MASTER THESIS IN ANALYTICAL ORGANIC CHEMISTRY

Analysis of the flavonoids and phenolics found in the marine angiosperm *Plantago maritima* collected in Norway

By Odd-Erik Tjønneland Lauvskard

Department of Chemistry

University of Bergen

2023

Acknowledgments

I would like to express my appreciation to Associate professor Monica Jordheim, my supervisor. She has been of tremendous help with insight and guidance during my research period. I would also like to thank Ph.D student Marie Emilie Wekre for her support, knowledge and guidance. Associate professor Jarl Underhaug, Ph.D Bjarte Holmelid and chief engineer Marit Bøe Vaage have my thanks for their help and teachings on use of the NMR, LC-MS and HPLC instruments.

Abbreviations

P. maritima – *Plantago maritima*

Chromatography

HPLC – High Pressure Liquid Chromatography

UHPLC – Ultra High-Pressure Liquid Chromatography

TLC – Thin Layer Chromatography

RP – Reverse Phase

DAD – Diode Array Detector

LC – liquid chromatography

UV – Ultraviolet

Vis – visible light

mAU – milli absorbance units

Rt – retention time

Prep – preparative

sh – shoulder

MS – Mass Spectrometry

LR – Low Resolution

HR – High Resolution

EI – electron impact ionization

ESI – electrospray ionization

TOF – Time Of Flight

m/z – mass to charge ratio

QqQ – triple quadrupole

SIM – Selected ion Monitoring

CID – collision – induced dissociation

TIC – total ion chromatogram

eV – electron volt

NMR analysis

NMR – Nuclear Magnetic Resonance

PMR – proton magnetic resonance

COSY – Correlated spectroscopy

HSQC – Heteronuclear single quantum coherence

HMBC – heteronuclear multiple bond correlation

NOESY – nuclear overhauser effect spectroscopy

TOSCY – total correlation spectroscopy

Å – angstrom

Coupl k – coupling constant

s – singlet

d – doublet

t - triplet

dd – double doublet

m – multiplet

2D – two dimensional

1D – one dimentional

ppm – part per million

δ – chemical shift

Chemistry

DMSO – dimethyl sulfoxide

PhGs – Phenylethyl Glycosides

CoA – Co-enzyme A

PAL – Phenylalanine Ammonia-Lyase

C4H – Cinnamic acid 4 – Hydroxylase

4CL – 4 – Coumarate: CoA Ligase

CHS – Chalcone Synthase

BNY – Bisnoryangonin

CTAL – 4-coumaroyltriacetic acid lactone

MeOH – Methanol

H_2O (Sdest) – super distilled water

HCOOH – Formic acid

ACN – Acetonitrile

Glu – glucose

Rha – rhamnose

MeO – methoxy

Arab – arabinoside

Rut – Rutinoside

Apiogluc – apio glucoside

Others

µm – micrometer

nm – nanometer

µL – microliter

Ref – reference

Abstract

This master project has a focus on extraction, separation and identification of flavonoids and other phenolic compounds in *Plantago maritima*. Previously in Norway there has only been done one small pilot study (bachelor project in Jordheim group) on the phenolic compounds in this plant using only DAD-HPLC, so the Norwegian polyphenol profile of this species isn't well documented. The polyphenolic profile of a species can show difference within geographical gradients due to different external parameters such as temperature, drought etc., normally this is seen for the quantitative amounts found. Qualitative polyphenolic profile variations are observed, however not to the same extent. Based on a literature survey, almost forty different polyphenols/phenolics are found in the genus in the classes of phenolic acids (cinnamic acid and hydroxybenzoic, and related esters), phenylethanoids and flavonoids. Both unsubstituted aglycones, mono and di-glycosylated compounds are seen. From literature ten polyphenols have been found in *P. maritima*: Caffeic acid (a), *p*-coumaric acid (b), ferulic acid (c), luteolin (14), chrysoeriol, diosmetin (17), apigenin-7-O-glucoside (2), luteolin-7-O-glucoside (3), verbascoside (10) and plantamajoside (1). In literature these ten compounds are confirmed through DAD-HPLC, ToF-MS (a, b, c, 14, 1 and 10) and MS/MS (2, 3 and 14).

Plantago maritima samples were harvested in Tømmervågen (60.440802°N, 5.302253°E) Bergen 23.06.2019 and initial DAD-HPLC analysis was performed. Extraction was performed with aqueous methanol (60:40), and extracts were combined and evaporated. The crude extract was purified with XAD-7, and finally with preparative HPLC. The different stages of purity and fractions were analyzed with DAD-HPLC and LC-MS in negative ESI mode. Selected preparative HPLC fractions were run on NMR. In addition, crude and purified fractions have been extensively analyzed with DAD-HPLC (UV-Vis and retention time) and LR-LC-MS (including MS/MS on glycosylated flavonoids). A total of 18 phenolics were identified in Norwegian *P. maritima.*

Only trace amounts were found from caffeic acid (a), p-coumaric acid (b) and ferulic acid (c). Plantamajoside (1) and luteolin (14) were confirmed with NMR (1D, 2D) analysis. These have previously only been tentatively identified in the species using HPLC, ToF-MS (1 and 14) and MS/MS (14). The flavonoid tricin (18), previously found only in *P. phaeostoma*, was identified with co - chromatography on HPLC and LC-MS using a tricin standard. A tricin glucoside (11) has also been identified (by LR-LC-MS and MS/MS) earlier found in *P. crassifolia*. Apigenin glucoside (2), luteolin 7 – O – glucoside (3), verbascoside (10) and diosmetin/chrysoeriol (17) were confirmed to be present (HPLC, LC-MS and MS/MS on 3 and 11). Ten compounds were for the first time in addition tentatively identified to be present within *P. maritima*: Campneoside I (4), nepitrin (6 – methoxy luteolin 7- glucoside) (6), luteolin glucuronide (7), quercetin arabinoside (8), tricin glucoside (11), rosmarinic acid (12), Apiin (apigenin 7 –

apioglucoside) (13), martynoside (15), apigenin (16) tricin (18). (HPLC, LC-MS and MS/MS on 6, 7, 11 and 13).

These have been found in the genus before by using DAD-HPLC, NMR (1, 3, 10, 11 and 15), TLC (12), MS/MS (1, 2, 4, 10, 14, 15, 16 and c), HR-MS (1, 2, 4, 10, 14, 15, 16 and c) In addition, two components tricin diglucoside (5) and diosmetin rutinoside (9) (HPLC, LC-MS and MS/MS on 5) were tentatively identified in both the species and in the genus for the first time.

Table of contents

1 Introduction

1.1. Motivation and purpose

The main aim of this master's project is to characterize the phenolic phenylpropanoid content of the marine plant *Plantago maritima* collected in Norway (Bergen), with a particular focus on the flavonoid content. The Norwegian *P. maritima* has not been examined before and a preliminary analysis based on DAD-HPLC (Bakke, 2020 – BSc project) indicated that the qualitative flavonoid content was different than previously seen in international studies (Beara et al. 2009). Beara et al studied the flavonoids in different *Plantago* species found in Serbia, and report on the flavone aglycones luteolin and apigenin, in addition to traces of the three substituted flavonol rutin (quercentin 3-rutinoside). Bakke 2020 did not find any traces of rutin in the Norwegian *P. maritima.* A study on the effects of elevated CO2 on phenolic secondary metabolites indicate the presence of plantamajoside, verbascoside and luteolin (Davey et al. 2004).

Considering the observations of the preliminary analysis, motivation was on further studies of the phenolic content of the Norwegian P. maritima. In order to improve the characterization accuracy, the crude extract was further purified using column chromatography (XAD-7) and preparative LC, and thorough analysis with DAD-HPLC, LR-MS, LC-MS/MS, reference standard and NMR.

This assignment is part of the research done in the Jordheim research group.

The research group has on-going studies of marine plants, analyzing and characterizing their flavonoid content. Marine plants are less studied than terrestrial plants, which makes them an interesting research topic (Maréchal 2019). (Marine plants are "terrestrial plants" adapted to the harsher marine environment, may change/alter their phenolic content).

1.2. Marine plants and angiosperms.

Angiosperms are vascular plants bearing flowers ("Plantago Maritima - an Overview | ScienceDirect Topics" 2022). Characteristically flowering plants has pollen (seed) and eggs (ovule). Angiosperms also have stems, roots and leaves("Angiosperms - NatureWorks" n.d.).

Plantago maritima is a salt tolerant marine plant, studies show *P. maritima* can tolerate saltwater due to its Na^+/H^+ antiport("Plantago Maritima - an Overview | ScienceDirect Topics" 2022). This allows efficient accumulation of Na^+ in the vacuole of *P. maritima*.

1.3. *Plantago maritima.*

Plantago maritima is classified in the plant kingdom as a vascular seedbearing angiosperm.("Plant Kingdom Plantae" 2022)

Plantago maritima is classified as an angiosperm, in the clade Eudicots, in Asterids of the Lamiales order in the Plantaginaceae family of the *Plantago* genus.("*Plantago Maritima*" 2020)

In the Norwegian species databank they have a map of registered observations of *P. maritima*, seeing as this marine plant is abundantly available along the entire coast, examining this plant and maybe finding some interesting substances would prove beneficial.("Plantago Maritima - Artsdatabanken" 2022)

When the chemical composition is better known it is possible to think about the chemical ecology of the plant. Because of *Plantago maritima's* abundance at the coast, it is possible to monitor the conditions of the local ecosystem and environment (Sævdal Dybsland et al. 2021).

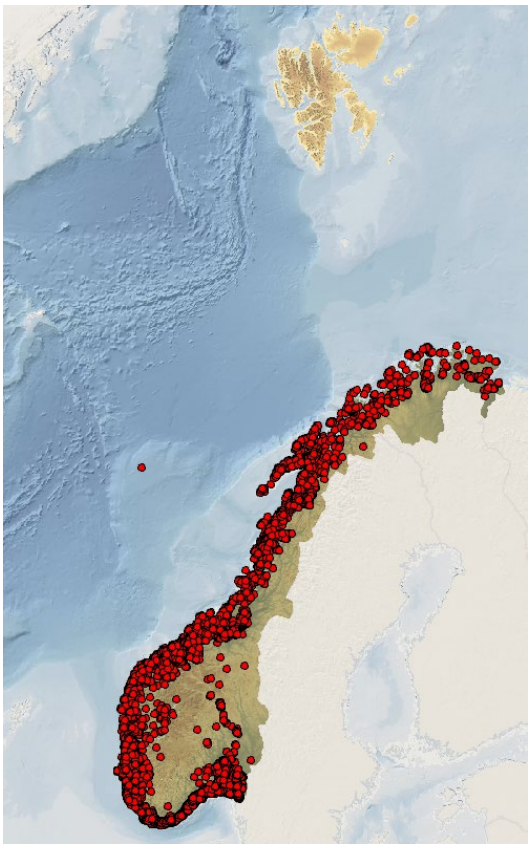

Figure 1.3.1: *P. Maritima* habitat map

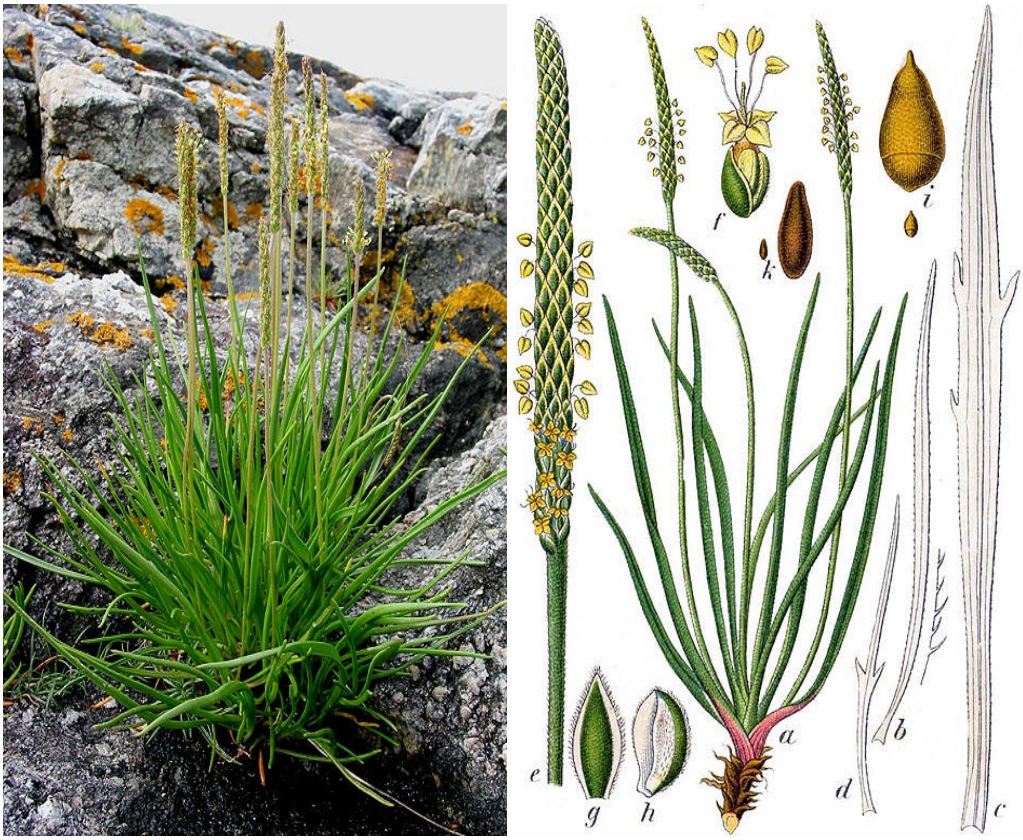

Figure 1.3.2: picture and illustration of *Plantago maritima*.(“Strandkjempe (Plantago Maritima)” 2022; “Gamle Tegninger Av Strandkjempe” 2022)

1.4. Polyphenols.

Polyphenols are compounds that are found in abundance in plants (Cory et al. 2018). Polyphenols are recognized for their antioxidant properties and probable role as a preventative measure against diseases associated with oxidative stress such as neurodegenerative disorders, cardiovascular diseases and cancer. Polyphenols cover a large group of compounds containing secondary metabolites in plants, chemically polyphenols are characterized as compounds with phenolic structural features. The least common denominator is that said compounds needs to contain at least one phenolic ring.

During synthesis, there are two metabolic pathways (Panche, Diwan, and Chandra 2016). The acetic acid pathway where simple phenols are the main products, and the shikimic acid pathway where phenylpropanoids are created.

Polyphenols	Phenolic acids	Hydroxybenzoic acid
		Hydroxycinnamic acid
		Phenylethyl
	Flavonoids	Flavones
		Flavonols
		Flavanones
		Isoflavonols
		Anthocyanins

Figure 1.4.1: Classification of polyphenols

1.5. Flavonoids.

Flavonoids are a group of natural substances with variable phenolic structures. (Panche, Diwan, and Chandra 2016) Flavonoids are natural products that are well known for their beneficial effects on health.

Flavonoids are found in most parts of flowers, bark, fruits, vegetables and grains.

Flavonoids are considered as highly important components in pharmaceuticals and medical applications. Flavonoids are known for being anti-oxidative, anti-inflammatory, anti-carcinogenic and anti-mutagenic. Research also shows that flavonoids have a preventative effect on coronary heart disease.

In plants themselves flavonoids are used as UV radiation blockers in new leaves, protecting the growing leaves. Flavonoids can inhibit certain enzymes, and are precursors for toxic compounds (Ludick 2020).

Flavonoids can be found in plants as aglycones, usually they are in a glycosylated form when produced in said plants (Ludick 2020). The glycosides from the glycosylated form can either be mono-, di or oligosaccharides. It's also possible for the glycosides to be sugar residues of galactose, rhamnose, xylose or arabinose. The fact that these flavonoids are glycosylated causes them to be more easily dissolved in water.

Flavonoids can be subdivided into different subgroups depending on the carbon of the C ring in which the B ring is attached and the degree of unsaturation and oxidation of the C ring.

An example is how isoflavones is attached to the C ring at position 3 and not position 2, where most others like flavones, flavonols and such are attached (Feng, Zhiyou, and Li 2017).

The A and B rings are responsible for emitting the wavelengths used to measure Flavonoids, the A ring has an absorption band at about 220-280 nm, while the B ring has a band at 300 - 400 nm.

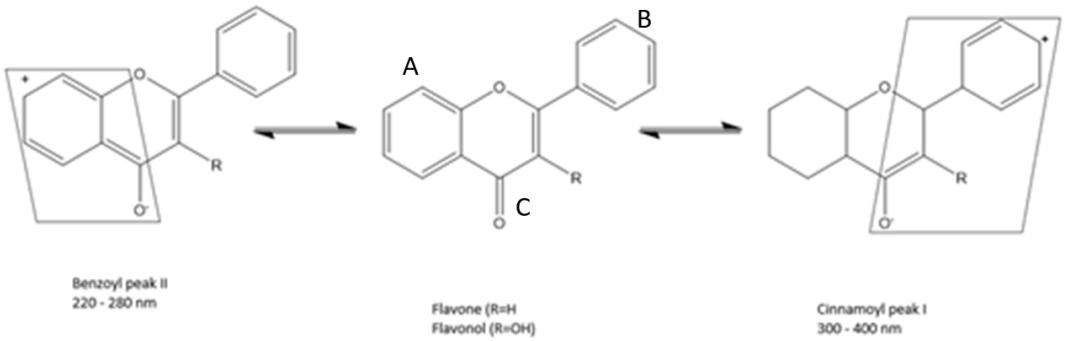

Figure 1.5.1: Flavonoid structure indicating UV peak origin, figure based on (Feng, Zhiyou, and Li 2017).

Table 1.5.1: Spectral characteristics of UV-VIS spectrum of flavonoids. Info aquired from (Feng, Zhiyou, and Li 2017).

Structure type	Band II (nm)	Band I (nm)
Flavone	250–280	304–350
Flavonol (3-OH is substituted)	250–280	328–357
Flavonol (3-OH is free)	250–280	358–385
Isoflavone	245–270	310–330 (shoulder peak)
Flavanone and flavanonol	270–295	300–330 (shoulder peak)
Chalcone	220–270 (weak peak)	340–390
Aurone	230–270 (weak peak)	370–430
Anthocyanidin	270–280	465–560

Substituents attached to rings A and B will affect the shapes of band I and II (Feng, Zhiyou, and Li 2017). An increase of hydroxyl groups in ring B results in an increase of red shift in band I. There is also an increase in red shift for band II when there is an increase in hydroxyl groups in ring A.

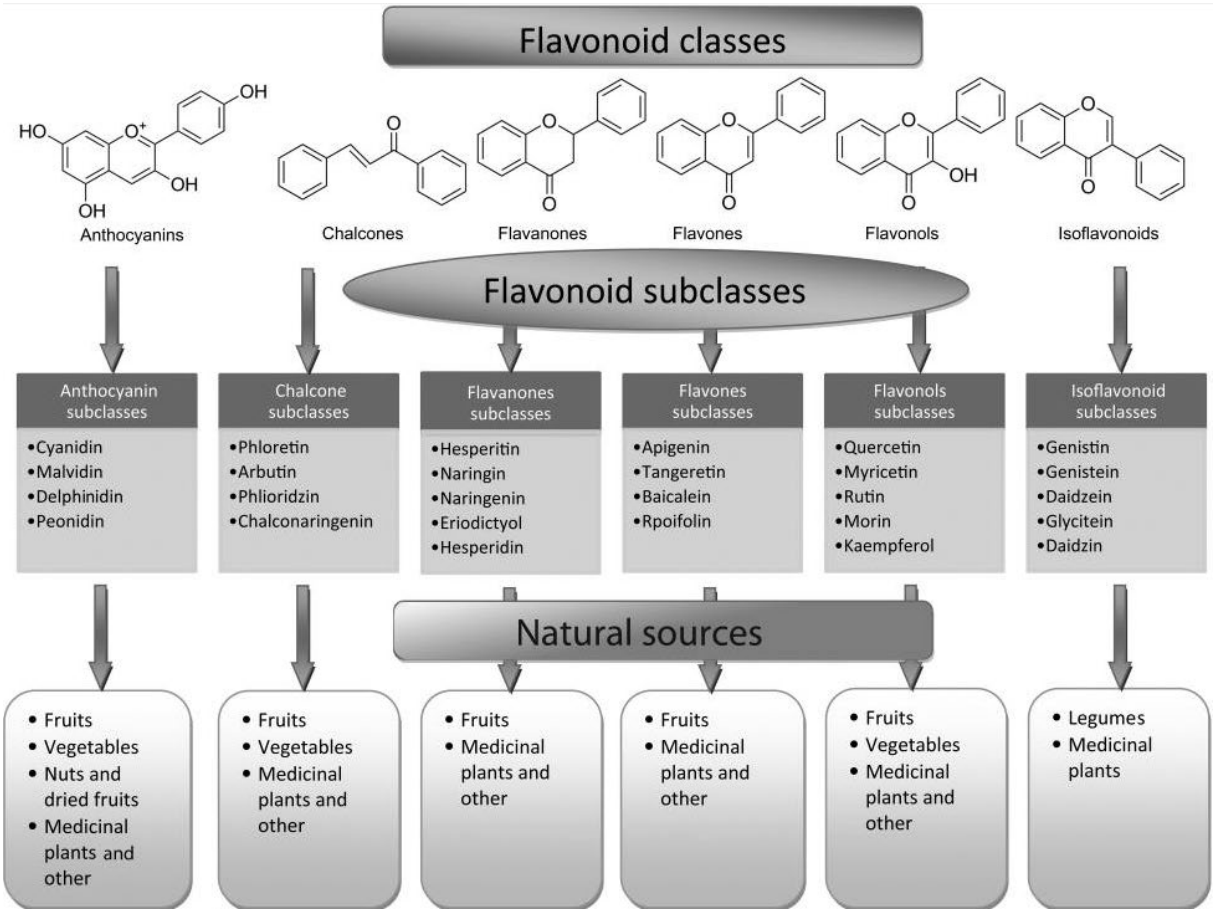

Figure 1.5.2: Flavonoid class and natural source chart acquired from(Panche, Diwan, and Chandra 2016).

1.6. Structure

The basic skeleton of flavonoids is built up of three rings. The A and B rings are benzene rings, the C ring is made of an oxygen and three carbon atoms. The B ring is usually attached at position 2, and for chalcones the C ring is split open.

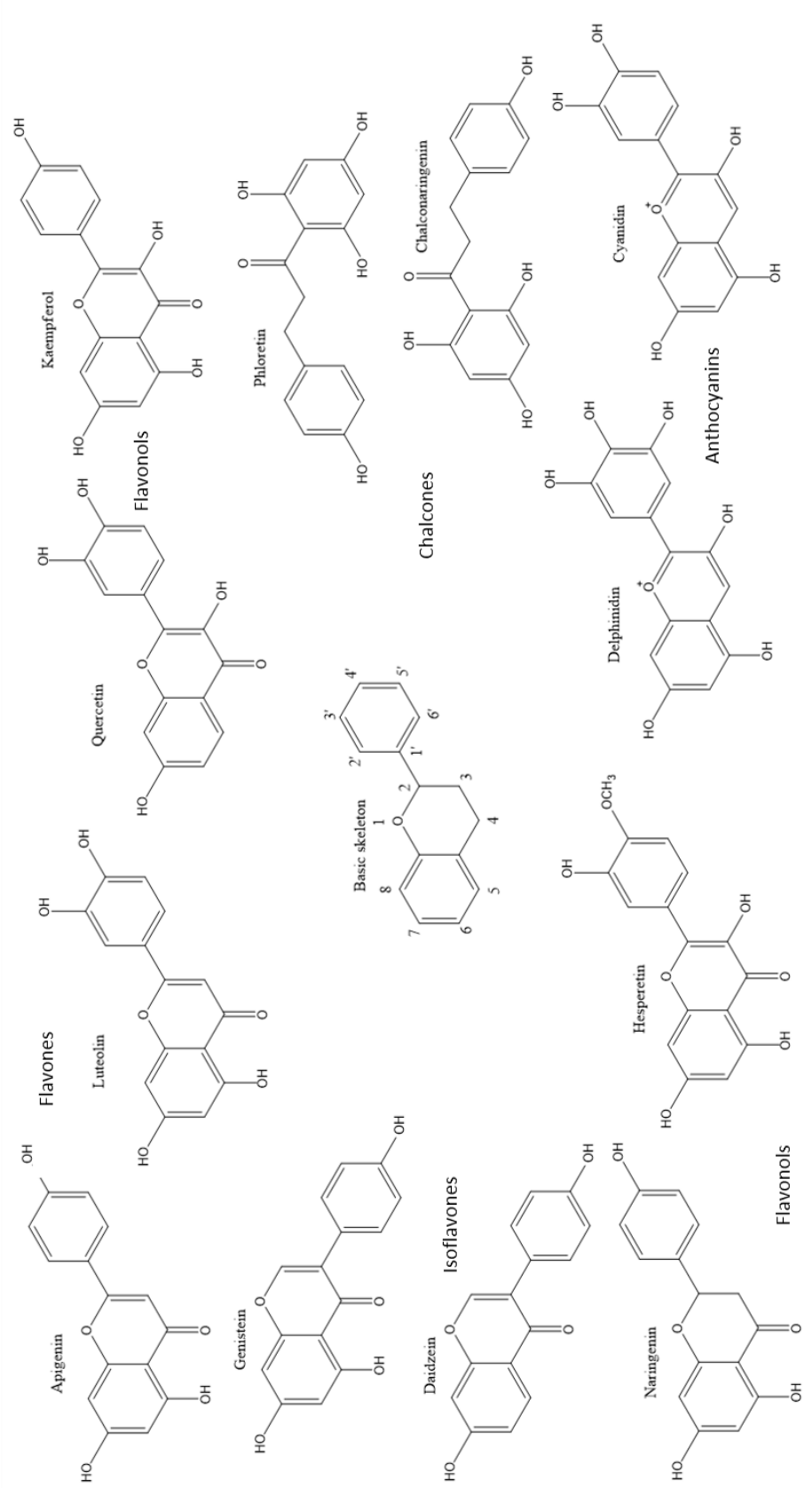

Figure 1.6.1: Basic skeleton for flavonoids and its classes. Modified after(Panche, Diwan, and Chandra 2016).

1.7. Flavones

Most flavones of vegetables and fruits have a hydroxyl group in position 5 on the A ring, another common hydroxylation position is carbon 7 in the A ring, or 3' and 4' in the B ring. Flavones have a double bond between positions 2 and 3 and a ketone at position 4 in the C ring (Panche, Diwan, and Chandra 2016). Good sources for flavones are celery, parsley, chamomile and ginko biloba. Citrus peels are rich in polymethoxylated flavones.

Flavones are highly diverse in methylation and hydroxylation, with the different glycosylation patterns (Panche, Diwan, and Chandra 2016). Flavones are perhaps the most common and largest subgroup of flavonoids in fruits and vegetables. Flavonols are flavonoids with a ketone group. Flavonols occur frequently in a variety of fruits and vegetables. Good sources for flavonols are onions, lettuce, tomatoes, apples, grapes and berries.

1.8. Flavanones

Flavanones are a precursor for a variety of flavonoids (Heldt and Piechulla 2021; Panche, Diwan, and Chandra 2016). Flavanones can be found in flowers, fruits, seeds, roots, bark, branches and peels. Flavanones lack double bond between C2 and C3 in the C ring. Two stereoisomeric forms of each flavanone structure are possible since carbon 2 is an asymmetric center. Flavanones are known for their free radical-scavenging properties and are the compounds that give fruits their bitter taste.

1.9. Phenylethyl glycosides (PhGs)

Some compounds have been associated with the biological activities in the *Plantago* genus (Samuelsen 2000). Plantamajoside and verbascoside are examples, they have been reported to have antibacterial, anti-inflammatory and antioxidant activities. Verbascoside is a potent inhibitor of the enzyme aldose reductase and protein kinase C. (Duynstee et al. 1999).

Verbascoside (acteoside) is part of the phenyletyl glycosides(-PhGs) group (Kawada et al. 2006). A rhamnose molecule is attached in the third position on the central glycoside molecule in verbascoside (figure 3.5.2), while plantamajoside is grouped as

a di-hydroxy phenylethyl glycoside. A glucose molecule is attached in the third position on the central glycoside molecule in plantamajoside.

1.10. Biosynthetic pathways of flavonoids.

The biosynthetic pathway responsible for synthesizing flavonoids in plants is the phenylpropanoid pathway (Falcone Ferreyra, Rius, and Casati 2012). By using phenylalanine that is transformed into 4-coumaroyl CoA, which then enters the flavonoid biosynthesis pathway. The pathway starts by building the main scaffold from which all flavonoids derive, which is chalcone.

The phenylpropanoid pathway also leads to the production of hydroxycinnamic acids such as sinapic and ferulic acids, leading into their corresponding esters.

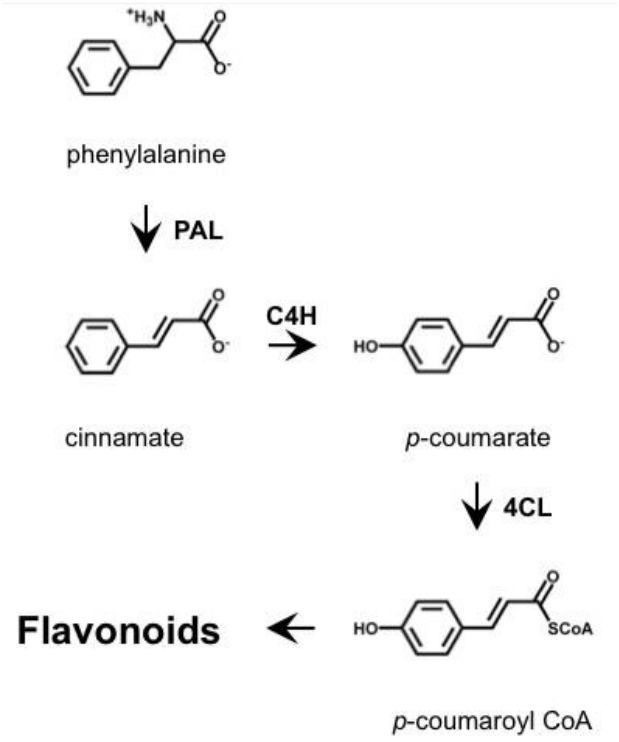

Schematic illustration of Phenylpropanoid pathway including enzyme catalyst.
Phenyalanine ammonia-lyase (PAL), Cinnamic acid 4 - hydroxylase (C4H), 4 - coumarate: CoA ligase (4CL)

Figure 1.10.1: Illustration of phenylpropanoid pathway(Fraser and Chapple 2011)

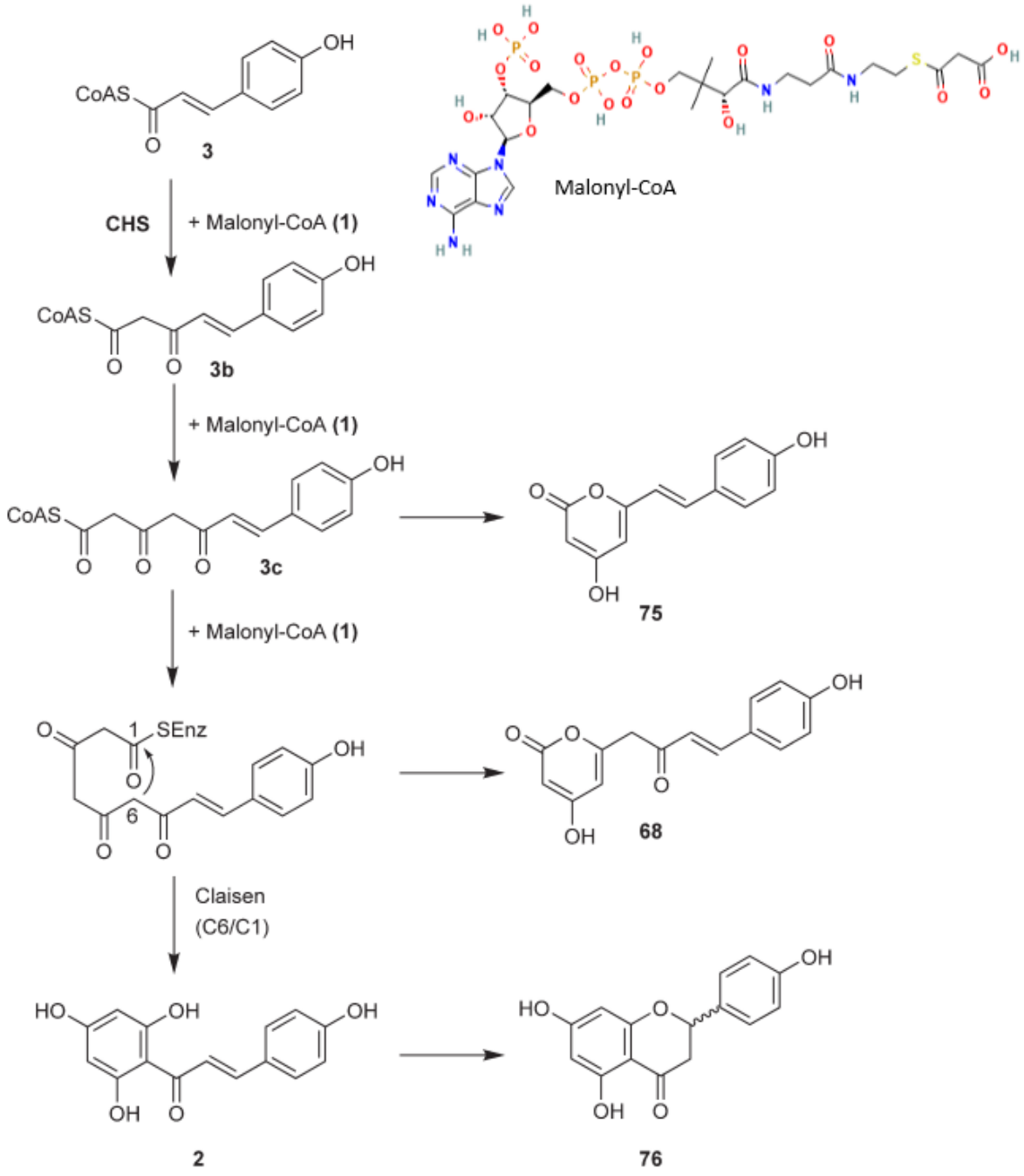

Proposed mechanism for the conversion of 4-coumaroyl-CoA (3) to naringenin chalcone (2), by-products bisnoryangonin (BNY) (75) and 4-coumaroyltriacetic acid lactone (CTAL) (68), and the tetraketide intermediate (3c).

Figure 1.10.2: Illustration of proposed mechanism regarding flavonoid synthesis.(Morita, Abe, and Noguchi 2010)

The Chalcone synthase (CHS) reaction is initiated by binding 4-coumaroyl-CoA, then by formation of a thioester at the active site of the enzyme (Morita, Abe, and Noguchi 2010). Naringenin chalcone is formed after three rounds of decarboxylative Claisen condensation, cyclization and aromatization of the enzyme bound tetraketide intermediate. This prosses leads to the flavanone naringenin (76).

1.11. Glycosides

Important derivatives of the monosaccharides are the glycosides (Bernatek, Uggerud, and Pedersen 2019). They occur when the hydroxyl group at carbon atom 1 in a monosaccharide reacts with a hydroxyl group in another compound (for example alcohol or amine), with decomposition of water.

Monosaccharides contain carbon, hydrogen and oxygen in ratios (CH2O) n where n = 3-7 and are called triosis (n = 3), tetrose (n = 4), pentose (n = 5) , hexose (n = 6) and heptulose (n = 7) (PHONE and FAX n.d.). Stereoisomers exist as D- or L-form. A chemical compound that rotates plane-polarized light to the right is called the dextrorotatory (D) and to the left levorotatory (L). Geometric D and L sugars. Glucose exists only as a D-isomer. D-glucose rotates plant-polarized light d + 52.7°, but D-fructose rotates -52.7°.

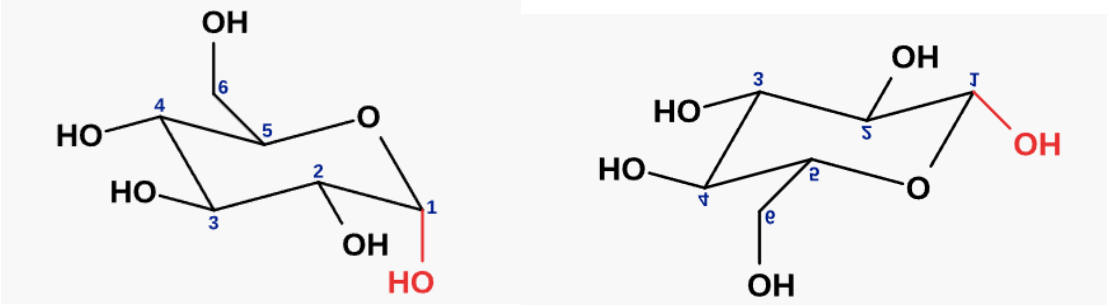

Figure 1.11.1: Alpha-(α) D-glucose Beta-(β) D-glucose
("Alpha(α) and Beta(β) Glucose: Comparison, Structures, Explanation" 2022)

α -glucose has axial (out of plane) configuration of the hydroxyl group on C1, β -glucose has an equatorial (along the plane) hydroxyl group on C1 (Budzianowska and Budzianowski 2022).

H-NMR can distinguish between alpha and beta glucoses, alpha glucose has a signature chemical shift value at 5.2 ppm while beta glucose has one at 4.6 ppm (evan 2014).

Below is a list of sugar molecules inclusive D-glucose, these molecules are variations that occur on flavonoids and other polyphenols contained in the *Plantago* family.

Xylose (wood sugar) as an aldopentose, a monosaccharide containing five carbon atoms and an aldehyde functional group. The chemical formula of xylose is $C_5H_{10}O_5$. (Wishart et al. 2009)

L-Rhamnose is a compound used as a component in chemical reactions and as a base material for organic compound synthesis (Kahraman 2019). Common originations for L-Rhamnose are from bacteria and plants. L-Rhamnose is one of the sugar components in Verbascoside.

L-Arabinose (L-arabinopyranose) is a pentose monosaccharide that is essentially neutral and exist in all living species (YMDB 2022).

Arabino furanose is the furanose form of arabinose. The compound is a pentose monosaccharide containing an aldehyde functional group, arabino furanose is a compound used in biological synthesis in plants and bacteria.

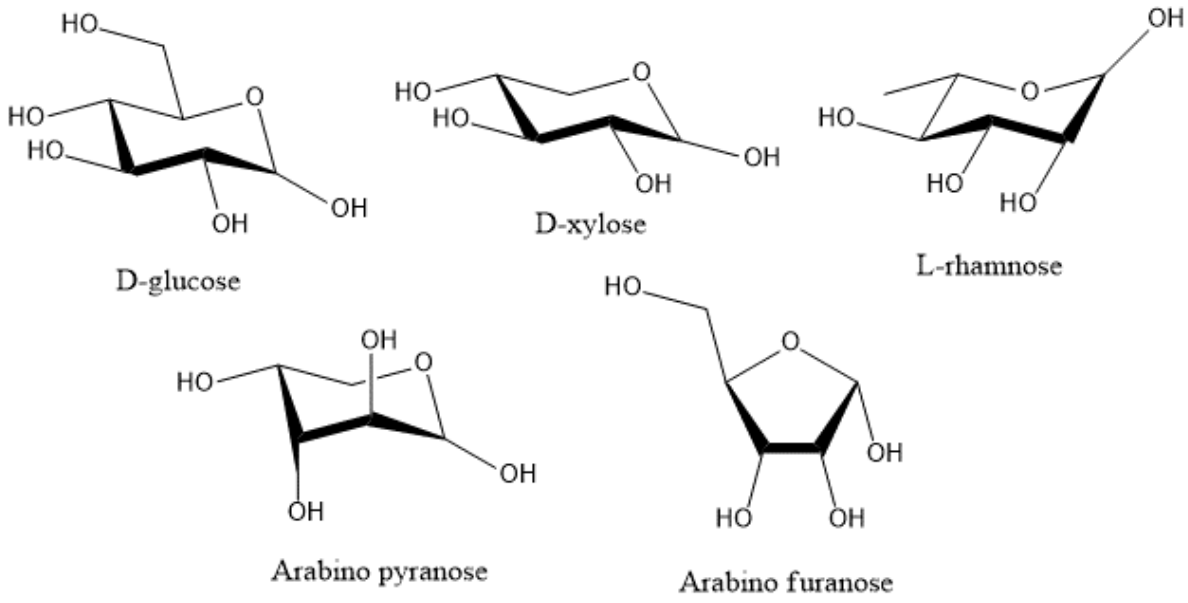

Figure 1.11.2: Illustration of sugar molecules found in phenolic compounds.

1.12. Components found in the *Plantago* genus.

To make a comprehensive list of compounds found in the *Plantago* genus in order to surmise possible candidates for phenolic acids, flavonoids and phenylpropanoids, including their glucosides that has an elevated chance of being found in *Plantago maritima.*

Table 1.12.1: Compounds (sorted by increasing molecular weight, MW) found in the *Plantago* genus including references. Compounds known to be in *P. maritima* are highlighted in grey.

No.	Compound	MW (g/mol)	*Plantago Ssp*	Reference
	protocatechuic acid	156.12	*depressa*	(Xu et al. 2020)
	p-coumaric acid	164.16	*maritima*	(Davey et al. 2004)
	gallic acid	170.12	*lanceolata*	(Sanna et al. 2022)
	caffeic acid	180.16	*maritima*	(Davey et al. 2004)
	quinic acid	192.17	*major*	(Beara et al. 2009)
	ferulic acid	194.18	*maritima*	(Davey et al. 2004)
16	apigenin	270.24	*argentea*	(Beara et al. 2009)
14	luteolin	286.24	*maritima*	(Davey et al. 2004)
	chrysoeriol	300.26	*maritima*	(Bakke 2020)
17	diosmetin	300.26	*maritima*	(Bakke 2020)
	quercetin	302.23	*major*	(Beara et al. 2009)
18	tricin	330.29	*phaeostoma*	(Kawashty et al. 1994)
	chlorogenic acid	354.31	*lagopus L*	(Fiz, Lanza, and Matellano 2000)
12	rosmarinic acid	360.3	*lagopus L*	(Fiz, Lanza, and Matellano 2000)
	magniferin	422.3	*atrata*	(Janković et al. 2012)
2	apigenin-7-O-glucoside	432.4	*maritima*	(Beara et al. 2009)
8	quercetin 3-O-arabinoside	434.3	*asiatica*	(Murai et al. 2015)
3	luteolin-7-O-glucoside	448.4	*maritima/ lanceolata*	(Beara et al. 2009; Fiz, Lanza, and Matellano 2000)
	luteolin-4'-glucoside	448.4	*ovata*	(Kawashty et al. 1994)
	ursolic acid	456.7	*major*	(Beara et al. 2009)

7	luteolin 7-O-glucronide	462.4	*phaeostoma*	(Kawashty et al. 1994)
	chrysoeriol 7-glucoside	462.4	*psyllium*	(Kawashty et al. 1994)
6	nepitrin (6-methoxy luteolin 7-glucoside)	478.4	*major*	("Plantago Major - Common Plantain" n.d.)
11	tricin 7-glucoside	492.4	*crassifolia*	(Zaghloul and Zaghloul 2000)
	apigenin 4',7-rhamnoside	562.5	*ovata*	(Patel et al. 2020)
13	apiin (Apigenin-7-apioglucoside)	564.5	*major*	(Beara et al. 2012)
9	diosmetin 7-O-rutinoside	608.5	**1*	
	rutin (quercetin 3-O-(6-O-rhamnosyl) glucoside)	610.5	*argentea*	(Beara et al. 2012)
	chrysoeriol 7-gentiobioside	624.5	*psyllium*	(Kawashty et al. 1994)
10	verbascoside	624.6	*maritima*	(Davey et al. 2004)
1	plantamajoside	640.6	*maritima*	(Davey et al. 2004)
15	martynoside	652.6	*lanceolata*	(Budzianowska, Skrzypczak, and Budzianowski 2004)
4	campneoside I	654.6	*depressa*	(Xu et al. 2020)
5	tricin 5-7-diglucoside	654.6		
	New phenylethanoid glycoside	756.25	*lanceolata*	(Budzianowska and Budzianowski 2022)

*1 Diosmetin is known to be in *P. maritima*, but diosmetin 7-O-rutinoside has yet to be found in the *Plantago* species.

2. Methods and procedures.

2.1. Samples.

Plantago maritima was harvested 23.06 2019 in "Tømmervågen" by Monica Jordheim, my supervisor.

The crude samples consist of flower, stem, and leaves, and was put in the freezer until use. Once ready to start, the samples were divided into flower, stem and leaves. Each part was dried separately at room temperature (23 ◦C) and each part was then extracted using a methanol and water solvent (60:40).

Later a new crude sample was made (extract 2), weighing in at 80.77 g. This sample was not separated into flower, leaf and stem, but instead made as a mix of all parts. The sample was then used for extraction, four extractions each using a liter of methanol and water (60:40) solvent were used.

2.2. Extraction.

To start off, there was a preliminary sample made from old leaf samples, to ascertain likeness between chromatographic results. Once this was achieved extractions of the flower, stem and leaf were all made. The solvent was an aqueous methanol solution (60:40) and the weights of the parts were flower: 1.298g, stem: 1.501g, and leaf: 1.189g.

Each sample was cut into smaller pieces and once solvent was added, each part was left on stirring for some time. Multiple extractions were made, some samples were stirred for an hour, some samples were stirred for over a full day. When separating the solvent from the flower samples, millipore membrane filters (0.45 μm) were used, once the liquid was separated all samples were dried into complete dryness on a rotavapor machine.

Plantago maritima flower extraction one (Ex. Pmf1) had a lot of particles that needed filtering out (presumably pollen). *Plantago maritima* leaf extraction one (Ex. Pml1) was mostly green with little to no visible particulates. Filtering still showed some results in cleaning up the green solvent. *Plantago maritima* stem extraction one (Ex. Pms1) was a lighter green liquid compared to the leaf extract. The steam extract contained small amounts of particulates that was removed by filtration.

Extract 2.

Extract 2 was made using a large amount of sample, weighing in at 80.77 grams. Four extractions, each using one liter of solvent was performed, each extraction lasting between 22-24 hours.

2.3. Column Chromatography – Amberlite XAD – 7 purifications.

Amberlite XAD 7 is a moderately polar powder made of acrylic ester, XAD 7 has a surface area of 450 m^2 per gram (Bertin et al. 2011). It has a pore diameter of 9 nm and a particle size of 0.3-1.2 mm.

After determining that the crude extract 2 contained too many substances, it was decided to use XAD 7 to wash the sample to remove unwanted sugar and acid substances. This was done by dissolving the dried sample into methanol and adding it to the gravimetric column containing XAD 7. Several liters of distilled water were used to wash away the unwanted substances, and once the water had cleared up enough when exiting the bottom of the column, methanol was used to remove the sample from the XAD 7 particles. Once the heat produced from water and methanol mixing reached the gathering spout, the sample was collected. The collected sample was then dried using roto-vapor.

2.4. (U)HPLC – (Ultra) High Performance Liquid Chromatography

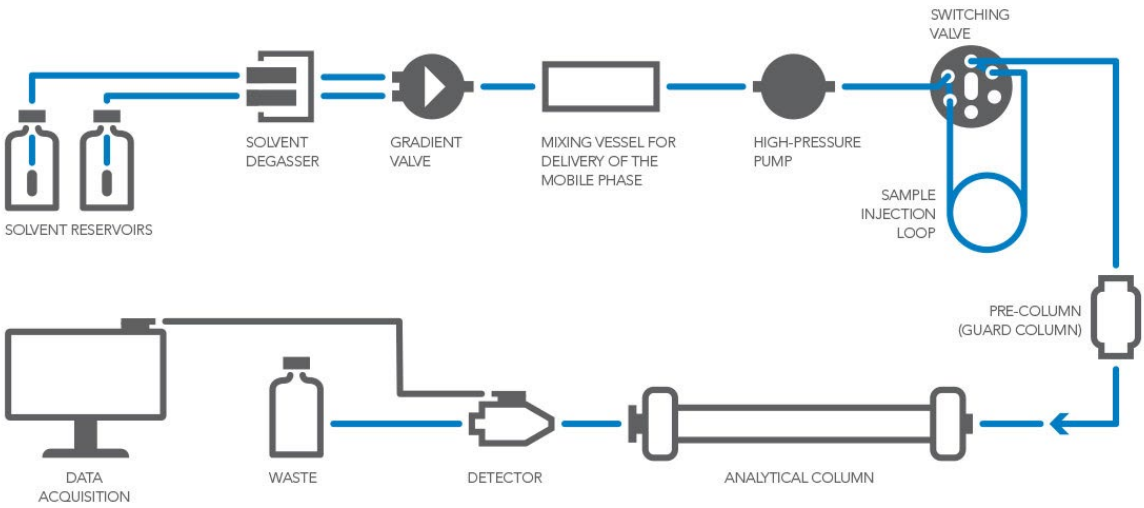

Figure 2.4.1: U/HPLC illustration ("HPLC Help Center" 2021)

The principle of HPLC is shown in figure 2.3.1. Solvents (two or more) get pumped and sent to the gradient valve where the amount of each solvent is controlled and sent to the mixing chamber (Moldoveanu and David 2012). After mixing the eluent is put under pressure and gets mixed with the sample in the sample injection loop. The sample then moves with the mobile phase trough the pre-column, then trough the analytical column. In the analytical column the substance in the sample gets separated and sent to the detector. Each substance has its own retention time (how long it takes to travel through the column) and therefore passes the detector at various times. The usual detector are UV/vis detectors, there are also MS detectors and fluorescence detectors. Once detection is done the raw data is sent to a computer and analyzed. The sample and solvents go into a waste bin.

A sample is comprised of analytes and matrix, analytes are the compounds of interest, matrix are all other compounds in the solution together with the analytes. Compounds have different retention times depending on their polarity and size and is used to separate them in the column (chromatographic separation). Retention is the prosses of compounds being retained on the solid phase, then getting released back into the mobile phase, polarity is what controls how long the solid phase retains each compound.

Isocratic elution is when the amount of each solvent stays the same during the entire elution (Moldoveanu and David 2012). Gradient elution is when the proportions of the solvents change over time during the elution while the total amount stays the same.

The two main types of chromatography are normal phase and reverse phase chromatography. The most common HPLC technique is Revers phase HPLC (RP-HPLC). This kind of chromatography has a non-polar stationary phase and a polar mobile phase. Non-polar stationary phases are widely available, some are produced by chemically bonding long hydrocarbon chains to the solid surfaces like silica. RP-HPLC is the most commonly used type of HPLC due to the large amount of compounds this type of chromatography can separate (Moldoveanu and David 2012).

Table 2.4.1: UHPLC specifications for *P. maritima* crude extract

Components	Specifications
UHPLC - Instrument	Aligent 1290 analytical HPLC (UHPLC)
Column	Luna Omega 1.6µm C18 100Å
UV – area	280 ± 20, 300 ± 10 320 ± 10, 360 ± 10, 380 ± 10
Injection volume	2µL
Flow	0.3mL/min
Solvent	A: H_2O(Sdest)+0.5%HCOOH. B: ACN +0.5% HCOOH

This Luna column is a fully porous silica C18 column, which means its packed with silica particles with C18 chains connected to the surface. The particle size is 1.6µm and the pore size is 100Å which converts into 10nm.

Table 2.4.2: HPLC specifications for *P. maritima* crude extract

Components	Specifications
HPLC - Instrument	Aligent 1260 analytical HPLC
Column	Hypersil 5 ODS Octadecyl 5µm C18 120Å
UV – area	280 ± 20, 300 ± 10 320 ± 10, 360 ± 10, 380 ± 10
Injection volume	20µL
Flow	1mL/min
Solvent	A: H_2O(Sdest)+0.5%HCOOH. B: ACN +0.5% HCOOH

Table 2.4.3: Gradient elution (HPLC)

Time (min)	0-30	30-34	34-35
%A	90	50	90
%B	10	50	10

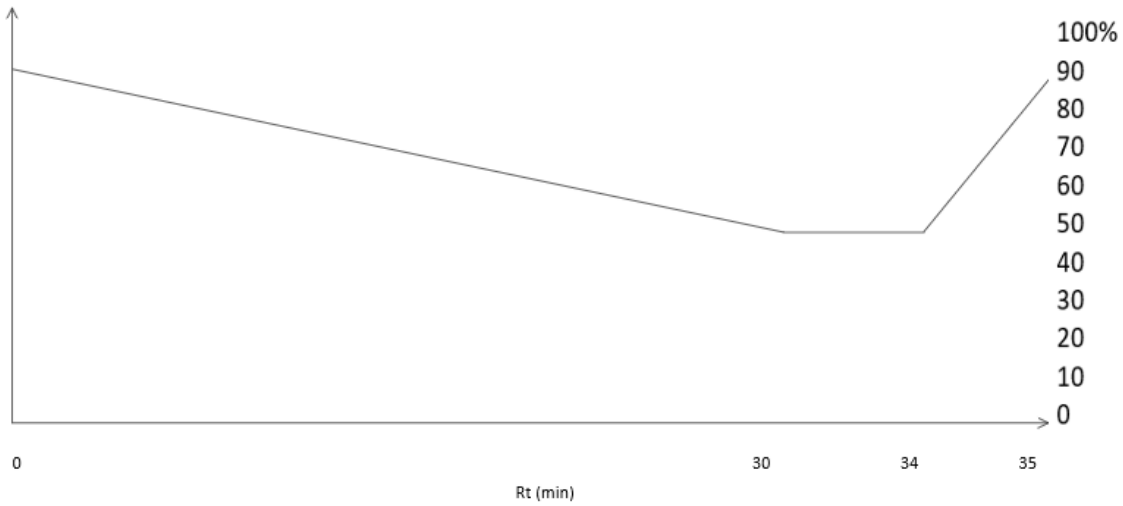

Figure 2.4.2: Graph showing the change in eluent during HPLC run.

A: H_2O(Sdest)+0.5%HCOOH. B: ACN +0.5% HCOOH

Table 2.4.4: Gradient elution used in UHPLC.

Time (min)	0	5	8	10	12	15	17	19	21	23	24	26	27	29
%A	95	85	80	75	70	45	40	35	30	30	0	0	95	95
%B	5	15	20	25	30	55	60	65	70	70	100	100	5	5

A: H2O(Sdest)+0.5%HCOOH. B: ACN +0.5% HCOOH

2.5. Preparative and analytical HPLC.

The main differences between (U)HPLC and preparative HPLC are pressure, column size, volume eluent used and during preparative HPLC it's possible to gather the sample post column passthrough ("Preparative Liquid Chromatography - an Overview | ScienceDirect Topics" 2022). The goal with preparative HPLC is to separate analytes from matrix in a sample, with the end goal of isolation and extraction of said analytes. Preparative HPLC is especially helpful in the separation of enantiomers. One of the difficulties that follows the use of preparative HPLC is the risk of overloading the column, resulting in lack of separation between compounds.

2.6. Mass Spectrometry (MS).

A mass spectrometer is an instrument that produces and weighs ions (Fleming and Williams 2020). Mass spectrometers can be divided into three fundamental parts: Ionization source, analyzer and detector.

When an analyte gets sent through MS, the molecule (M) gets ionized (M^+). After ionization the ions are separated by their mass / charge ratio (m/z). The ions usually have a charge of one because of one single electron, m/z can be referred to as the mass of the ion.

Table 2.6.1: Gradient elution used in LC-MS.

Time (min)	0	2	5	8	10	12	15	18	19	23	24	26	34
%A	99	95	95	80	75	70	50	35	35	30	0	0	95
%B	1	5	5	20	25	30	50	65	65	70	100	100	5

A: H2O(Sdest). B: ACN

Electron impact ionization (EI).

To achieve ionization, electrons are repelled from a heated filament and attracted to an anode, the potential difference from this is about 70 eV (Mark 1982). Electrons with this potential energy can remove electrons from molecules, given that the required energy for ionization is about 7-10 eV. Using this prosses of potentially charged electrons ions is made, $M + e \rightarrow M^{*+} + 2e$.

Electrospray ionization (ESI).

Ionization using ESI occurs when a solution is ejected from the needle tip, and the solution is vaporized due to the strong electric field present at the needle tip (Pavia et al. 2014). this method using a strong electric field makes the small droplets in the highly charged mist, and the mist is at atmospheric pressure. This method is popular because the solution used can be an effluent directly from a HPLC column.

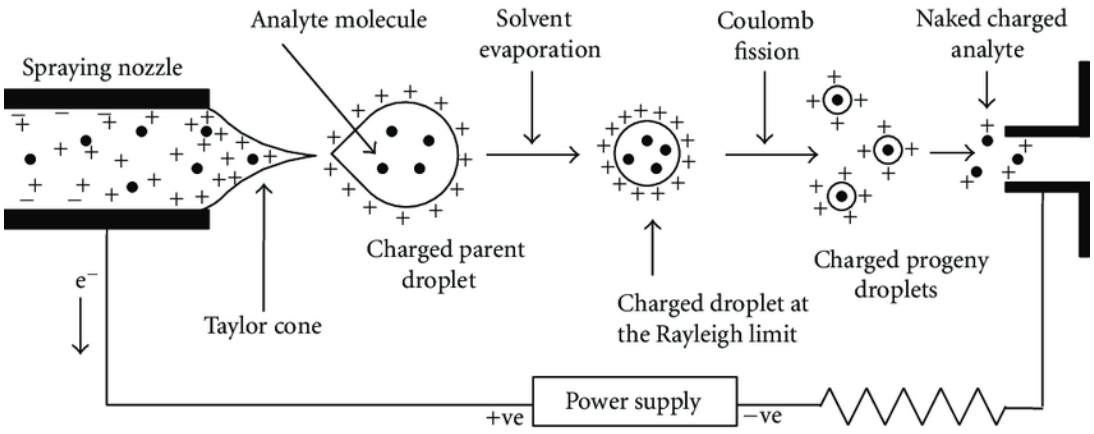

Figure 2.6.1: Electrospray ionization (ESI)("Figure 6: Schematic Representation of the Electrospray Ionization Process." 2022)

The ionized gas is sent to an ion analyzer to measure and separate ions according to m/z ratios. The most common analysis method is the magnetic analyzer, this method uses a magnetic field to deflect the ions, and the amount of deflection correlates to their mass. The larger ions are deflected less than the small ions.

Another method of analysis is time-of-flight (TOF) analysis.

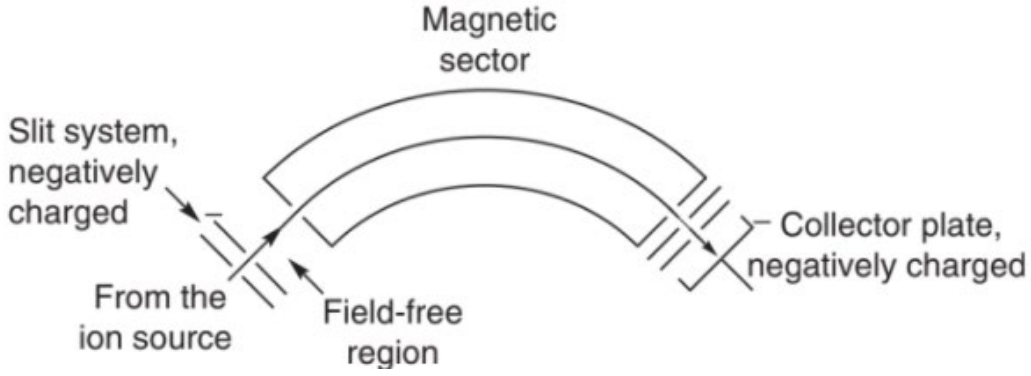

Figure 2.6.2: TOF analysis illustration.

This method has the advantage of detecting all ions instead of just the masses meeting the set requirements at any given time (Fleming and Williams 2020). As the name suggests TOF analysis utilizes the time of flight in correlation to the distance traveled to measure the mass of the ions.

Quadrupole mass analyzer.

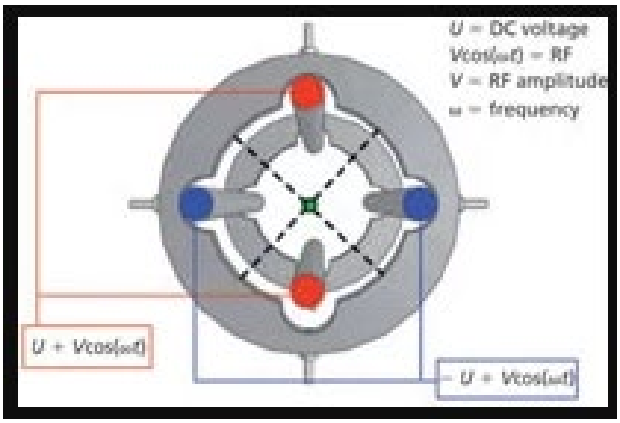

Figure 2.6.3: Illustration of quadrupole mass analyzation device.(McDowall 2012)

Electric fields are used in order to separate ions according to their m/z ratio, the ratio of mass in Daltons (Da) to the integer number of charges (z), as the masses pass along the central axis of the parallel and equidistant rods (Pavia et al. 2014; McDowall 2012). The rods are often made of molybdenum alloys since the rods then gain an inertness and lack of activity. The rods polarity oscillates between positive and negative. The oscillation determines the m/z ratio that gets to travel to the analyzer.

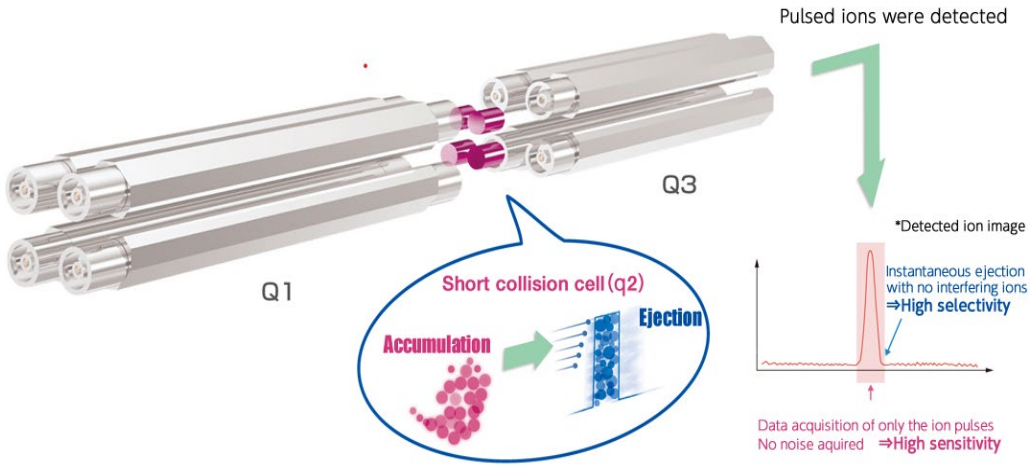

Figure 2.6.4: QqQ MS.

A quadrupole is two pairs of metal rods equally distanced from an axis; each pair generates an electric field when DC voltage is run through them ("JEOL USA Blog | A Quick Introduction to Triple-Quadrupole Mass Spectrometry" 2022). The current is flipped at a certain frequency to create an oscillating field that only accepts certain m/z ratios. QqQ is when there are two large quadrupoles with a small quadruple in the middle as shown in the picture above.

MS fragmentation.

When using MS, it's important to track the charge and radical sites carefully to prevent miss assigning which fragments are ionic and neutral, and to not draw highly unlikely fragmentations (Pavia et al. 2014). It's also important to remember that fragmentations during MS happens while the compounds are in gas phase where ions are in a highly exited vibrational state, meaning one can't draw chemical reactions.

During MS the compound of interest M gets ionized to M+, then fragmentated to F_1^+ - F_x^+.

High Resolution Mass Spectrometry (HR-MS).

HR-MS is an incredibly useful tool when researching unknown compounds to figure out their structure. HR-MS finds the exact mass of the molecule down to the fifth decimal space, which makes it possible to differentiate between most compounds. The level of precision HR-MS gives makes the data point towards only one formula, where the only obstacle would be when isotopes are involved.

MS scan mode.

In scan mode the MS machine detects for signals over a mass range, said range could for example be from 50 to 800 m/z (Packard 1998). During the scan period the MS electronics scan trough the mass range in intervals over a period to get the entire range. The stored spectra represent the signals detected throughout the entire range. Because the full range is covered, scan mode is typically selected for qualitative analysis, or quantitative if all masses are not known in advance.

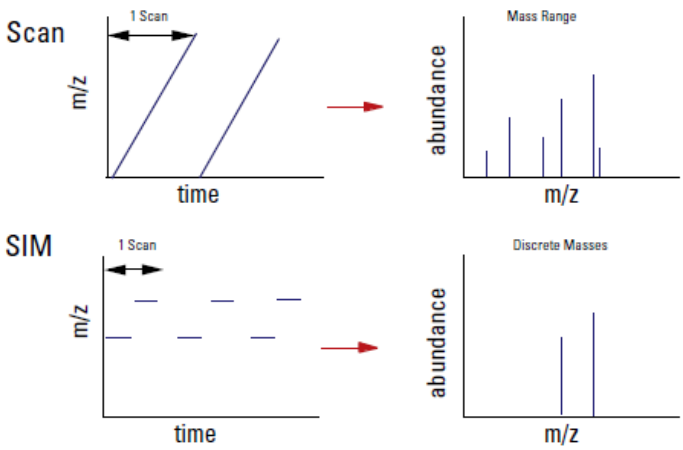

Figure 2.6.5: Illustration showing Scan and SIM data acquisition.

MS SIM mode.

Mass spectrometers can also operate in a mode called Selected Ion Monitoring (SIM)(Packard 1998). Rather than scanning continuously through a range they can be set to only monitor a few mass-to charge ratios (m/z). only looking for selected masses results in a smaller scan time which increases the sensitivity. Moreover, because the cycle time between data points is often shorter than in scan mode, quantitative precision and accuracy are improved through optimal peak shape profiling. Since the m/z values that will be sampled must be set in advance, SIM is most often used for target compound analysis. When an analysis consists of multiple targets, the m/z value sampling can be programed to match the time of the compound's elution time window.

There are two ways to introduce samples to the machine, either by using direct injection or inject the sample into a loop that sends the sample trough a HPLC column. When using direct injection, the scan range needs to be narrowed down since the peak width will be narrow because the sample gets introduced all at once.

Collision-Induced Dissociation (MS/MS).

The process called collision-induced dissociation (CID) is how MS/MS is accomplished (Packard 1998). The CID process breaks ions apart as a result of molecules colliding with one another. By using electrospray ionization, a CID spectrum can be produced with only one quadrupole system.

By using various levels of voltage, it's possible to achieve various degrees of fragmentation. With higher voltage, the degree of fragmentation increases.

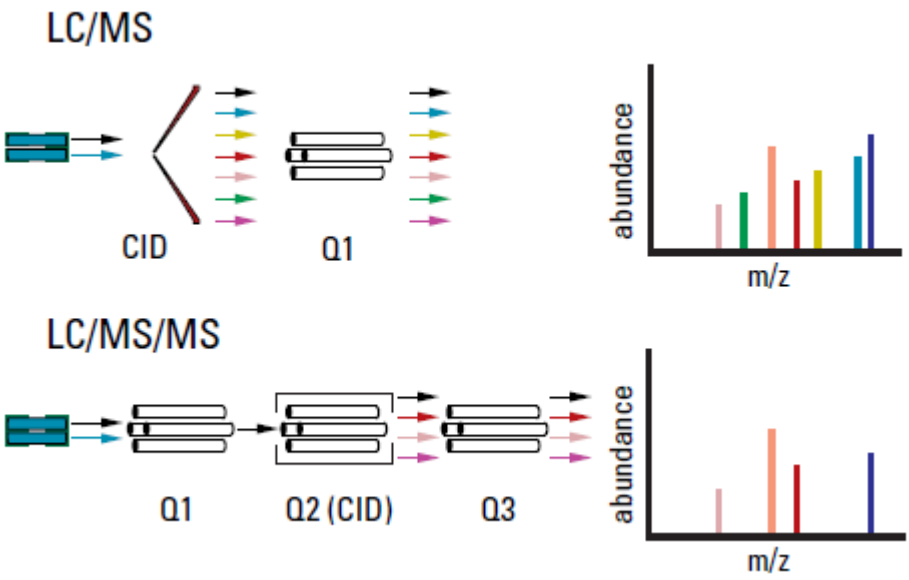

Figure 2.6.6: CID with single quadrupole and triple quadrupole mass spectrometers (Packard 1998)

While using MS there are two ionization modes positive (+) ESI and negative (-) ESI Depending on the setup of the instrument, only positive or negatively charged ions are yielded (Harrata 1995). The formation of ions occurs in large amounts. In positive ion mode protonated analyte molecules are observed in the mass spectra. Negative mode deprotonated analyte molecules are observed. When analyzing m/z of +ESI true mass is obtained by removing one proton, while -ESI requires an additional added proton to acquire true mass.

2.7. NMR Nuclear Magnetic Resonance.

NMR is a highly useful spectroscopic method used by organic chemists given that NMR utilizes hydrogen and carbon nuclei, of which organic compounds are mainly built of (Pavia et al. 2014).

Nuclear magnetic resonance spectroscopy involves transition of a nucleus from one spin state to another with the resultant absorption of electromagnetic radiation by spin active nuclei (having nuclear spin not equal to zero) when they are placed in a magnetic field. The energy associated with NMR experiments is incapable of disrupting even the weakest chemical bonds. Nuclear magnetic resonance spectroscopy pertains to nuclei and only one type of nucleus at a time, e.g., all 1H, 13C or 15N nuclei. When the frequency of the rotating magnetic field and that of the processing become equal, they are said to be in resonance and absorption or emission of energy by the nucleus

can occur. A plot of the peak intensities versus the frequencies of absorption constitutes an NMR spectrum.

APPLICATIONS USED (1H, COSY, HSQC, HMBC and NOESY)

^{1}H-NMR: The 1H nucleus is by far the most commonly studied by NMR spectroscopy because of its high natural abundance (99,98%) and the fact that it is invariably present in the majority of organic compounds (Pavia et al. 2014). Proton Magnetic Resonance (PMR) spectrum provides information about the number of different types of protons and regarding the nature of the immediate environment of each of them.

COSY: Shows which pairs of protons in a molecule that are coupled to each other showing 2JHH and 3JHH (most common). Correlated spectroscopy (COSY) pertain to coherent transfer of magnetization (through scaler coupling) and are particularly important for examining large biological molecules or polymers where both the extremely large number of resonances and severe overlapping of signals make stepwise (one dimensional) selective decoupling experiments impossible.

HSQC: Heteronuclear Single Quantum Coherence is used frequently in NMR spectroscopy of organic molecules and is of particular significance in the field of protein NMR. The resulting spectrum is two-dimensional (2D) with one axis for proton (1H) and the other for a hetero nucleus (an atomic nucleus other than a proton), which is usually 13C or 15N. The spectrum contains a peak for each unique proton attached to the hetero nucleus being considered so it shows 1JCH.

HMBC: Heteronuclear Multiple Bond Correlation experiment gives correlations between carbons and protons that are separated by two, three, and, sometimes in conjugated systems, four bonds (3JC-H > 2JC-H > 4JC-H > 5JC-H) the J coupling in H-C J stands for «the elastic potential difference between the linear and nonlinear elastic bodies with the same geometric variables». Direct one-bond correlations are

suppressed. This gives connectivity information much like a proton-proton COSY.(Enerstvedt 2018; Pavia et al. 2014)

NOESY: Nuclear Overhauser Effect Spectroscopy is a two-dimensional spectroscopy method that makes use of the overhauser effect (Pavia et al. 2014). COSY and NOESY are quite similar, but COSY only shows through-bond interactions shown in cross peaks, while NOESY also shows cross peaks that arise through-space interactions. An important note is that in practice the through-space interaction must be within 5 **Å**. An example of the through-space effect shown in spectra would be how two different cross peaks appear in the figures shown below (Pavia et al. 2014). In figure A the cross peak occurs between a methyl group and an N-H signal, which creates a cross peak between the signals 8.8ppm (N-H) and 2.13 ppm (C-H) while in figure B the cross peak is between 7.49 ppm(aromatic) and 2.13 ppm(C-H).

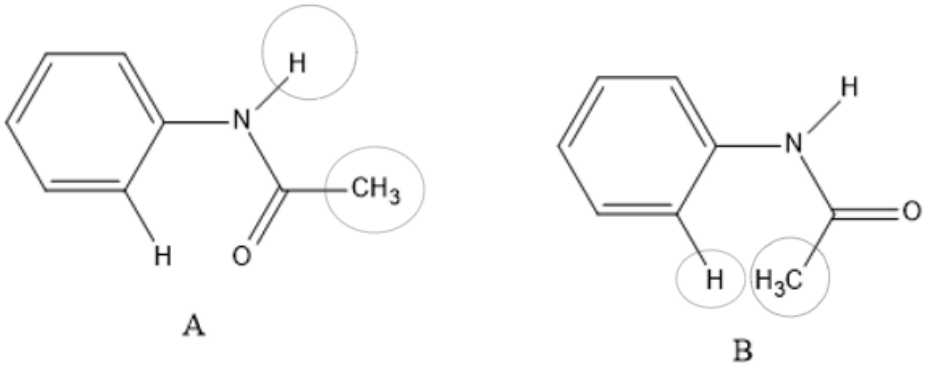

Figure 2.7.1: Isomeric structures with highlighted areas that create differing cross peaks during NOESY (Pavia et al. 2014).

3. **Results.**

Aqueous methanol (60:40) was used for extraction. Preliminary extraction was performed on the stem, leaves and flowers of *Plantago maritima* separately.

3.1. **HPLC**

After extraction HPLC was performed. The figures below show differing concentration of compounds, but the profiles overlap neatly, meaning that the compounds in the different parts are mostly the same.

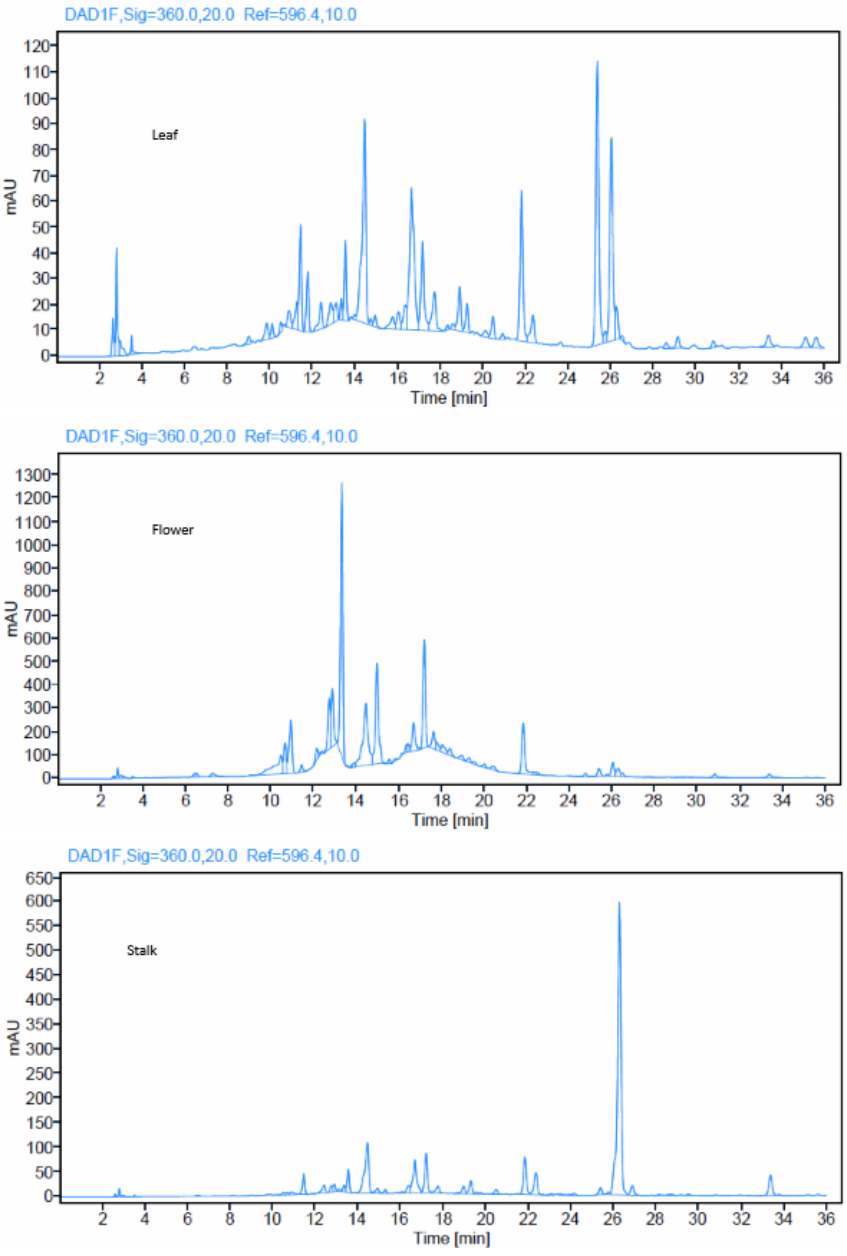

Figure 3.1.1: Aligned HPLC chromatograms (recorded at 360±20nm) of P. maritima extract from flower (top), leaf (middle) and stalk (bottom).

Given that the three separate parts mostly contain the same compounds, the parts were combined during a larger extraction.

After initial HPLC analysis it was decided to wash the sample using gravimetric column separation, the column being packed with XAD-7. The purified sample was run through preparative HPLC, 41 vials were collected and analyzed using HPLC.

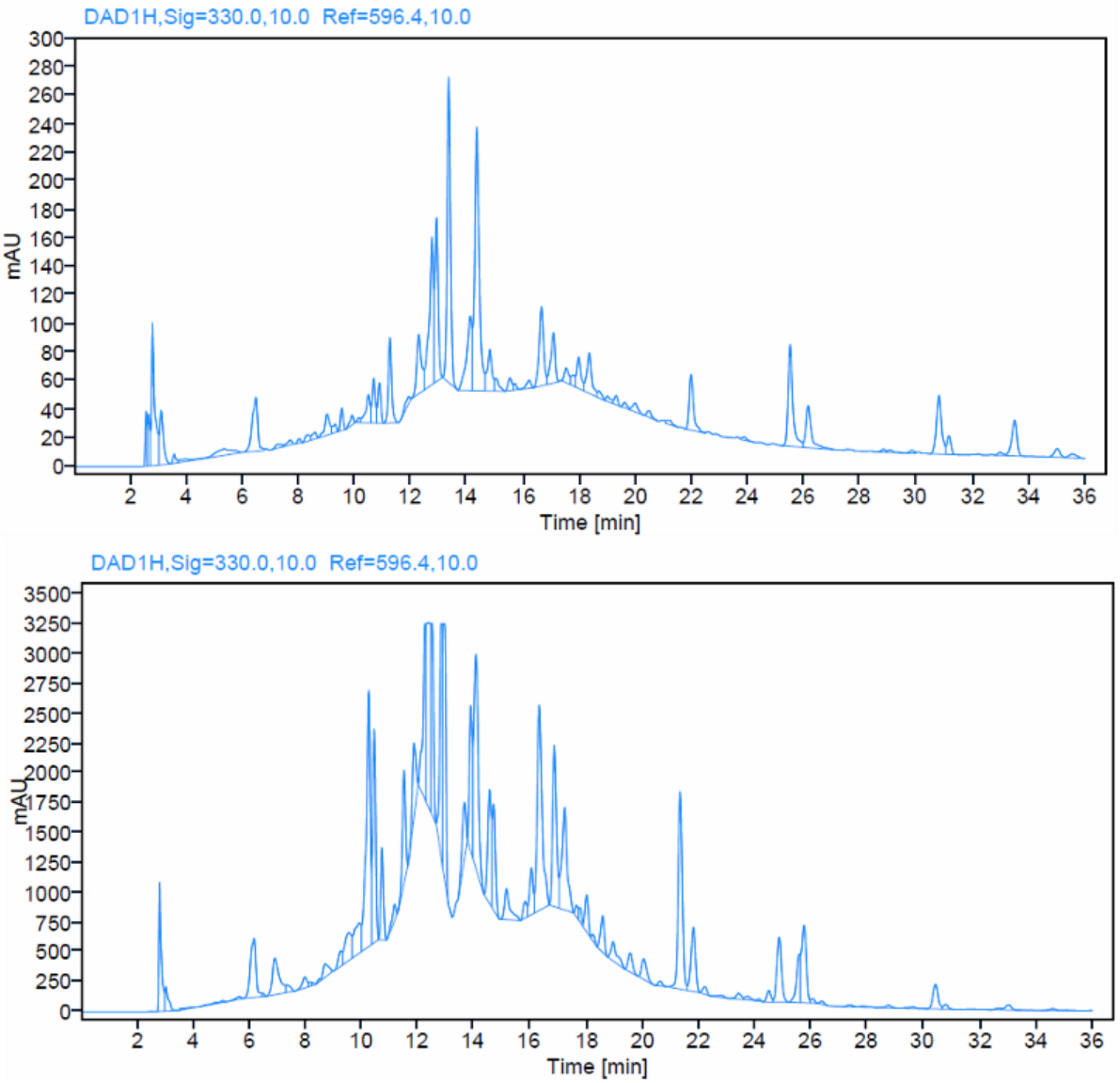

Figure 3.1.2: Aligned HPLC chromatograms (recorded at 330±10nm) of crude *P. maritima* extract (top) compared to a XAD-7 purified *P. maritima* extract (bottom). The increased phenolic purity is observed from the higher relative intensities (mAU) seen from the XAD-7 purified extract (bottom) compared to the crude extract (top).

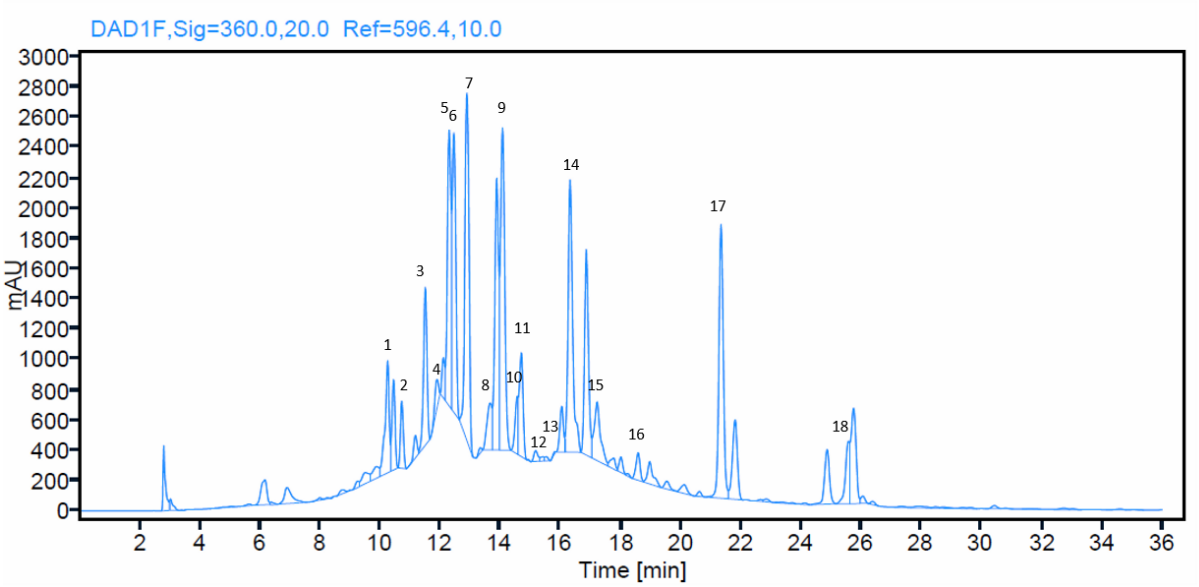

Figure 3.1.3: HPLC chromatogram of XAD-7 purified crude sample showing compounds found and (tentatively) identified.

Table 3.1.1: list of compounds found and tentatively confirmed from XAD-7 purified crude extract of *P. maritima*. Compounds known to be in *P. maritima* are highlighted in grey.

No.	Component	Crude Rt HPLC
1	plantamajoside	10.232
2	apigenin glucoside	10.706
3	luteolin 7 glucoside	11.493
4	campneoside I	11.846
5	tricin diglucoside	12.272
6	nepitrin (6-methoxylutelin glucoside	12.437
7	luteolin glucuronide	12.926
8	quercetin arabinoside	13.866
9	diosmetin rutinoside	14.046
10	verbacoside	14.532
11	tricin glucoside	14.679
12	rosmarinic acid	15.139
13	apiin (Apigenin 7-apioglucoside)	15.806
14	luteolin	16.306
15	martynoside	17.206
16	apigenin	18.559
17	diosmetin/chrysoeriol	21.319
18	tricin	25.559

3.2. Preparative HPLC.

After extraction, HPLC analysis of each part (leaf, stem and flower) was preformed, it was concluded that separating the parts was unnecessary because the parts contained mostly the same compounds but with varying concentrations. A large extraction was done in one sample. HPLC analysis of main sample showed the necessity to wash the sample to eliminate unnecessary compounds. Once XAD-7 purified, preparative HPLC was performed on the sample.

Table 3.2.1: Overview of the preparative (prep.) HPLC fractions (1-43) and their time of collection. The table also shows the analytical HPLC retention times of the collected preparative fractions (Rt) (example prep 17 figure 3.2.1).

Prep No.	Prep. time(min)	Analytical LC, Rt (min)	Prep No.	Prep. time(min)	Analytical LC, Rt (min)	Prep No.	Prep. time(min)	Analytical LC, Rt (min)
1	8-9	7,5-13	16	22.8-24	12-15	31	35-35.5	17-20
2	9-10	10-13	17	24-25	12- 17	32	35.5-36.9	18-20
3	10-11	10-13	18	25-25.8	13-17	33	36.9-38.1	19-22
4	11-12	10-13	19	25.8-27	14-18	34	38.1-39.5	20-23
5	12-13	10-13	20	27-27.7	13-18	35	39.5-40	21-24
6	13-14	10-13	21	27.7-28.5	14-18	36	40-40.5	21-26
7	14-15	10-13	22	28.5-29.8	14-18	37	40.5-41	25-27
8	15-16	10-14	23	29.8-30	14-18	38	41-41.9	25-27
9	16-17	10-15	24	30-30.8	15-18	39	41.9-42.4	25-27
10	17-18	10-14	25	30.8-31	16-18	40	42.4-43.5	25-27
11	18-19	10-14	26	31-33.8	16-19	41	43.5-44.6	25-27
12	19-19,5	10-15	27	33.8-34	16-20	42	44.6-45.5	-
13	19.5-20.5	11-15	28	34-34.4	17-20	43	45.5-46	-
14	20.5-21.9	12-15	29	34.4-34.9	17-20			
15	22-22.8	12-15	30	34.9-35	17-20			

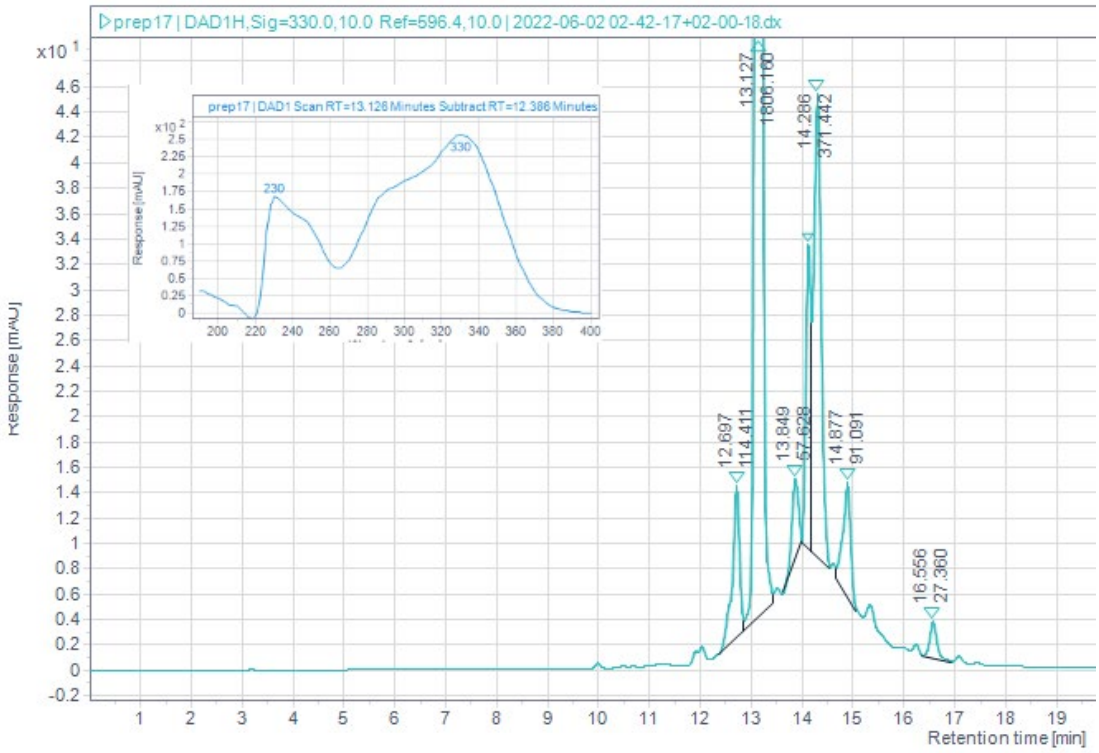

Figure 3.2.1: HPLC of prep 17 and UV spectrum (330 nm) of the major peak (Rt 13.13 min). The major peak is tentatively confirmed to contain plantamajoside (UVmax 330, local UV 230).

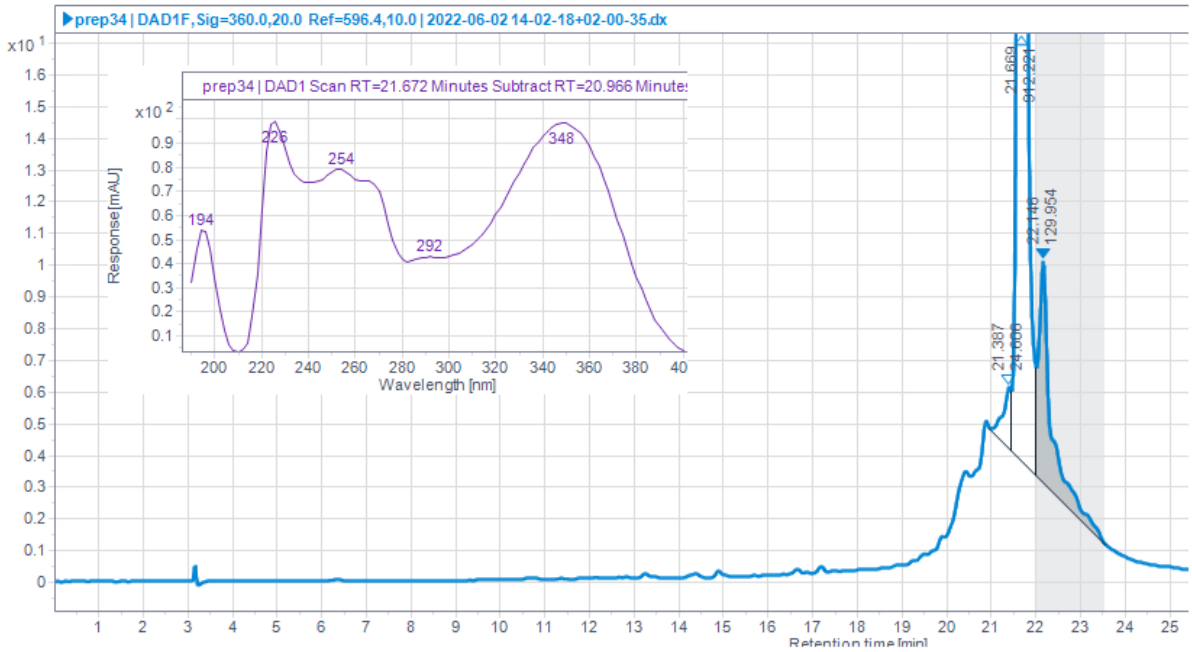

Figure 3.2.2: HPLC of prep 34 and UV spectrum (348 nm) of the major peak (Rt 21.67 min). The major peak is tentatively confirmed to contain luteolin (UVmax 348, local UV 254).

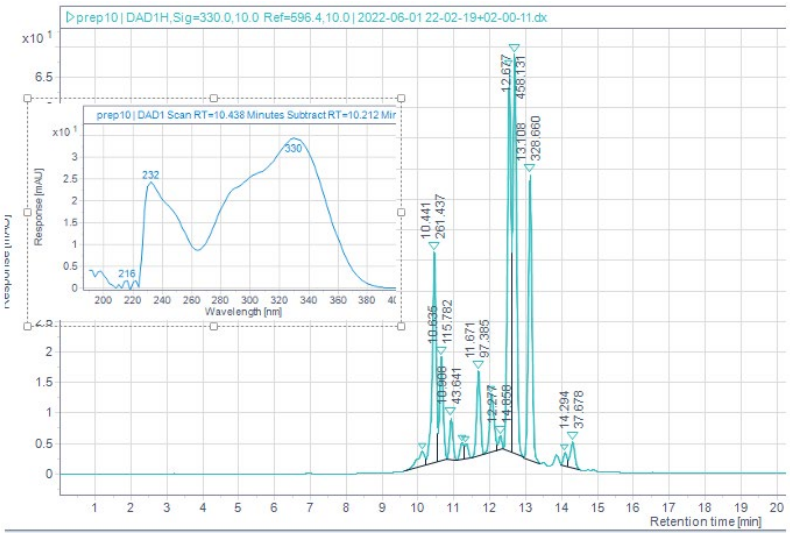

Figure 3.2.3: HPLC of prep 10 and UV spectrum (330 nm) of the minor peak (Rt 10.44 min). The minor peak is tentatively confirmed to contain campneoside I (UVmax 330, local UV 232).

Figures 3.2.1-3 are respectively examples of medium (prep 17), low (prep 34) and high (prep 10) number of varying compounds.

Table 3.2.2: overview of measured UV in prep samples, compared to reference UV of compounds assumed to be contained in mentioned prep sample. Compounds known to be in *P. maritima* are highlighted in grey.

Compound	Prep	Reference UV (nm)	Measured UV (nm)
luteolin	34	347 267 255	348 254
apigenin	37	337 269 212	338 268 212
tricin	37	349-346 269	350 266
diosmetin/chrysoeriol	39	348 292 268 252	348 266
apigenin glucoside	5	335 269 254	336 274
quercetin arabinoside	14	354 255	350 254 (raw 352 256)
luteolin 7-O-glucoside	22	349 254sh 205	348 266
nepitrin	23	346 272 255	348 270 256
luteolin glucuronide	23	348 266sh 256 205	348 266sh
tricin glucoside	24	341 269 253	342 266
tricin diglucoside	22	351 265-270	350 264
diosmetin rutinoside	22	348 268 252	348 252
apiin (apigenin 7-apioglucoside)	24	335 272	334 290
rosmarinic acid	24	329 287 sh	328
plantamajoside	17	332	330
verbascoside	18	330	330
campneoside I	10	332 296sh	330
martynoside	25	330 287 220	332 206

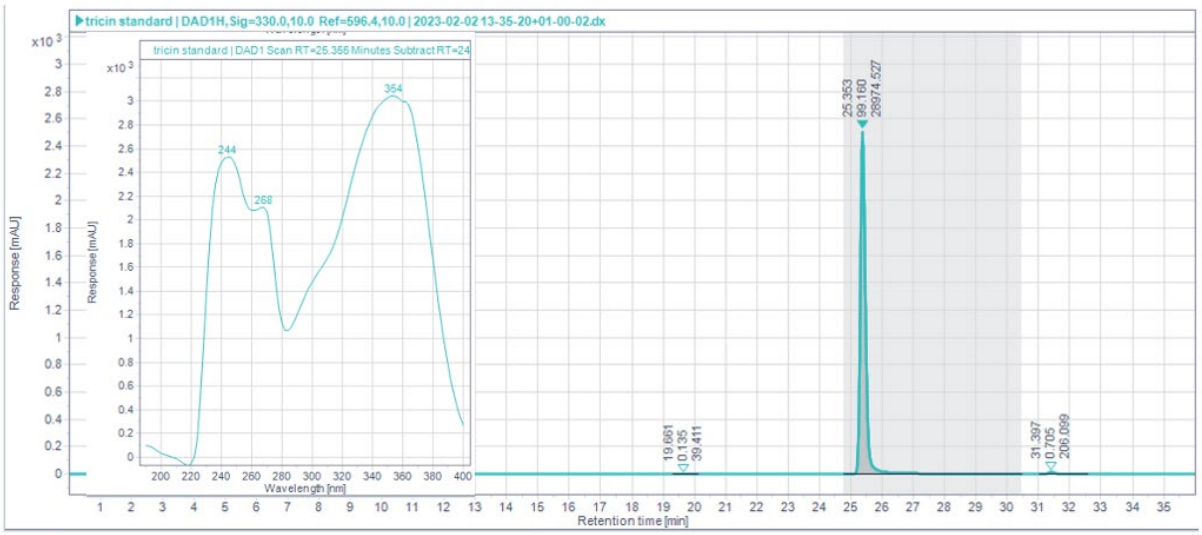

Figure 3.2.4: HPLC chromatogram and UV spectrum of reference sample tricin.

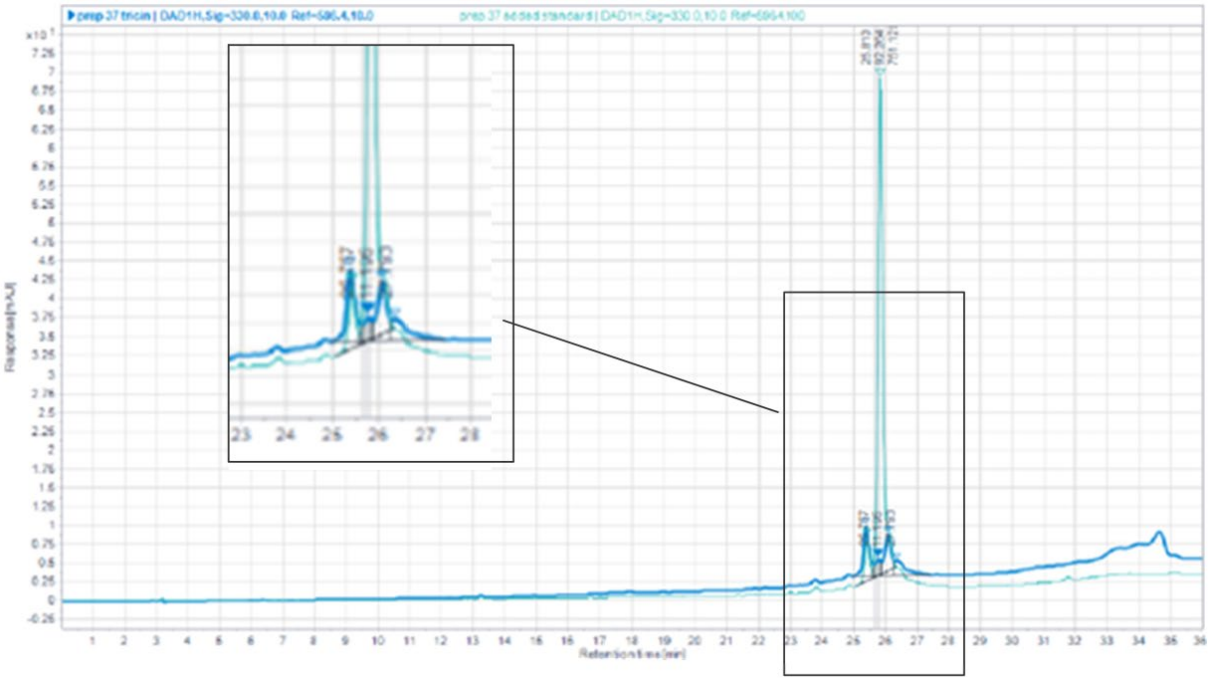

Figure 3.2.5: HPLC co - chromatogram of overlaid prep 37 with and without tricin standard added.

Reference UV values for tricin are 349-346 nm and 269 nm, tricin standard sample gave UV values of 352 nm and 269 nm. The Rt value for the peak suspected to be tricin is 25.756 minutes while Rt for the standard sample is 25.811 minutes.

3.3. **LC-MS.**

LC-MS was run for the HPLC samples whose UV spectrum indicated that the sample might contain a UV active polyphenolic compound. The LC-MS is configured with an UV DAD that reads UV of the sample roughly ten seconds before the TIC of the sample is read. Using this the TIC peaks of interest were picked out by verifying whether the peaks had a UV peak that was slightly ahead of the TIC. By reading the UV spectrum of the LC-MS and comparing it visually to the UV spectrums from HPLC it was decided whether the peaks match between HPLC and LC-MS.

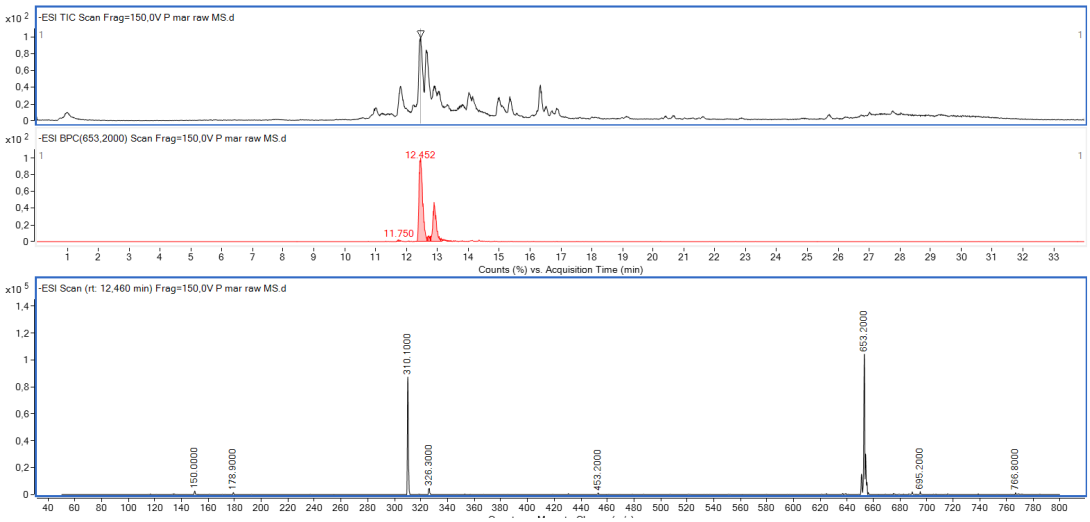

Figure 3.3.1: Illustration of large content present (l), UV active, campneoside I with m/z⁻ 653.2.

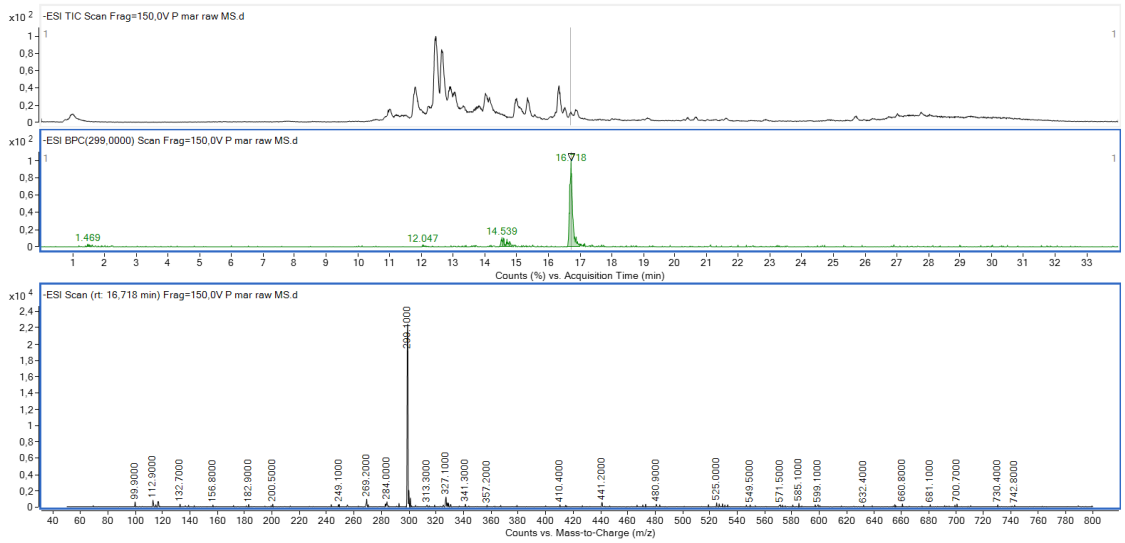

Figure 3.3.2: Illustration of medium content present (m), UV active, diosmetin with m/z⁻ 299.

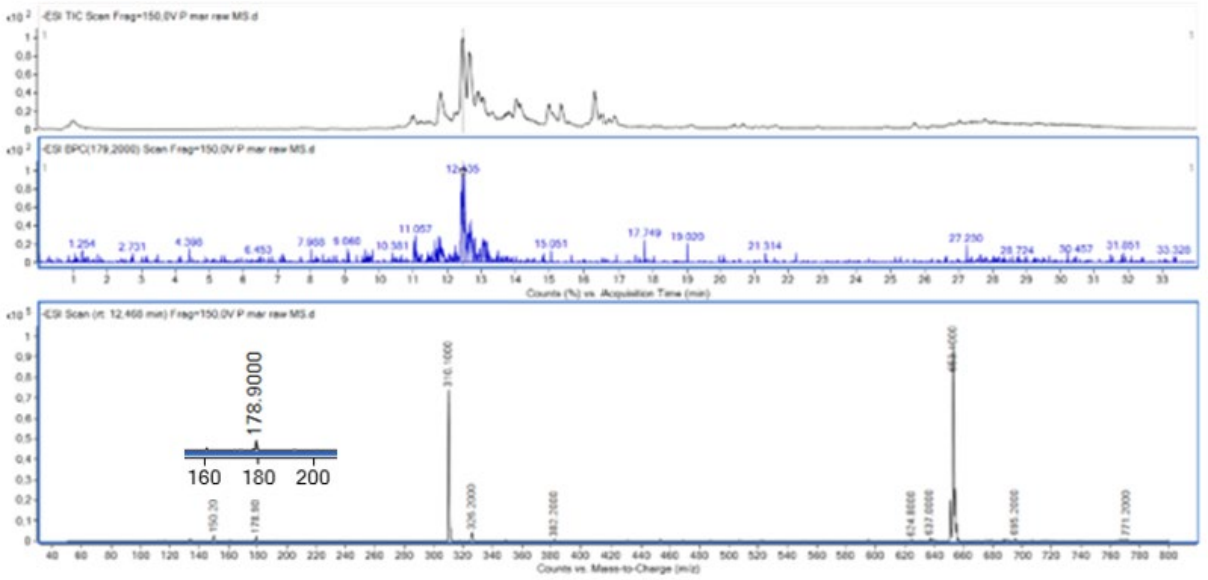

Figure 3.3.3: Illustration of trace amounts preset (t), UV active, caffeic acid with m/z$^-$ 178.8.

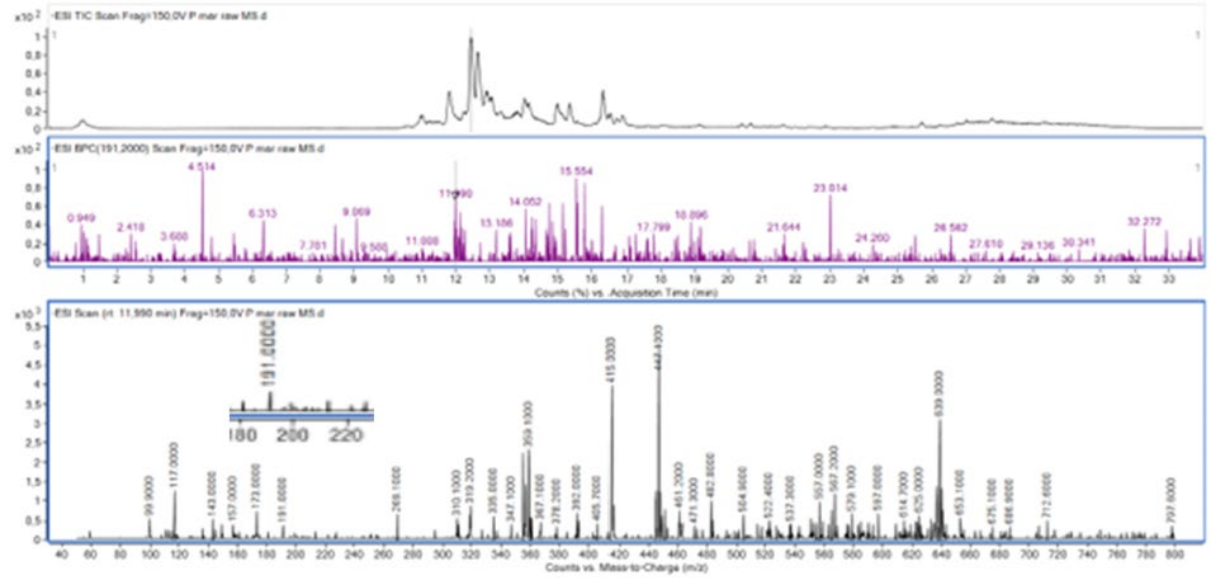

Figure 3.3.4: Illustration of not detected (nd), quinic acid scan for m/z$^-$ 191.2.

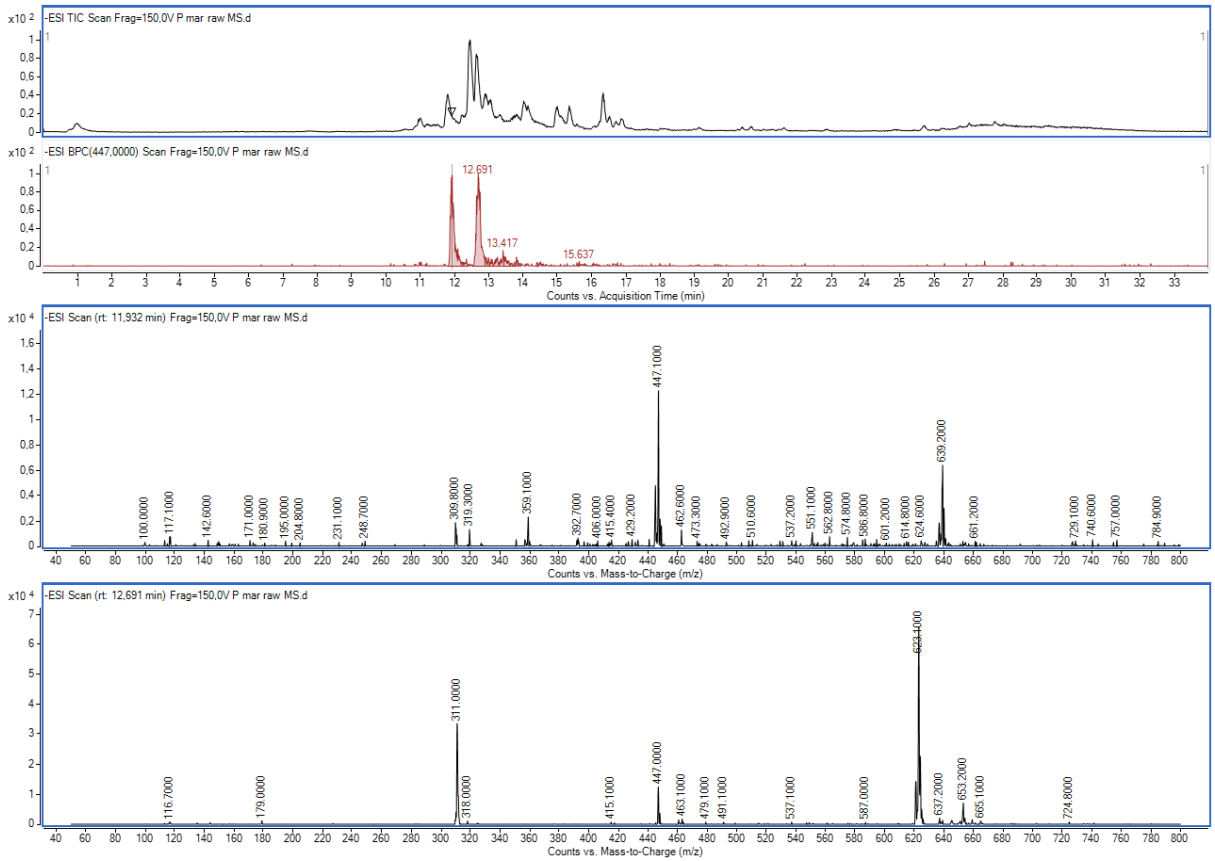

Figure 3.3.5: Illustration of 2 components with same weight (m/z^- 447) but different Rt times (11.932 and 12.691).

Table 3.3.1: Component list earlier found in the *Plantago* genus. Trace amounts present – t, medium content present – m, large content present – l, not detected – nd. All LC-MS samples were run only in ESI negative mode. Compounds known to be in *P. maritima* are highlighted in grey. * = same wight 2 components with different Rt present. luteolin-7-O-glucoside and luteolin-4'-glucoside

	***Plantago* species**	**Component**	**Weight**	**MS crude**
	depressa	protocatechuic acid	156.12	nd
	maritima	*p*-coumaric acid	164.16	t
	lanceolata	gallic acid	170.12	t
	maritima	caffeic acid	180.16	t
	major	quinic acid	192.17	nd
	maritima	ferulic acid	194.18	t
16	*argentea*	apigenin	270.24	l
14	*maritima*	luteolin	286.24	l
	maritima	chrysoeriol	300.26	m
17	*maritima*	diosmetin	300.26	m
	major	quercetin	302.23	t
18	*phaeostoma*	tricin	330.29	m
	lagopus L	chlorogenic acid	354.31	nd
12	*lagopus L*	rosmarinic acid	360.3	t
	atrata	magniferin	422.3	t
2	*maritima*	apigenin-7-O-glucoside	432.4	m
8	*asiatica*	quercetin 3-O-arabinoside	434.3	l
3	*maritima*	luteolin-7-O-glucoside	448.4	m *
	ovata	luteolin-4'-glucoside	448.4	m *
	major	ursolic acid	456.7	nd
7	*phaeostoma*	luteolin 7-O-glucronide	462.4	t *
	psyllium	chrysoeriol 7- glucoside	462.4	t *
6	*major*	nepitrin	478.4	t
11	*crassifolia*	tricin 7-glucoside	492.4	m
	ovata	apigenin 4',7-Rhamnoside	562.5	t
13	*major*	apiin (Apigenin 7-apioglucoside)	564.5	m
9		diosmetin rutinoside	608.5	m
	argentea	rutin (quercentin 3-rutinoside)	610.5	t
	psyllium	chrysoeriol 7-gentiobioside	624.5	m *
10	*maritima*	verbascoside	624.6	l *
1	*maritima*	plantamajoside	640.6	l
15	*lanceolata*	martynoside	652.6	m
4	*depressa*	campneoside I	654.6	l *

5		tricin 5-7-diglucoside	654.6	l *
	lanceolata	new phenylethanoid glycoside	756.25	t

Below is a figure (3.3.6:) which show the structure of the new phenylethanoid glycoside found in *Plantago lanceolata* with a weight of 756.25 g/mol(Budzianowska and Budzianowski 2022). The speculated structure was created in the same research document that first found the new compound.

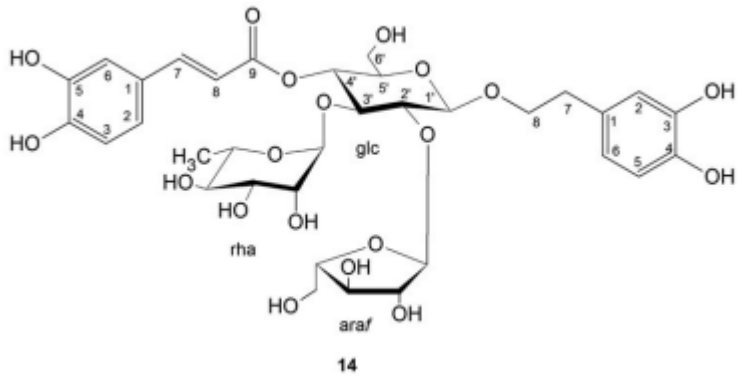

Figure 3.3.6: New phenylethanoid glycoside (copy from (Budzianowska and Budzianowski 2022))

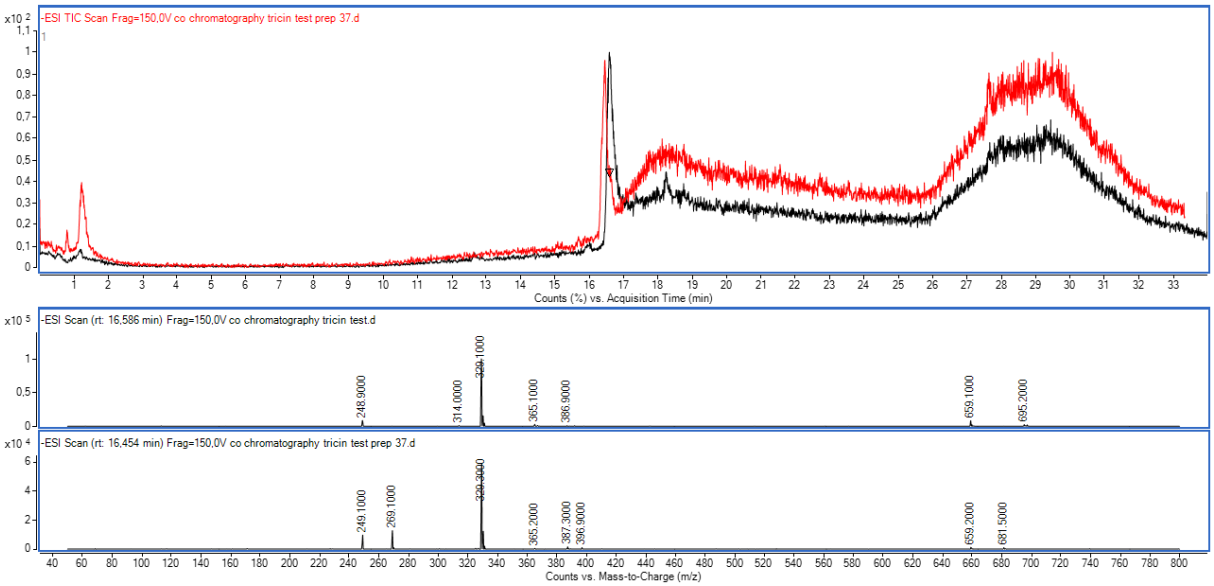

Figure 3.3.7: LC-MS co - chromatography of tricin standard sample (black) and prep 37 (red), m/z$^-$ 329.1(Tricin) and m/z$^-$ 329.3 (prep 37). Rt is 16.586 (Tricin) and 16.454 (prep 37).

3.4. LC-MS/MS to check glycosylated state of suspected flavonoids.

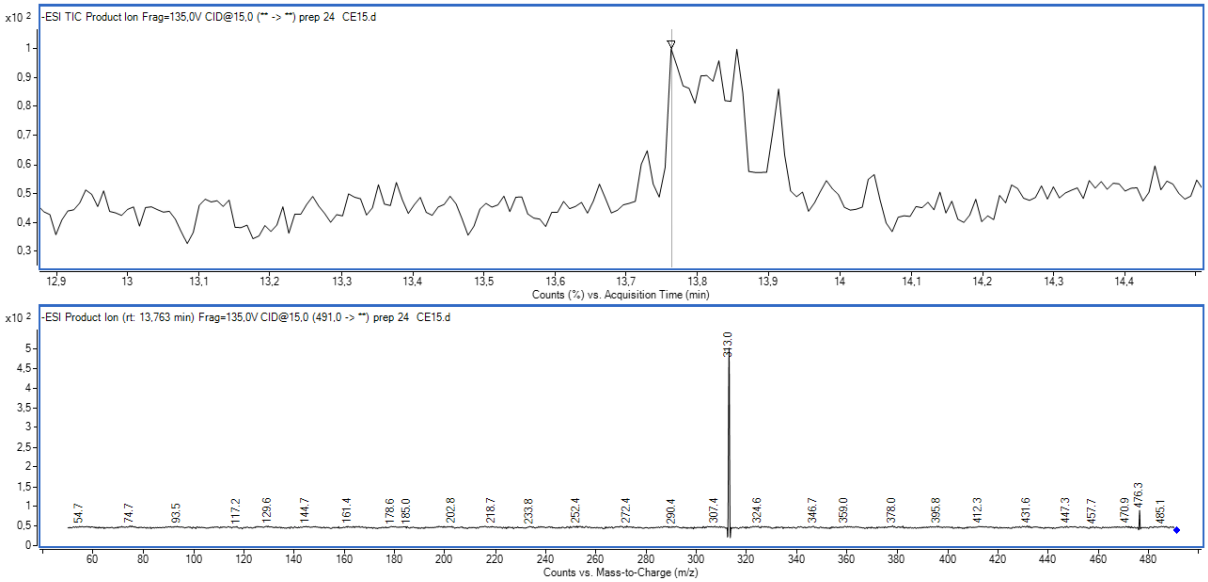

Figure 3.4.1: LC-MS/MS CE 15 tricin with glucose removed.

Tricin glucoside (11).

A sample of prep 24 previously assumed to contain tricin glucoside (11) with a molecular weight of 492.4 g/mol was run on LC-MS/MS to remove the glucoside.

Figure 3.3.7 shows a success in removing the glucoside, having lost a m/z$^-$ 178.1 (mass loss) leaving behind a fragment with m/z$^-$ 313. A fragment with m/z$^-$ 313 is what is assumed to appear if glucoside is removed and tricin is left behind.

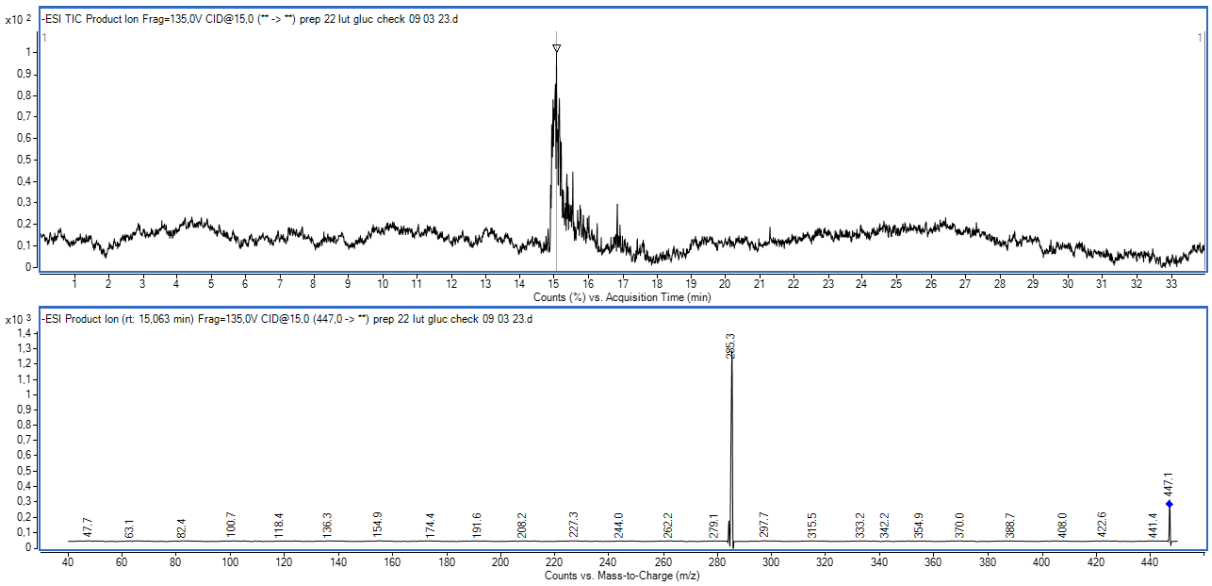

Figure 3.4.2: LC-MS/MS of prep 22 checking for luteolin7-O- glucoside (3).

Luteolin7-O- glucoside (3).

Using MS/MS on prep 22 assumed to contain luteolin 7-O-glucoside (m/z^- = 447), -ESI gave a fragment of m/z^- = 285.3 which means a mass loss of 161.7 corresponding with a loss of glucoside. This data fits the assumption of prep 22 containing luteolin glucoside as luteolin in -ESI will show a m/z^- = 285, the mass loss of 161.7 fits despite glucose having a MW of 180 because during fragmentation in this occasion the oxygen bonding luteolin and glucose together stayed with the luteolin fragment. By combining all the data, it is tentatively confirmed that *P. maritima* contains luteolin glucoside.

Tricin diglucoside (5).

Using MS /MS on prep 22 (Figure A 21) assumed to contain tricin diglucoside (m/z^-= 653.1), -ESI gave a fragmentation with a fragment mass of 329.2 and tricin is known to have m/z^- = 329. The mass of the lost fragment is 323.9, which one of the predicted possible fragments values of diglucoside. By combining all the data, it is tentatively confirmed that *P. maritima* contains tricin diglucoside.

Nepitrin (6).

Using MS MS on prep 22 (Figure A 22) assumed to be containing nepitrin (nepetin glucoside) (m/z^-= 477.1). -ESI gave fragmentation where the main fragment has m/z^- = 314.2 which fits expectations as this mass corresponds to nepitrin (methoxyluteolin) which has a MW of 316.2 g/mol. The mass loss is 163 which is as expected loss of glucoside. By combining all the data, it is tentatively confirmed that *P. maritima* contains nepitrin.

Luteolin glucuronide (7).

Using MS MS on prep 24 (Figure A 23) assumed to contain luteolin glucuronide (m/z^- = 461), – ESI fragmentation gave signals at 299.5, 298, 255.1 and 284.8 m/z^-. of these fragments, 284.8 m/z^- is the one of interest as this confers a mass loss of 176.2 which corresponds to a loss of glucuronide and the remaining mass being luteolin. By combining all the data, it is tentatively confirmed that *P. maritima* contains Luteolin glucuronide.

Apiin (13).

Using LC-MS/MS on prep 24 (Figure A 24) assumed to contain apiin (m/z^-=563.1), - ESI fragmentation gave no signals. No signal was recorded from m/z^-=563.1. The LC-MS machine has been checked and the problem seems to be that the collision cell is not properly evacuating its content as intended. Troubleshooting proved that using MS/MS only yielded results some of the time. Both product ion scan and MRM were used to confirm the problem was in the machine. Possible solutions would have been to use HR QTOF MS/MS, but time restraints made this unviable.

Apigenin glucoside (2).

Using LC-MS/MS on prep 5 (Figure A 25) assumed to contain apigenin glucoside (m/z^-=431.1), - ESI fragmentation gave no signals. No signal was recorded from m/z^-=431.1. The same problems during analysis appeared as described in apiin.

Quercetin arabinoside (8).

Using LC-MS/MS on prep 15 (Figure A 26) assumed to contain quercetin arabinoside (m/z^-= 433.2), - ESI fragmentation gave no signals. No signal was recorded from m/z^-=433.2. The same problems during analysis appeared as described in apiin.

Diosmetin rutinoside (9).

Using LC-MS/MS on prep 22 (Figure A 27) assumed to contain quercetin arabinoside (m/z^-= 607), - ESI fragmentation gave only a signal at 607 m/z^- but no signal was found at the expected 299 m/z^- value. The same problems during analysis appeared as described in apiin.

3.5. NMR Nuclear Magnetic Resonance.

All samples deemed pure enough to attempt NMR on were run on 600 MHz at 23°C using DMSO-d_6 solvent.

Preparative sample 17 was dried and dissolved in DMSO – d_6 to be run on NMR. The data showed that the sample contained multiple compounds to the degree where certain signals from the compound of interest were hidden.

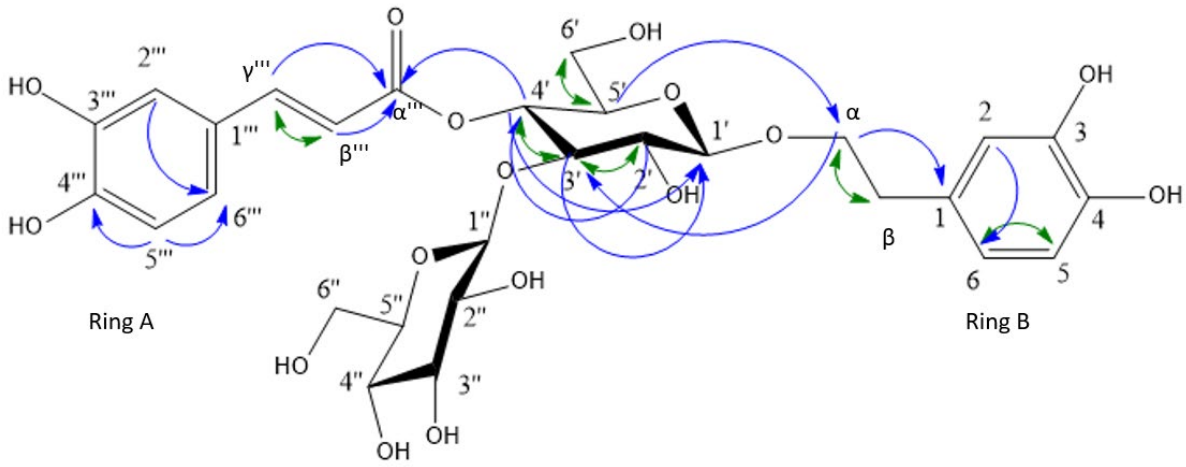

Figure 3.5.1: Proposed structure for major compound in prep 17 plantamajoside. Blue arrows illustrating HMBC data, arrows show H-C J3- H-C J5 signal correlation. All arrows start from a hydrogen and end at a carbon. Green arrows show COSY data. Figure framework referenced from (Arnold et al. 2002). Signal description shown in table 3.5.1.

Table 3.5.1: NMR data of signals from the major peak in prep 17, tentatively confirming plantamajoside. Table shows proton and carbon signals for the given marks. Marks reference in figure 3.4.1.

Proton ^{1}H	**δ ^{1}H (ppm)**	**δ ^{13}C (ppm)**	**Area**	**1H**	**Signal type**	**Neighbor ^{1}H/^{13}C (ppm)**	**HMBC ^{13}C (ppm)**	**Coupling constant J (Hz)**
H1	-	102						
H2	7.02	115	0.91	1	d		122	2.1
H3	-							
H4	-							
H5	6.76	116	1.47	1	d	6.97/122	122	8.2
H6	6.97	122	1.23	1	dd	6.76/116	116	8.3 2.1
Hβ	2.70	35	1.58	2	m	3.89/70.7	70.7 116	

Hα	3.89	70,7	1.38	2	m	2.70/35	35 102	
H1’	3.20	75		1				
H2’	3.69	79	0.62	1	s	4.35/102	70	
H3’	4.35	102	1.01	1	d	3.69 4.70	75	7.8
H4’	4.70	70	1.51	1	t	4.35/102	75 79 70.7 166	
H5’	3.10	72		1		0.95/18.7	70 70.7	
H6’	0.95	18.7	2.76	2	d	3.10/72	72	6.2
H1’’-H5’’	3.20-3.38	61-80		5	m			
H6’’	3.67	71	1.60	2	s		101	
Hα’’’	-	166						
Hβ’’’	7.45	146	1	1	d	6.19/114	114 166	15.8
Hγ’’’	6.19	114	1.01	1	d	7.45/146	146 166	15.9
H1’’’	-							
H2’’’	6.62	116.4	0.90	1	s		120 129.5	
H3’’’	-							
H4’’’	-	129.5						
H5’’’	6.63	115.7	0.80	1	d		120 129.5	4.8
H6’’’	6.49	120	0.92	1	dd		116.4	8.0 2.1

In acidic aromatic Oh-groups, the ^{1}H will be exchanged with deuterium in protic solvents such as methanol-d_4. The exchange leads to the aromatic OH signals disappearance from the spectrum due to falling out of the detectable range. During this thesis DMSO-d_6 is used as solvent for NMR which is a less protic solvent where the methyl groups of DMSO are only weakly acidic. It is however still possible for the OH signals to disappear due to H-D exchange with the solvent.

The placement of signal β’’’ (7.45 δ) is derived from the fact that it is the most deshielded signal, making it highly likely that this signal is close to the enoate. COSY shows that signal β’’’ is neighbor with signal γ’’’ (6.19 δ). Signal β’’’ has coupling constant 15.8 and signal γ’’’ has a coupling constant of 15.9. This indicates that both are in trans position.

Ring A (figure 3.5.1:) (1’’’-6’’’) is expected to have three signals at about the same value. The H signals in the ring are 5’’’,6’’’ and 2’’’.

Ring B (Figure 3.5.1:) (1-6) is supposed to have the same signal setup as ring A. The H signals in ring B are 2, 5 and 6. Signals 5 and 6 are neighbors as shown in figure 3.5.6.

HMBC shows connection between signals 2, 5 and 6.

The two-carbon chain from ring B to the glucose molecule with low chemical shift are assigned signal α and β, COSY shows α and β are neighbors. As shown in figure 3.5.1 there are two glucose molecules present in plantamajoside. The central glucose molecule has been elucidated. The signals in the middle glucose ring are 6’ (0.95 δ), 5’ (3.10 δ), 1’ (3.20 δ), 2’ (3.69 δ), 3’ (4.35 δ) and 4’ (4.70 δ). 3’ was found to be neighboring both signals 2’ and 4’ as shown by COSY in figure 3.5.7. Using COSY from figure 3.5.6 one can see that 6’ (0.95 δ) is neighbor to 5’ (3.10 δ).

Given the difficulty of elucidating glucose molecules without both COSY and TOCSY, the last molecule was not properly elucidated. An approximate elucidation for the central glucose molecule was done, the lower glucose molecule (connected to central glucose at C3’ (figure 3.5.1:)) contains signals 6’’ (3.67 δ) and 1’’-5’’ (3.20 δ - 3.38 δ).

Using HSQC (figure 3.5.5) to connect hydrogen signals to carbon signals, we get these connections: ^{1}H7.45 - ^{13}C146, ^{1}H 7.02 - ^{13}C 114, ^{1}H 6.97 - ^{13}C 122, ^{1}H 6.76 - ^{13}C 116, ^{1}H 6.63 - ^{13}C 115.7, ^{1}H 6.62 - ^{13}C 116.4, ^{1}H 6.49 - ^{13}C 120, ^{1}H 6.19 - ^{13}C 114, ^{1}H 3.89 - ^{13}C 70.7, ^{1}H 2.70 - ^{13}C 35, ^{1}H 0.95 - ^{13}C 18.7, ^{1}H 3.10 - ^{13}C 72, ^{1}H 3.20 - ^{13}C 75, ^{1}H 3.20/3.38 - ^{13}C 61/80, ^{1}H 3.67 - ^{13}C 71, ^{1}H 3.69 - ^{13}C 79, ^{1}H 4.35 - ^{13}C 102, ^{1}H 4.70 - ^{13}C 70.

By reading the H-NMR spectra, plantamajoside or verbascoside are both possible compounds. Both compounds have two glucoside molecules, given that only COSY was performed, and not also TOCSY, the order of the glucoside molecules and their coupling constants become hard to conclude.

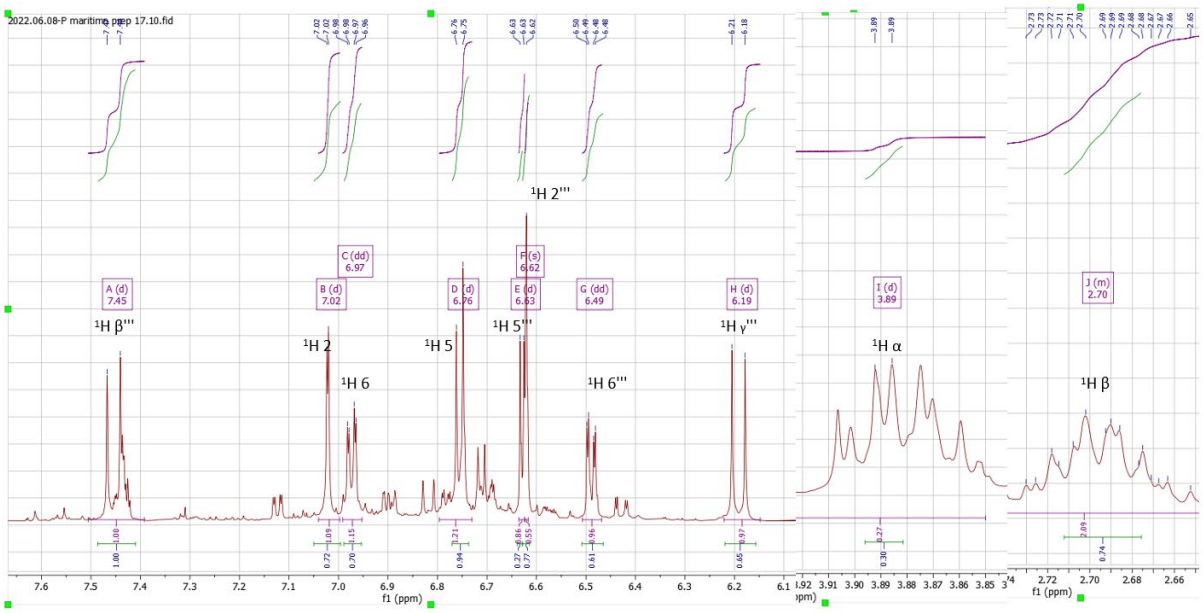

Figure 3.5.2: ^{1}H-NMR of prep 17 run on 600 MHz at 23°C using DMSO-d_6 solvent. By interpreting the signals in the aglycol area and the glucose area, it is possible to conclude that the signal pattern corresponds with plantamajoside.

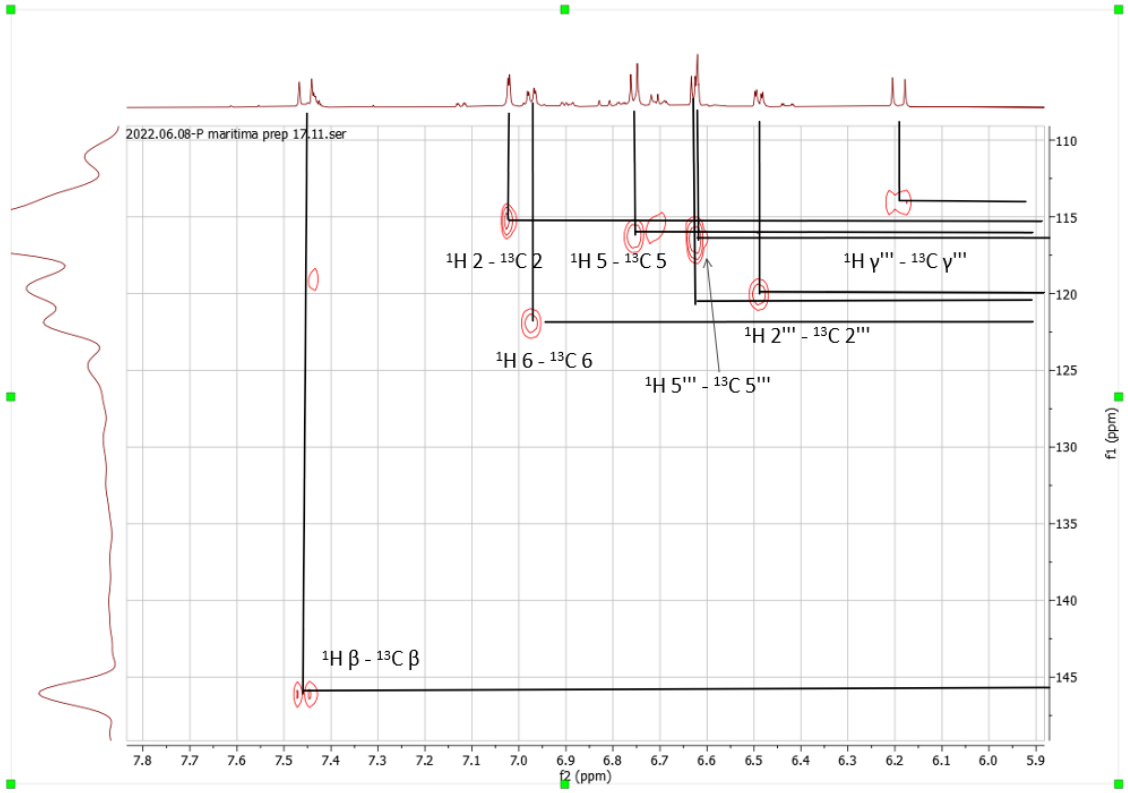

Figure 3.5.3: HSQC prep 17 aglycol area showing H-C 1J connection.

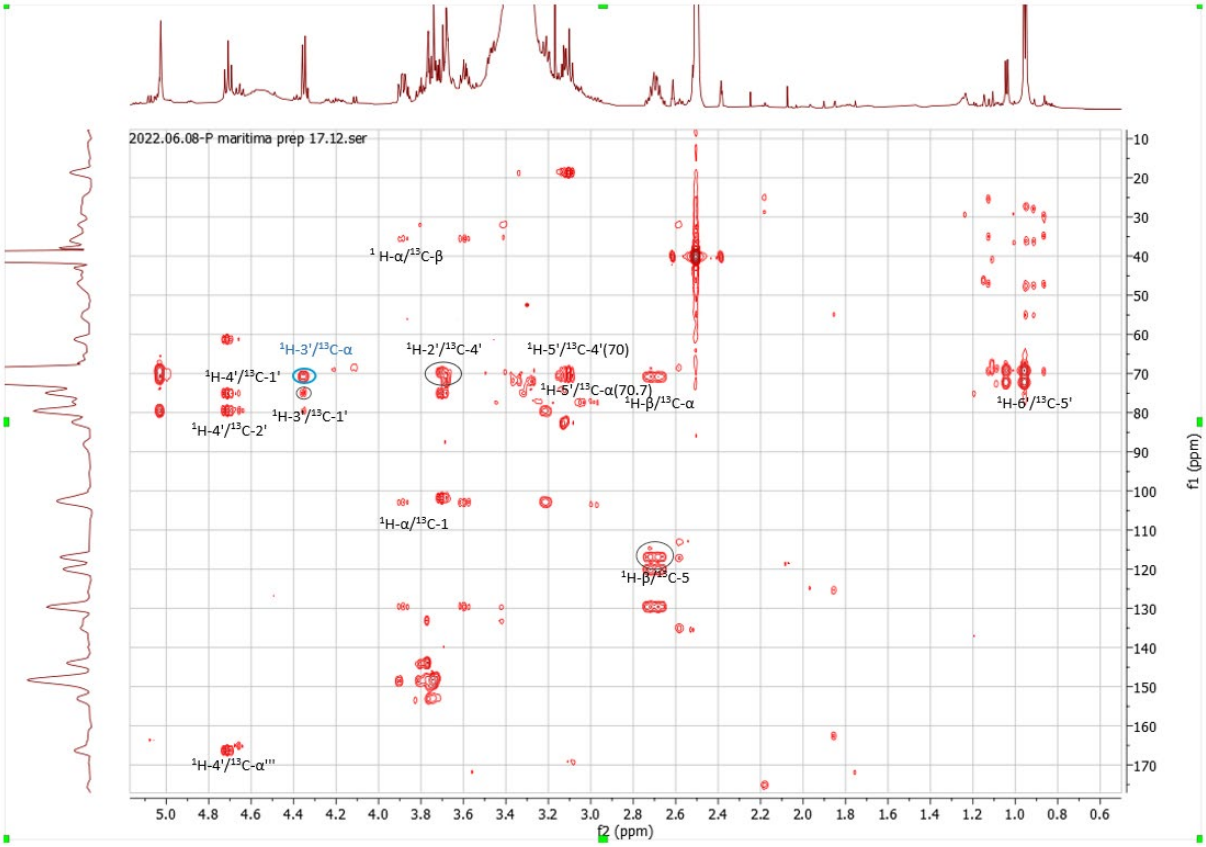

Figure 3.5.4: HMBC data of H-C J3-5 correlation of prep 17 between 0.5-5.5 ppm. Correlation written in table 3.5.1

HMBC shows that all parts of plantamajoside see the connections that is expected, except for ring A which does not connect to the γ''' area.

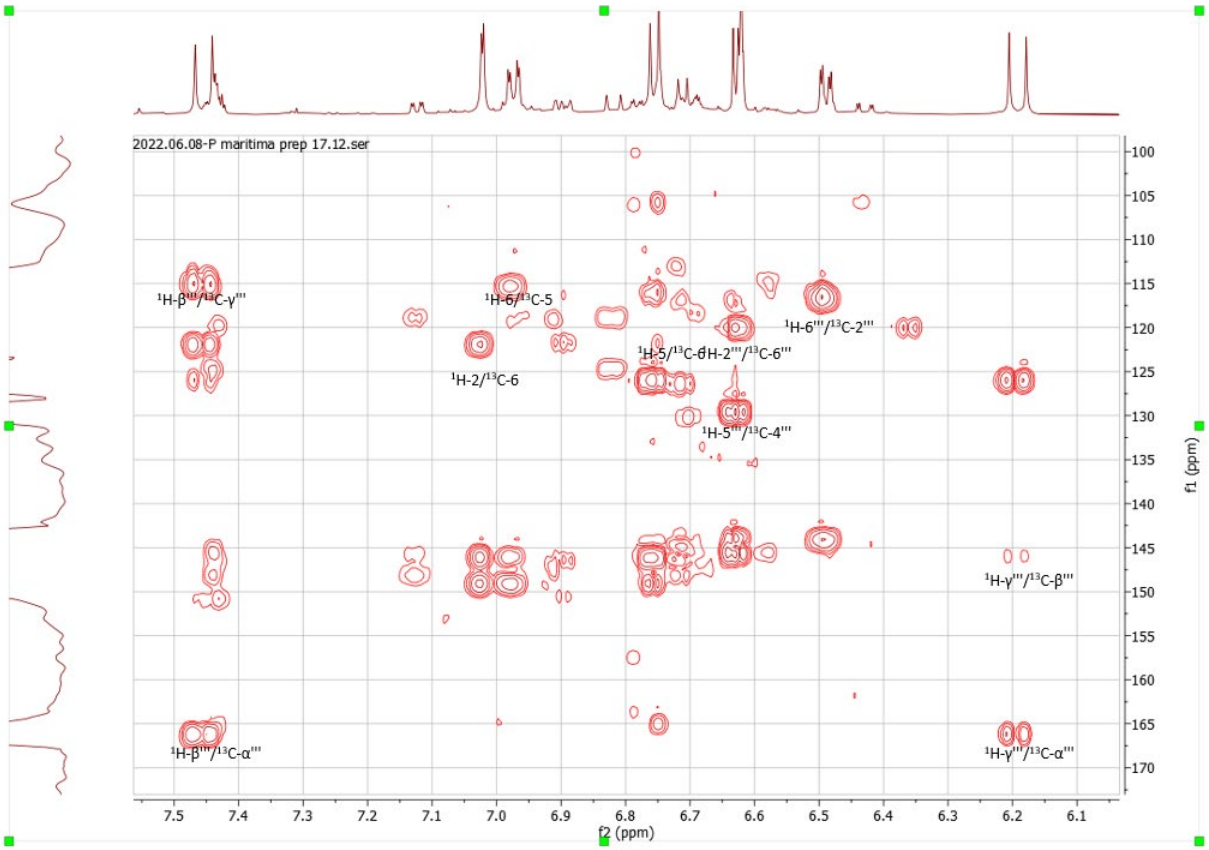

Figure 3.5.5: HMBC data H-C J3-5 correlation of prep 17 aglycol area LC-MS data shows several other components present in the sample, using this knowledge only relevant data was assigned and marked.

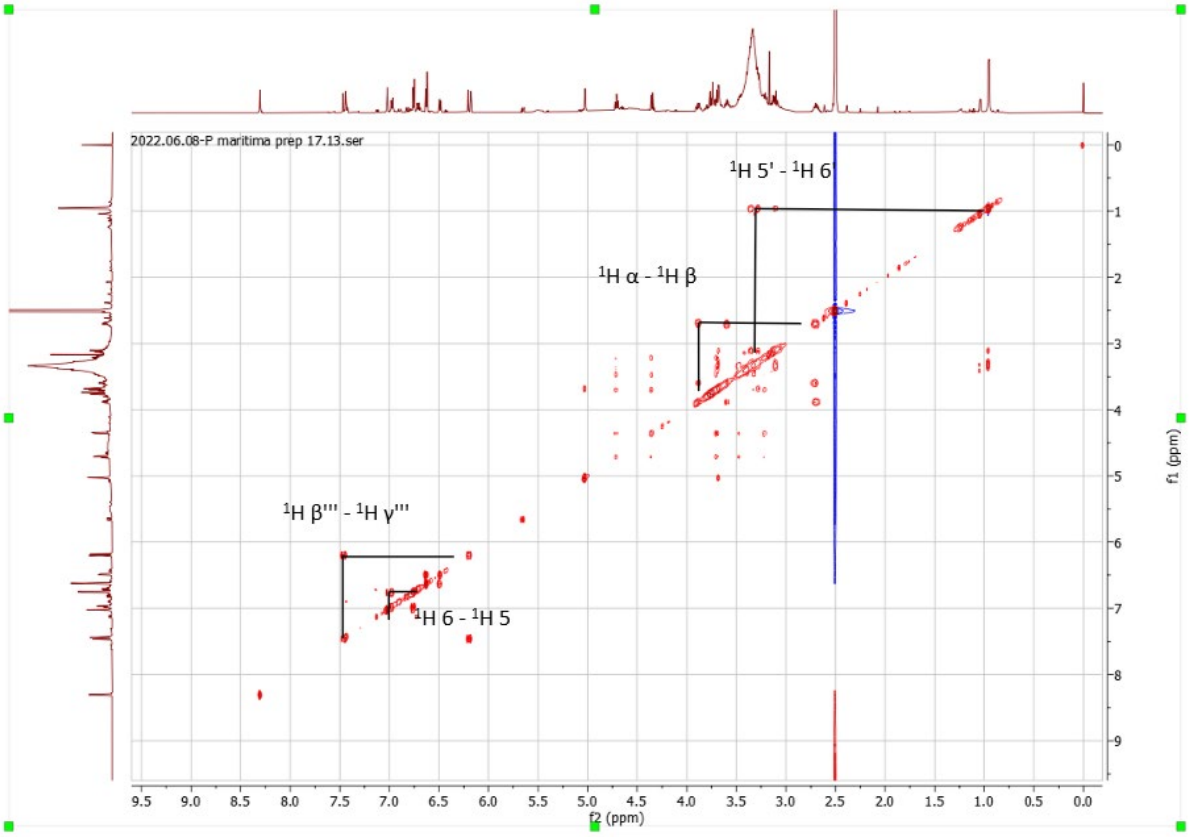

Figure 3.5.6: COSY prep 17 MR data from figure 3.5.6 shows four sets of neighboring protons, first set is 7.45 and 6.19, second set is 6.97 and 6.76, third set is 3.89 and 2.70 and lastly 3.10 and 0.95.

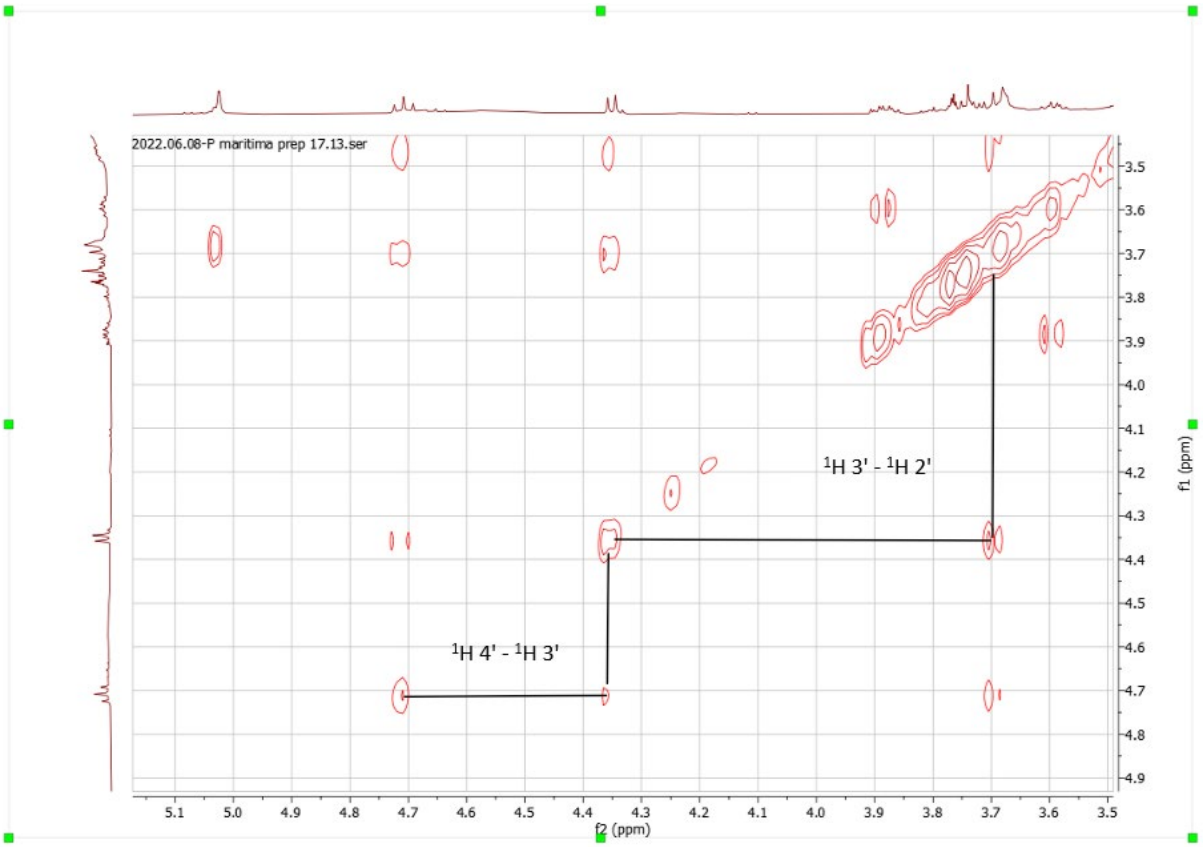

Figure 3.5.7: COSY prep 17 Shows that proton 4.35 is neighboring with both 3.69 and 4.70.

Prep 34 tentatively containing luteolin.

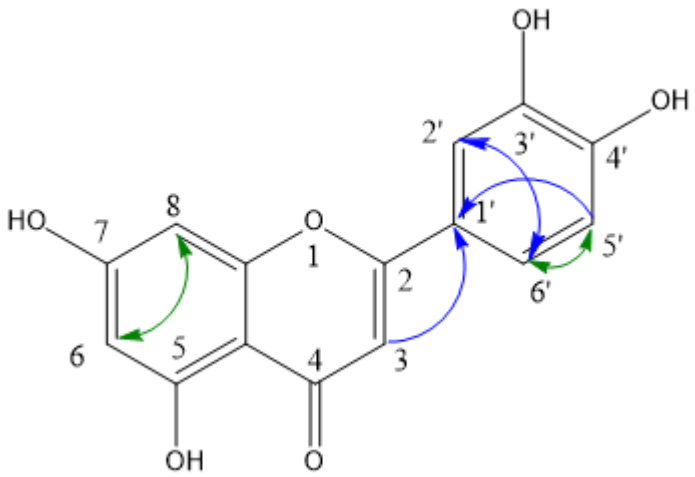

Figure 3.5.8: Proposed structure for major compound in prep 34 luteolin, green arrows showing COSY and blue showing HMBC data of H-C J3-5 correlation.

Table 3.5.2: NMR data from the major peak tentatively luteolin from prep sample 34.

Proton ^{1}H	δ ^{1}H (ppm)	δ ^{13}C (ppm)	Area	^{1}H	Signal type	Neighbor $^{1}H/^{13}C$ (ppm)	HMBC ^{13}C (ppm)	Coupling constant J (Hz)
1	-			0				
2	-			0				
3	6.67	103	1.53	1	s		104 122	-
4	-			0				
5	-			0				
6	6.44	94	1.27	1	d	6.18	99 104	2.1
7	-			0				
8	6.18	99	1.25	1	d	6.44	94 104	2,1
1’	-	122		0				
2’	7.40	114	2.02/2*	1	m		119	-
3’	-			0				
4’	-			0				
5’	6.87	118	1.29	1	d	7.40	110 122	-
6’	7.40	119	2.02/2*	1	m	6.87	114	-

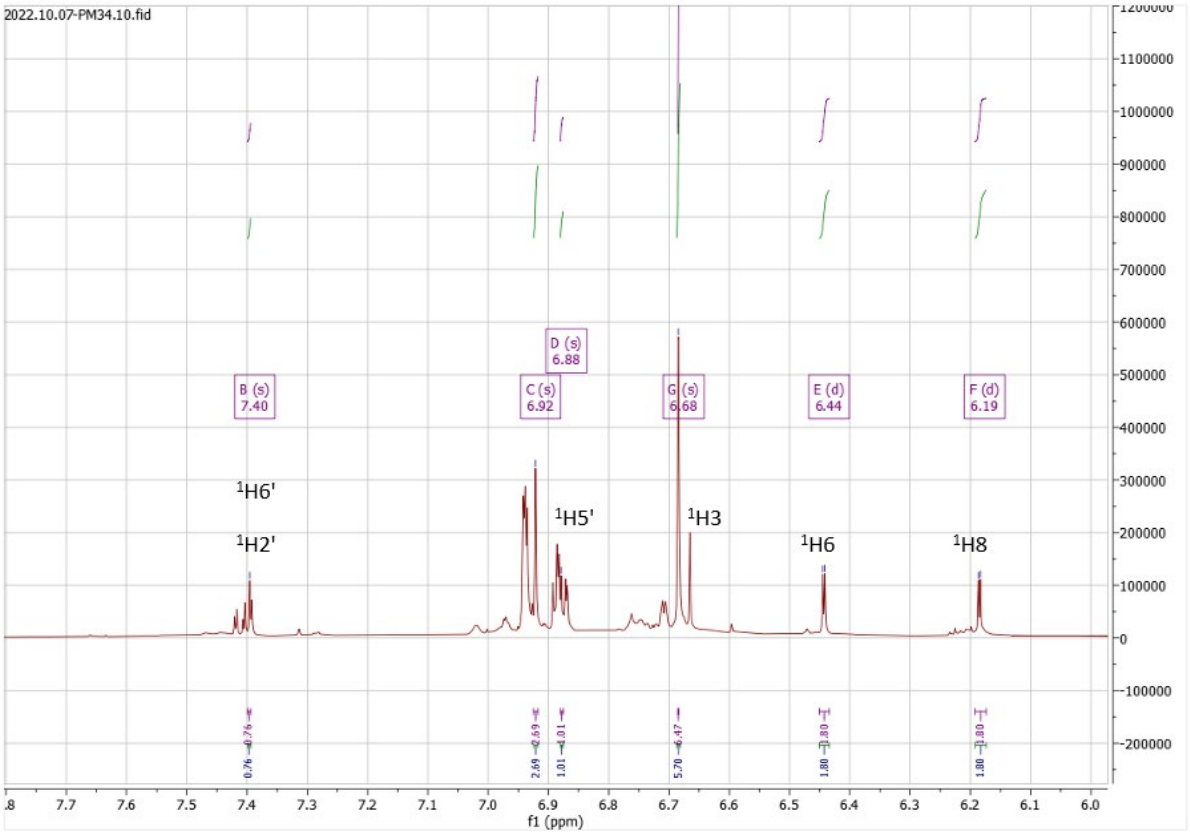

Figure 3.5.9: ^{1}H-NMR prep 34 run on 600 MHz at 23°C using DMSO-d_6 solvent in the aglycol area (6-8 ppm). The focus while interpreting NMR spectra was the aglycone

area (6-8 ppm). The were some other substances present in the sample, which gave extra signals, making the interpretation more difficult.

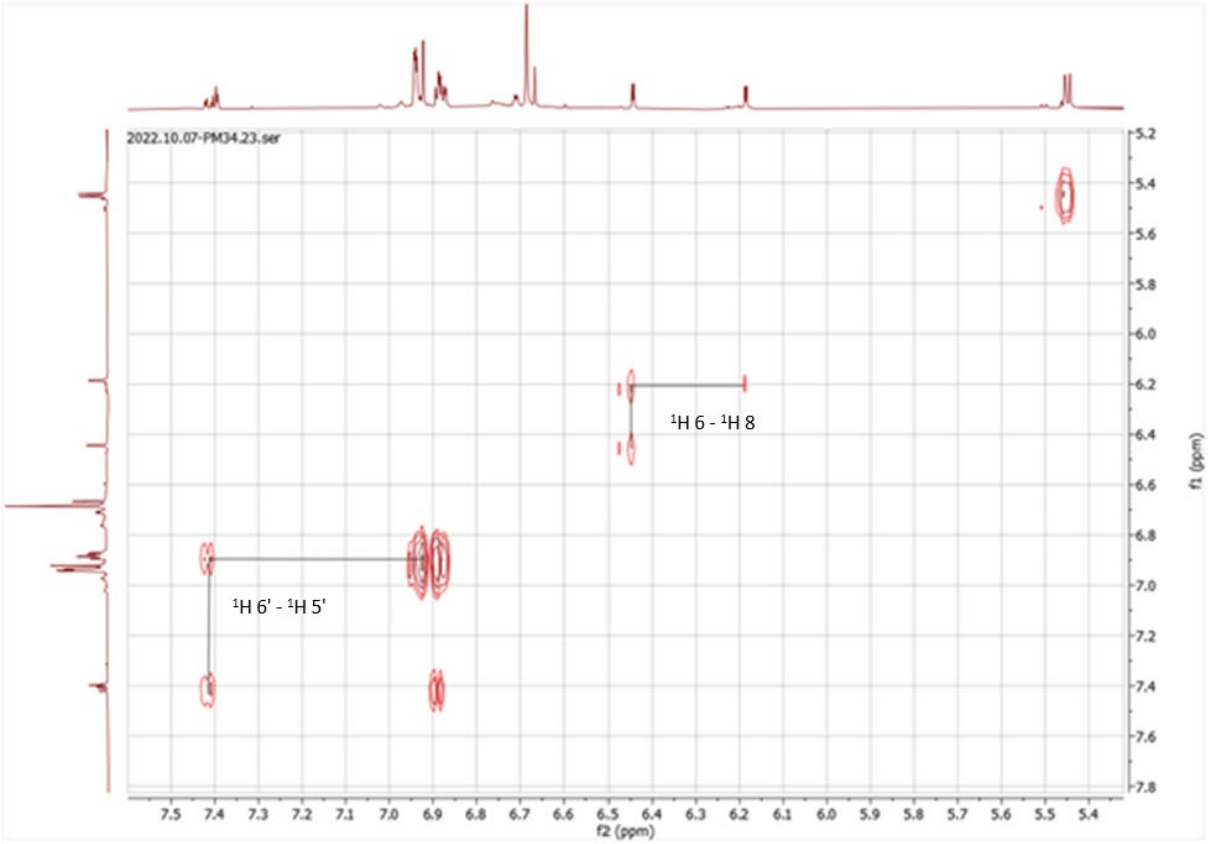

Figure 3.5.10: COSY of prep 34 showing that 6’ (7.40) are neighbors with 5’ (6.87) and 6 (6.44) is neighbor with 8 (6.18).

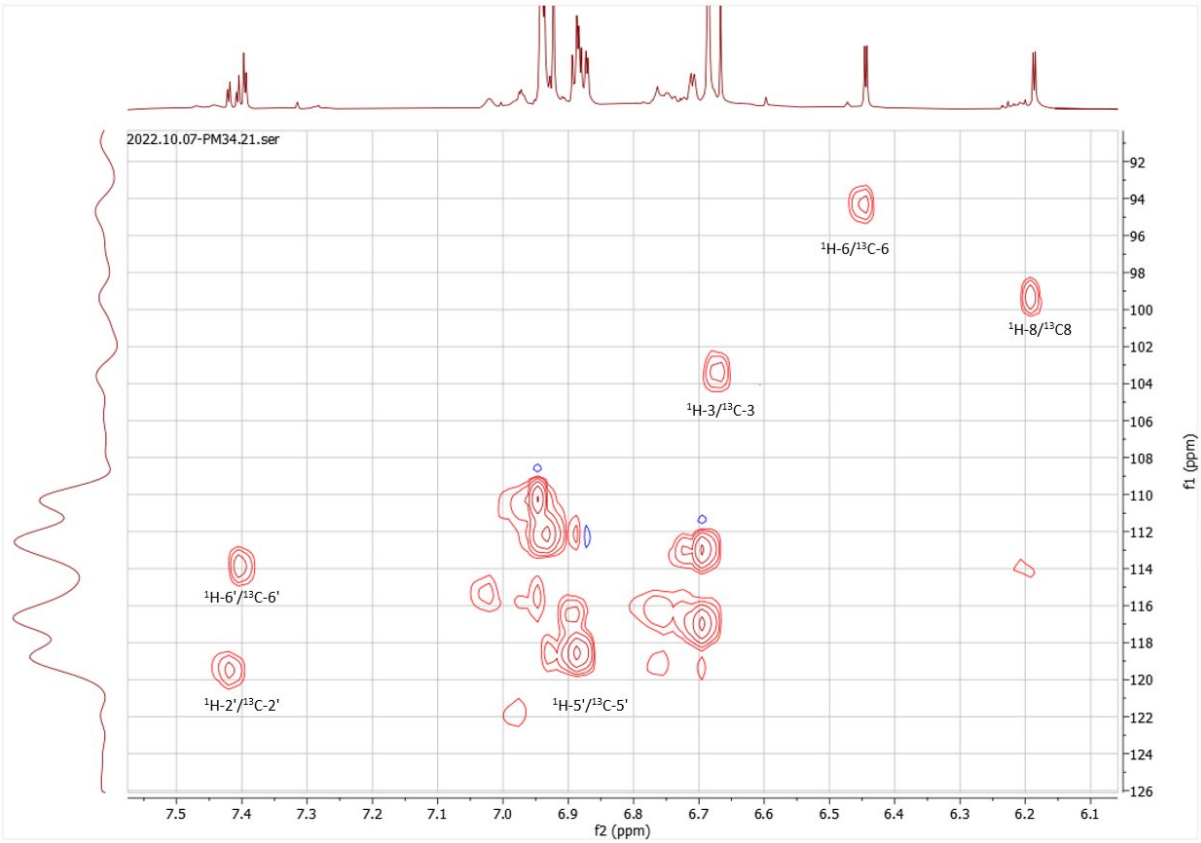

Figure 3.5.11: HSQC of prep 34 showing H-C J1 correlation data.

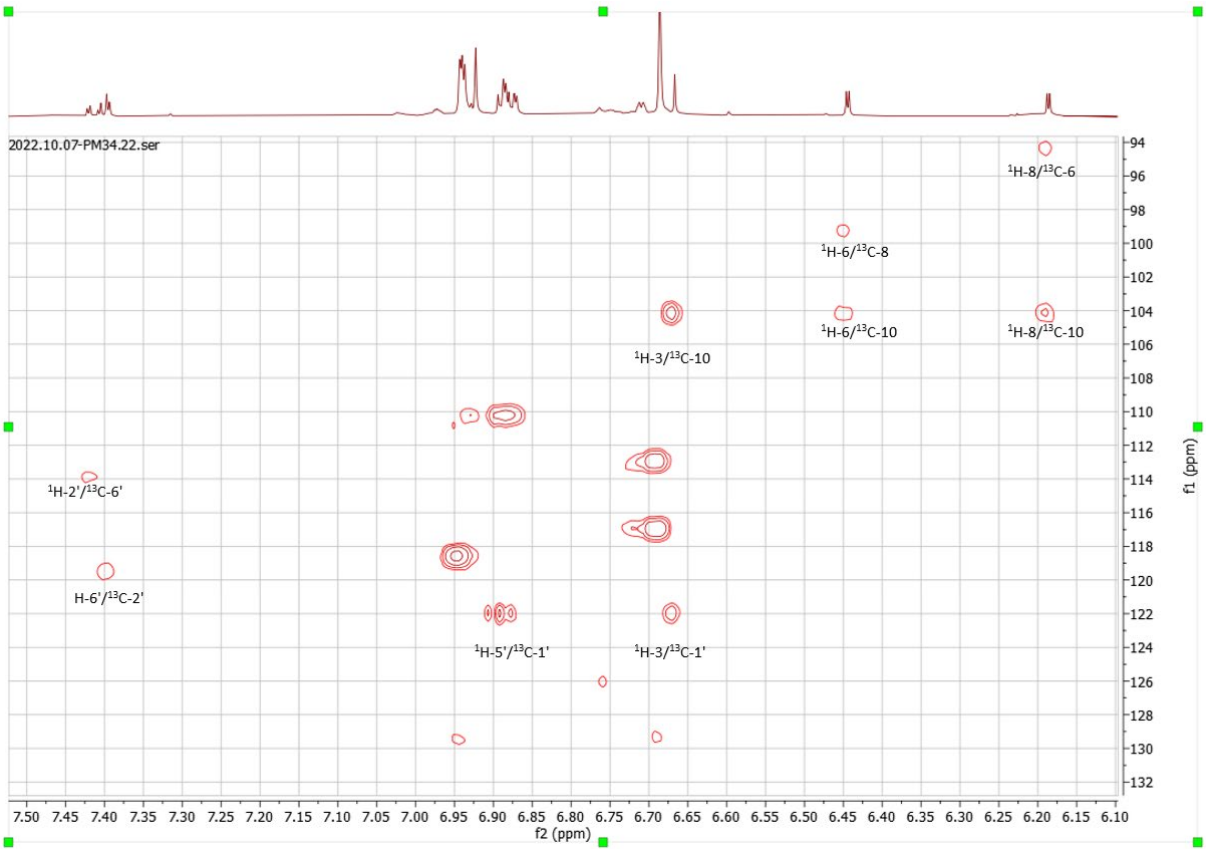

Figure 3.5.12: HMBC of prep 34 showing H-C J3-5 correlation data.

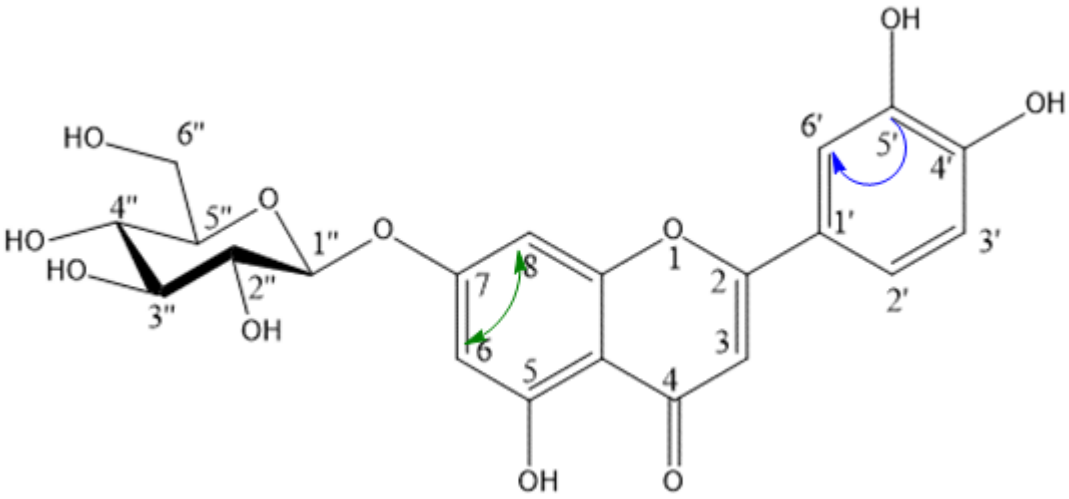

Figure 3.5.13: luteolin 7-O-glucoside structure, the compounds is tentatively present in prep 22.

Table 3.5.3: ^{1}H-NMR data regarding prep 22 tentatively luteolin 7-O-glucoside.

Proton ^{1}H	**δ ^{1}H (ppm)**	**δ ^{13}C (ppm)**	**Area**	**^{1}H**	**Signal type**	**Neighbor ^{1}H/^{13}C (ppm)**	**HMBC ^{13}C (ppm)**	**Coupling constant J (Hz)**
1	-			0				
2	-			0				
3	6.71	113	0.66	1	s			-
4	-			0				
5	-			0				
6	6.45	99	0.52	1	m	6.18	27	
7	-			0				
8	6.18	114	0.66	1	s	6.45	46 49 126	
1’	-	122		0				
2’	7.47	116	0.44	1	s		121	-
3’	-			0				
4’	-			0				
5’	6.87	115	0.52	1	s		106	-
6’	7.44	119	0.66	1	s		115	-

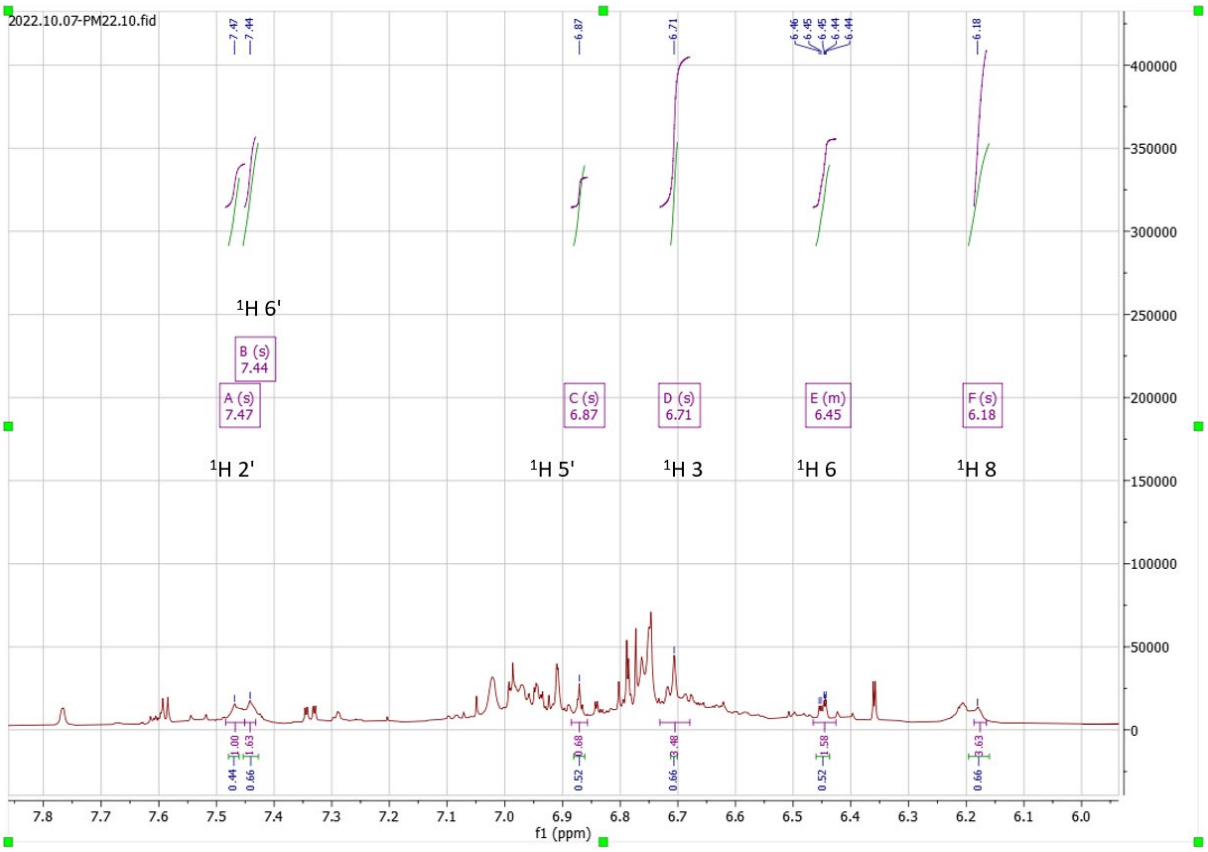

Figure 3.5.14: ^{1}H-NMR prep 22 run on 600 MHz at 23°C using DMSO-d_6 solvent in the aglycol area (6-8 ppm).

The focus while interpreting NMR spectra was the aglycone area (6-8 ppm).

The were some other substances present in the sample, which gave extra signals, making the interpretation more difficult.

By comparing luteolin with luteolin 7-O-glucoside, the H-NMR spectra shows similarities.

In the glucoside area, the amount of other interfering compounds that hinders elucidation of the molecule.

An attempt to find a connection between the 6 and 8 position in ring A and the glucose in the 3-4 ppm area to see whether the glucose might be in the 7 position, the attempt did not succeed. Luteolin 7 - O - glucoside has been confirmed in *lanceolata* by NMR in the paper "Polyphenolic Compounds from *Plantago lagopus L.*"(Fiz, Lanza, and Matellano 2000).

4. **Discussion and conclusion**.

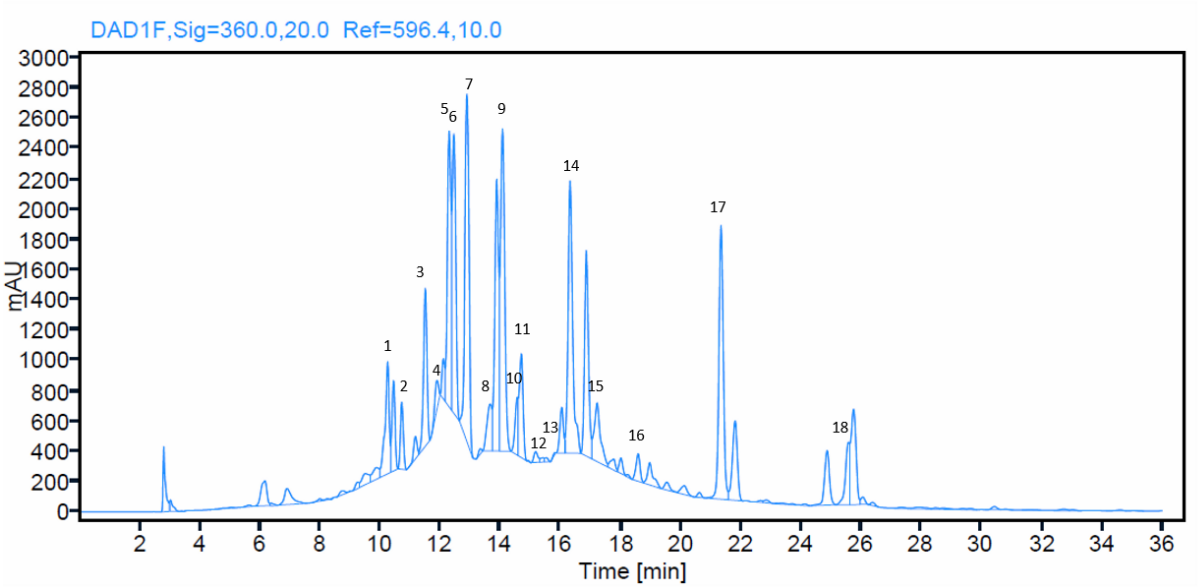

Figure 4.1.1: HPLC chromatogram of XAD-7 purified *P. maritima* (leaf, flower and stalk combined) detected at 360 ± 10 nm. Eighteen major and minor peaks have been labeled (1-18). See table 3.5.1 for spectroscopy and chromatogram data.

Table 4.1.1: HPLC chromatography data from analysis of XAD-7 purified *P. maritima* sample combined with data from LC-MS to tentatively identified compounds.

No.	Component	Refernce UV(nm)	Measured UV (nm)	Crude Rt HPLC	Prep nr	Mw (g/mol)	-ESI m/z^-
1	plantamajoside	332	330 238	10.232	17	640.6	639
2	apigenin glucoside	335 269 253	336 274 250	10.706	5	432.4	431.1
3	luteolin 7-O-glucoside	349 254sh 205	344 270 242	11.493	22	448.4	447
4	campneoside I	332 296sh	330 240	11.846	10	654.6	653.1
5	tricin diglucoside	351 270-265	354 274	12.272	22	654.6	653.1
6	nepitrin (6-methoxylutelin 7-glucoside	346 272 255	350 280	12.437	23	478.4	477.1
7	luteolin glucuronide	348 266sh 256 205	350 302 280 250	12.926	24	462.4	461
8	quercetin arabinoside	354 255	352 256	13.866	14	434.3	433.2
9	diosmetin rutinoside	348 268 252	352 268	14.046	22	608.5	607
10	verbacoside	330	332 246	14.532	18	624.6	623
11	tricin glucoside	341 269 253	342 272	14.679	24	492.4	491.1
12	rosmarinic acid	329 287sh	328	15.139	24	360.3	359

13	apiin (Apigenin 7-O-apioglucoside)	335 272	328 238	15.806	24	564.5	563.1
14	luteolin	347 267 255	348 266	16.306	34	286.24	285
15	martynoside	328 284 233 220 205	332	17.206	25	652.6	651
16	apigenin	337 269 212	336 256	18.559	37	270.24	269
17	diosmetin/chrysoeriol	348 292 268 252	350 254	21.319	39	300.26	299.1
18	tricin	349-346 269	348 250sh	25.560	37	330.29	329

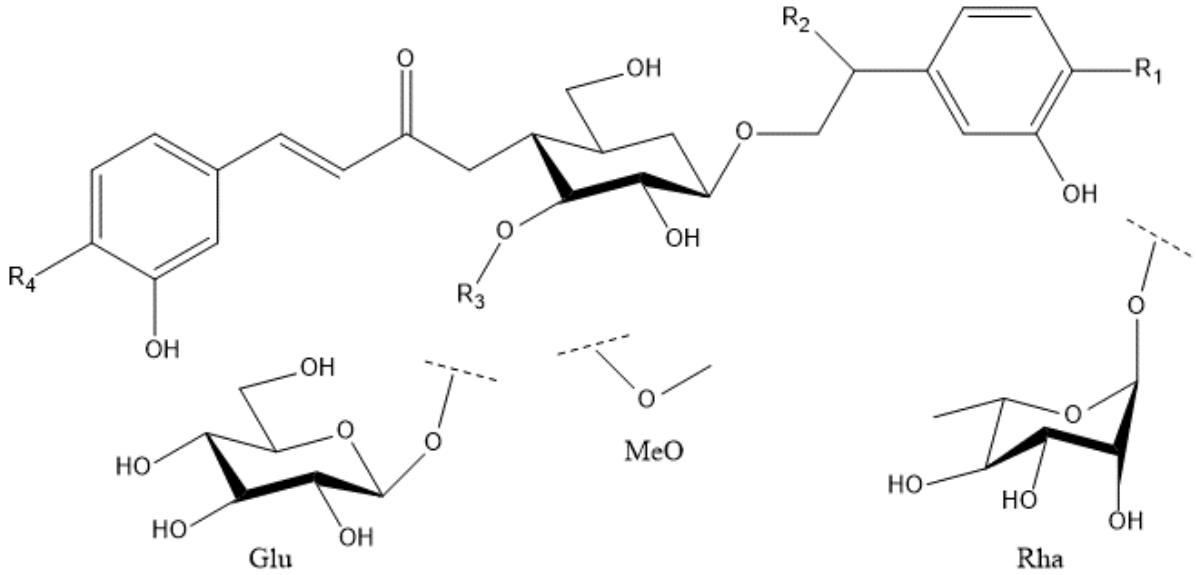

Figure 4.1.2: Main structure with differentiating groups.

Table 4.1.2: List of compounds tentatively found in *Plantago maritima* extraction. Structure explained when combined with figure 4.1.2.

Compound	**R_1**	**R_2**	**R_3**	**R_4**
plantamajoside (1)	OH	H	Glu	OH
verbascoside (10)	OH	H	Rha	OH
campneoside I (4)	OH	MeO	Rha	OH
martynoside (15)	MeO	H	Rha	MeO

Both verbascoside and plantamajoside are found to be present in *Plantago maritima* in earlier research (Davey et al. 2004). The main difference between these two compounds is that in the third position on the central glucose there are different sugar molecules connected. Verbascoside has a rhamnose molecule while plantamajoside has a glucose molecule in the third position(Kawada et al. 2006; Duynstee et al. 1999).

Plantamajoside (1) has a molecular weight of 640.6 g/mol. The reference value for UV (Davey et al. 2004) is 332 nm (table 4.1.1:). Measured UV value was 330 nm. Plantamajoside is the major UV active compound in prep 17. (Figure A 1 and B 2).

A study indicate that plantamajoside is a caffeic acid sugar ester(H. Ravn and Brimer 1988). Plantamajoside is a dihydroxy phenethyl glucoside from the polyphenolic compounds group (H. W. Ravn et al. 2015). Preforming NMR on prep 17 gave signals that matched both plantamajoside and verbascoside, given that the sugar molecule in third position on the central glucoside is the only difference between the two compounds, the signals originating from the common part of the compounds overlap (see table 3.2.1 for signal elucidation). Given the UV-, NMR-, and LC-MS data one can conclude that both plantamajoside and verbascoside is tentatively present in the extract. Plantamajoside is more prominent in prep samples 16 and 17, while verbascoside is mostly allocated to prep 18.

Campneoside I (4) has a molecular weight of 654.6 g/mol and is categorized as a phenylethanoid glycoside. Research shows campneoside I has been found in the Plantago genus (*Plantago depressa*) (Xu et al. 2020). Reference UV (Torres-Vega et al. 2021) for campneoside I is 332 and 296sh nm (Table 4.1.1:). Found UV signal is 330 nm (figure B 19). LC-MS of prep 10 shows a major peak with m/z^- of 653.1 which corresponds to campneoside I (figure A 15). Campneoside I is almost identical to verbascoside with the only difference being a methoxy group at the chain between the central glucose molecule and the benzene ring. Given the UV data and the LC-MS data, campneoside I is tentatively present.

Verbascoside (10) has a molecular weight of 624.6 g/mol. Verbascoside is a phenylethanoid glycoside (Alipieva et al. 2014). Reference UV (Davey et al. 2004) signals are 330 nm(Table 4.1.1:). Measured UV signal was found to be 330 (Figure 3.5.1). Using negative mode ESI during LC-MS on prep 18, the m/z^- value of 623 was found, this mass corresponds to verbascoside (Figure A 2 and B 5).

Martynoside (15) has a molecular weight of 652.6 g/mol and is categorized as a phenylethanoid glycoside. Research shows martynoside has been found in the *Plantago* genus (*Plantago lanceolata*) (Budzianowska, Skrzypczak, and Budzianowski 2004). Reference UV (ERSÖZ et al. 2002) for martynoside is 330, 287 and 220 nm(Table 4.1.1:). Measured UV signals were 332 and 206 nm. (Figure B 20) Compared to other phenylethanoid glycosides, martynoside has a methoxy group instead of an alcohol group at positions 4 and 4’’’. LC-MS of prep 25 shows a minor peak with m/z^- of 651.1 which corresponds with martynoside (figure A 16). Given the UV and LC-MS data martynoside is tentatively present.

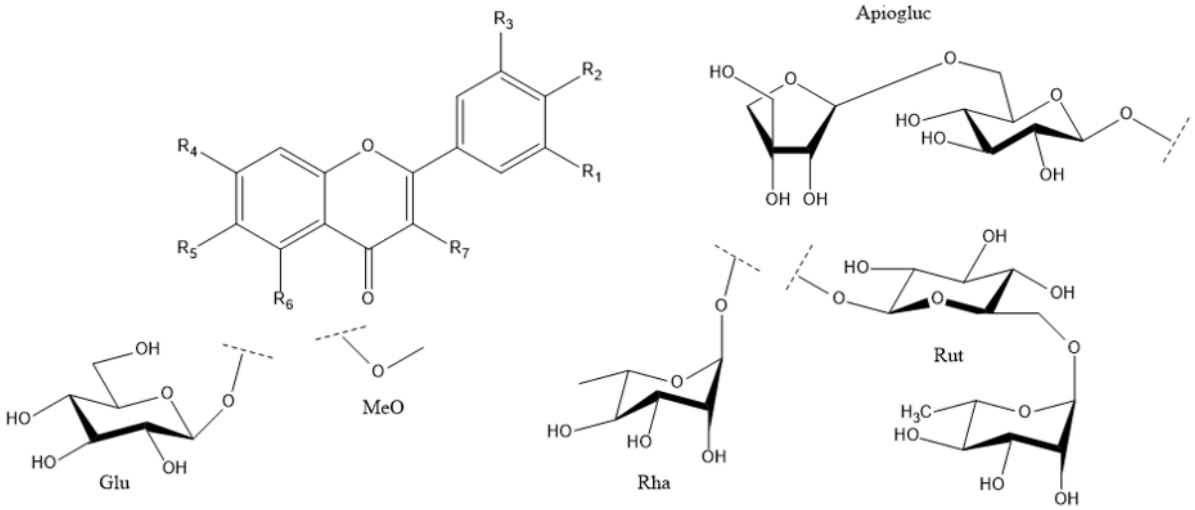

Figure 4.1.3: Main skeleton for flavonoids and R groups used in table 4.1.3:

Table 4.1.3: List of compounds tentatively found in *Plantago maritima* extraction. Structure explained when combined with figure 4.1.3.

Compound	R1	R2	R3	R4	R5	R6	R7
luteolin	H	OH	OH	OH	H	OH	H
apigenin	H	OH	H	OH	H	OH	H
quercetin	H	OH	OH	OH	H	OH	OH
tricin	MeO	OH	MeO	OH	H	OH	H
diosmetin	H	MeO	OH	OH	H	OH	H
chrysoeriol	H	OH	MeO	OH	H	OH	H
apigenin 7-O glucoside	H	OH	H	Glu	H	OH	H
quercetin 3-O-arabinoside	H	OH	OH	OH	H	OH	Arab
luteolin 7-O-glucoside	H	OH	OH	Glu	H	OH	H
tricin 5-7-diglucoside	MeO	OH	MeO	Glu	H	Glu	H
nepitrin	H	OH	OH	Glu	MeO	OH	H
luteolin 7-O-glucuronide	H	OH	OH	Glu	H	OH	H
tricin 7-O-glucoside	MeO	OH	MeO	Glu	H	OH	H
diosmetin 7-O-rutinoside	H	MeO	OH	Rut	H	OH	H
apigenin 7-apioglucoside	H	OH	H	Apiogluc	H	OH	H

Apigenin glucoside (2) has a molecular weight of 432.4 g/mol and is categorized as a flavone glucoside. Apigenin glucoside has been found in *Plantago maritima* in earlier research (Beara et al. 2009). Reference UV (Goufo, Singh, and Cortez 2020) are 335, 269 and 253 (Table 4.1.1:). Apigenin glucoside has been found in prep 5 and has UV values of 336 and 274 (Figure B 3). The results are inconclusive about its presence, but tentatively confirmed in prep 5.

Luteolin 7-O-glucoside (3) has a molecular weight of 448.4 g/mol and is a flavone glucoside. Luteolin 7-O glucoside has been found in *Plantago maritima* in earlier research (Beara et al. 2009). Reference UV (Goufo, Singh, and Cortez 2020) is found to be 349, 254sh and 205 nm (Table 4.1.1:). The UV values found in prep 22 are 348 and 266 nm (figure B 7). NMR data regarding prep 22 (figure 3.4.13) in the aglycol area (6-8 ppm) signals are like the NMR data belonging to Luteolin. LC-MS of prep 22 contains the m/z^- value 447 (figure A 4).
By combining the results from LC-MS, HPLC and NMR it's tentatively confirmed that prep sample 22 contains luteolin 7-O glucoside.

Tricin diglucoside (5) has a molecular weight of 654.6 g/mol and is categorized as a methylated flavone diglucoside. Tricin diglucoside has yet to be found in the *Plantago* genus. Reference UV(Wilson 1985) is 351 and 265-270 nm. Found UV values in prep 22 are 350 and 264 nm (figure B 14) (Table 4.1.1:). LC-MS of prep 22 contains a m/z^- of 653.1 (figure A 10 in appendix). LC-MS/MS of prep 22 confirmed tricin diglucoside through mass loss and remaining fragment size. Tricin diglucoside has not been confirmed in *Plantago maritima* previously, nor has it been found in the *Plantago* genus. with the data from LC-MS/MS, it is tentatively confirmed that tricin diglucoside is in *Plantago maritima.*

Nepitrin (6-methoxy luteolin 7-glucoside) (6) has a molecular weight of 478.4 g/mol and is categorizer as a 6-methoxyflavone. Nepetin-7-glucoside is found in the *Plantago* genus ("Plantago Major - Common Plantain" n.d.). Reference UV (Lee et al. 2018) is 346, 272 and 255 nm (Table 4.1.1:). Found UV values in prep 23 are 348, 270 and 256 (Figure B 15). LC-MS of prep 23 shows m/z^- 477.1 which indicates nepitrin (figure A 11). given the UV – and LC-MS data, this tentatively confirms the presence of nepetin-7-glucoside.

Luteolin glucuronide (7) has a molecular weight of 462.4 g/mol and is categorizer as a flavone glucuronide. Luteolin glucuronide is found in the *Plantago* genus(*Plantago lanceolata*) (Mo et al. 2022). the reference UV (华玉强 2006) is 348, 266sh, 256 and 205 nm (Table 4.1.1:). UV signals found in prep 23 are 348 and 266sh nm (figure B 17). LC-MS of prep 23 shows a m/z^- of 461 which indicates luteolin glucuronide (figure A 13). the combination of UV and LC-MS data tentatively confirms that luteolin glucuronide is present in prep 23. A study show that glucuronide might have the function of curing cardiovascular diseases, reduce blood fat and improve micro circulation (华玉强 2006).

Quercetin arabinoside (8) has a molecular weight of 434.3 g/mol and is categorized as a flavonol arabinoside. Research shows quercetin arabinoside has been found in the *Plantago* genus (*Plantago asiatica*) (Murai et al. 2015). Reference UV (dos Santos et al. 2014) for quercetin 3-O-arabinoside are 354 and 255 nm (Table 4.1.1:). Found UV signals in prep 14 are 350 and 254 nm (figure B 18). LC-MS of crude XAD-7 purified *P. maritima* shows a peak with m/z^- of 433.2 which corresponds to quercetin arabinoside (figure A 14). Given the UV data and LC-MS data, quercetin arabinoside is tentatively confirmed to be present in *Plantago maritima.*

Diosmetin rutinoside (9) has a molecular weight of 608.5 g/mol and is categorized as a methylated flavone glucoside. The base molecule diosmetin has been found in *Plantago Maritima*, but diosmetin rutinoside has yet to be found. Reference UV (Lin and Harnly 2007) is 348, 268 and 252 nm (Table 4.1.1:) while found UV values are 348 and 252 in prep 22 (figure B 22 in appendix). LC-MS of prep 22 shows the sample contains a m/z^- peak of 607.0 (Figure A 18 in appendix). Given the UV and m/z^- data found, diosmetin rutinoside is tentatively confirmed to be contained in prep 22.

Tricin glucoside (11) has a molecular weight of 492.4 g/mol and is categorized as a methylated flavone glucoside. Tricin glucoside has been found in the *Plantago* genus, but no research shows whether tricin glucoside has been found in *Plantago maritima (Plantago crassifolia*) (Zaghloul and Zaghloul 2000). Reference UV (M. Li et al. 2016) is

341, 269 and 253 nm (Table 4.1.1:). Tricin glucoside is suspected to be in *Plantago maritima* prep 24, UV was found to be 342 and 266 nm (figure B 13). LC-MS of prep 24 shows a m/z^- of 491.1 which corresponds with tricin glucoside (figure A). LC-MS/MS of prep 24 gave fragmentation which confirmed tricin glucoside through mass loss and fragment m/z^-. Given the data available it is tentatively confirmed that tricin glucoside is present in prep 24.

Apiin (Apigenin 7-apioglucoside) (13) has a molecular weight of 564.5 g/mol and is categorized as a flavone di glycoside. Apiin has been found in the *Plantago Major* (Beara et al. 2012), but yet to be found in *Plantago Maritima.* Reference UV (Pradas Del Real et al. 2017) is 335 and 272 nm (Table 4.1.1:) while found UV values are 334 and 290 in prep 24 (B 24 in appendix). LC-MS of prep 24 shows the sample contains a m/z^- peak of 563.1 (A 19 in appendix). Given the UV and m/z^- data apiin is tentatively confirmed to be contain in prep 24.

Luteolin (14) has a molecular weight of 286.24 g/mol and is categorized as a flavone. According to previous research (Davey et al. 2004) luteolin is present in *Plantago maritima*. Reference values for UV (Kotova, Kotov, and Kotov 2021) are 347, 267 and 255 nm (Table 4.1.1:). UV signals found during HPLC of prep 34 were 348 and 254 nm. (Figure B 9)

The NMR data shown in figure 3.4.11 indicates towards luteolin. MS data shown in figure A 3 shows a mass of 285 m/z^- which would be the expected mass for luteolin in negative ESI mode. By analyzing the three sets of data one can conclude that prep 34 tentatively contains luteolin.

Apigenin (16) has a molecular weight of 270.24 g/mol and is categorized as a flavone. Apigenin has been found in *Plantago maritima* in earlier research (Bakke 2020). Reference UV (B. Li, Robinson, and Birt 1997) for apigenin is 337, 269 and 212 nm (Table 4.1.1:). Results suggest that apigenin is the major peak in Prep 37 and the UV values found are 338, 268 and 212 nm (figure B 10). LC-MS of prep 37 shows a minor peak with a mass corresponding to apigenin (figure A 5). and the UV spectrum measured in the same area during LC-MS contains peaks at approximately 337 and 269

nm. Given the MS and UV data it is tentatively confirmed that prep 37 contains apigenin.

Diosmetin/chrysoeriol (17).

Figure 4.1.3 in combination with table 4.1.3 shows that the only difference between diosmetin and chrysoeriol is that an OH group swaps places with a MeO group in position R_2 and R_3. This makes NMR the only viable option for differentiating between the two compounds.

Diosmetin/chrysoeriol has a molecular weight of 300.26 g/mol and is categorized as a flavone. Compounds 17 has been found in *Plantago maritima* in earlier research (Bakke 2020). LC-MS of prep 39 found a m/z^- of 299.1 in negative ESI mode (figure A 12). Reference UV (Lech, Witkoś, and Jarosz 2014) for diosmetin are 348, 292, 268 and 252 nm (Table 4.1.1:).

UV peaks found in prep 39 are 348 and 266(figure B 16).

The UV data combined with the LC-MS data tentatively confirms that prep 39 contains diosmetin/chrysoeriol.

Tricin (18) has a molecular weight of 330.29 g/mol and is categorized as a methylated flavone. Tricin has been found in the Plantago genus, but not yet confirmed in *Plantago maritima* (*Plantago phaeostoma boiss*) (Kawashty et al. 1994). Reference UV (M. Li et al. 2016) is 349-346 and 269 nm (Table 4.1.1:). In prep 37 the peak suspected of being tricin has UV peaks at 350 and 266 (figure B 12). LC-MS of prep 37 shows a main peak with m/z^- 329, given the – ESI mode run during MS the actual weight is 330 (figure A 8). Looking at the UV spectrum of the LC-MS run of prep 37 the signal shows peaks at around 348 nm. Co - chromatography of a tricin standard sample and prep 37 show similar mass, Rt time and UV signals. With the given results it is confirmed that tricin is in *Plantago maritima*.

Rosmarinic acid (12) has a molecular weight of 360.3 g/mol and is categorized as a hydroxycinnamic acid and is an ester of caffeic acid. Rosmarinic acid is known to be in *Plantago lagopus L*(Fiz, Lanza, and Matellano 2000)*,* but has yet to be found in *Plantago maritima.* Reference UV (Shekarchi et al. 2012) values are 329 and 287sh nm while found UV values are 328 nm in prep 24 (B 23 in appendix). LC-MS of prep 24 shows that the sample contains a m/z^- peak of 359.0 (A 20 in appendix). given the UV and LC-MS data rosmarinic acid is tentatively confirmed to be contained in prep 24.

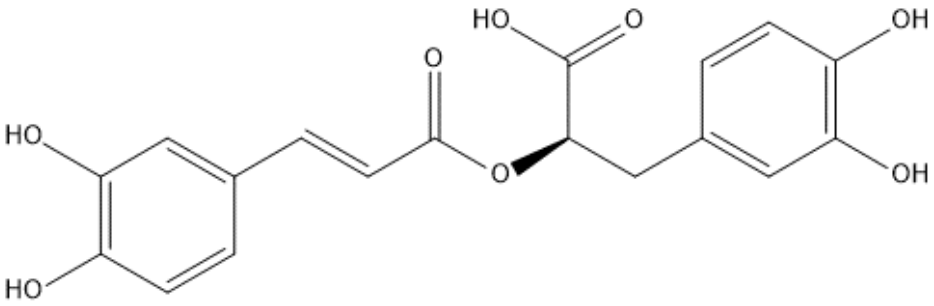

Figure 3.5.4 Rosmarinic acid

Only trace amounts were found from caffeic acid, p-coumaric acid and ferulic acid (table 3.3.1:). This is because these acids co elude with other compounds that are major peaks while the acids are trace amounts leading to them being hidden in HPLC UV chromatograms (figure 4.1.1:).

Conclusion

Compounds confirmed to be present in *Plantago maritima* are plantamajoside (1) and luteolin (14). Methods used for confirmation are HPLC, LC-MS and NMR.
Tricin (18) is checked by co - chromatography with a tricin standard sample and prep 37. Co chromatography show that both samples have the same mass and similar Rt time in LC-MS and HPLC data respectively. With the given results it is confirmed that tricin is in *Plantago maritima*.

Compounds tentatively confirmed to be present in *Plantago maritima* (already known to be present) are apigenin glucoside (2), luteolin 7 – O - glucoside (3), verbascoside (10) and diosmetin/chrysoeriol (17), the methods used for tentative confirmation are HPLC and LC-MS.
Only trace amounts were found from caffeic acid (a), p-coumaric acid (b) and ferulic acid (c) using LC-MS.

Compounds tentatively confirmed to be present in *Plantago maritima* (that are known to be in the *Plantago* genus) are campneoside I (4), nepitrin (6), luteolin glucuronide (7), quercetin arabinoside (8), tricin glucoside (11), rosmarinic acid (12), apiin (13), martynoside (15), apigenin (16). The methods used for tentative confirmation are HPLC and LC-MS.

Compounds tentatively confirmed to be present in *Plantago maritima* (that are not known to be in the *Plantago* genus) are tricin diglucoside (5) and diosmetin rutinoside (9). The methods used for tentative confirmation are HPLC and LC-MS.

LC-MS/MS has been run on tricin glucoside (11), luteolin7-O- glucoside (3), tricin diglucoside (5), nepitrin (6), and luteolin glucuronide (7), and have strengthened the tentative status of these compounds in *Plantago maritima*.

LC- MS/MS has been run on apiin (13), apigenin glucoside (2), quercetin arabinoside (8) and diosmetin rutinoside (9). Results have been inconclusive most likely due to errors during injection.

Of the 10 compounds known to be in *Plantago maritima*, 6 were found to be present in significant amounts, with corresponding UV and MS data. 10 compounds previously known to be in the *Plantago* genus has been tentatively discovered in *Plantago maritima*. 2 completely new compounds not known to be in either the *Plantago* genus or *Plantago maritima* has also been tentatively discovered.

About 40% of the phenolic peaks in the HPLC profile (major and minor peaks) have not been identified in this master project. This is due to the challenging phenolic matrix, with many compounds with similar structures and properties, creating a crowded HPLC profile. Further work should focus on increasing the resolution of the HPLC gradient, both for analytical and preparative HPLC, to increase the number of isolated compounds to be analyzed with HR-LC-MS and NMR. It would also be advisable to increase the amount of dried raw sample, a reasonable amount would be 160-250g.

Appendix A. LC-MS figures used for reference in results and discussion.

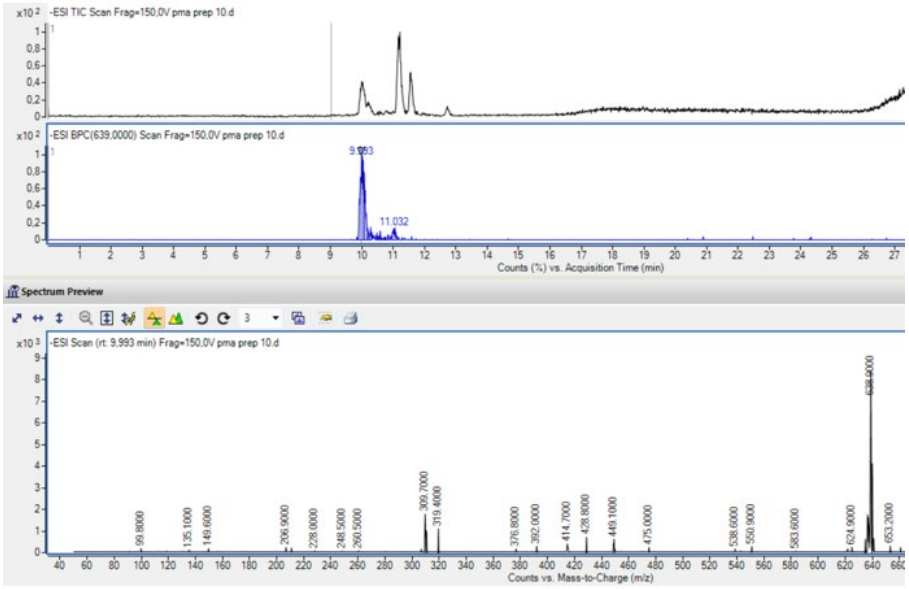

Figure A 1: Plantamajoside MS prep 17 m/z$^-$ 639

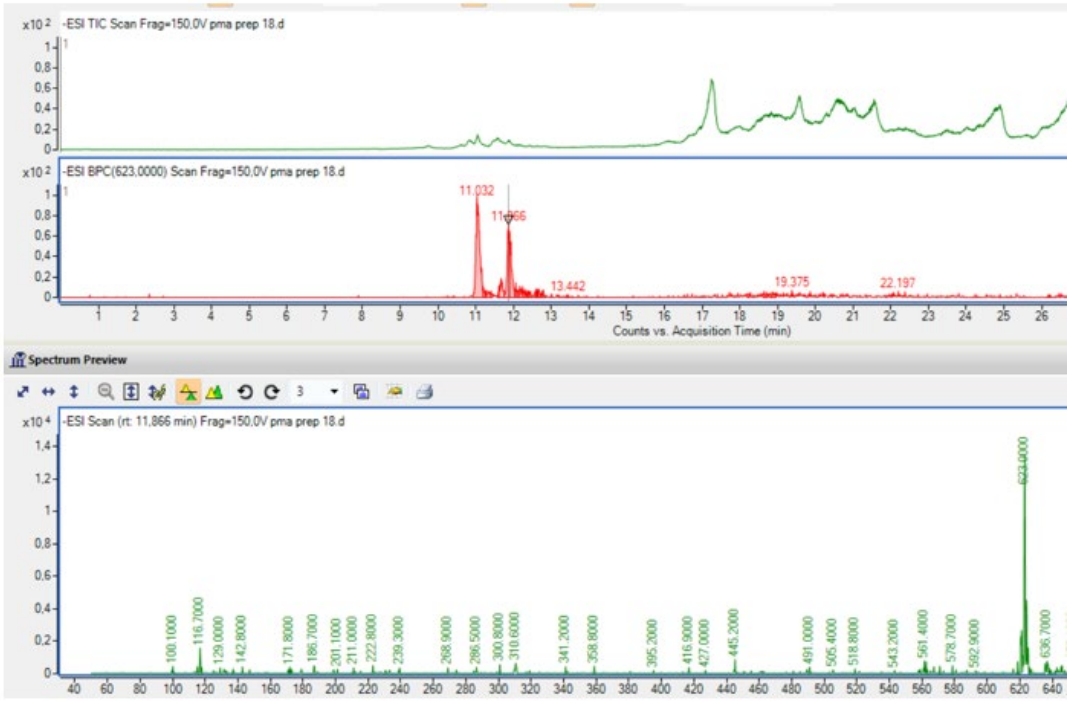

Figure A 2: Verbascoside MS prep 18 m/z$^-$ 623 indicates towards verbascoside.

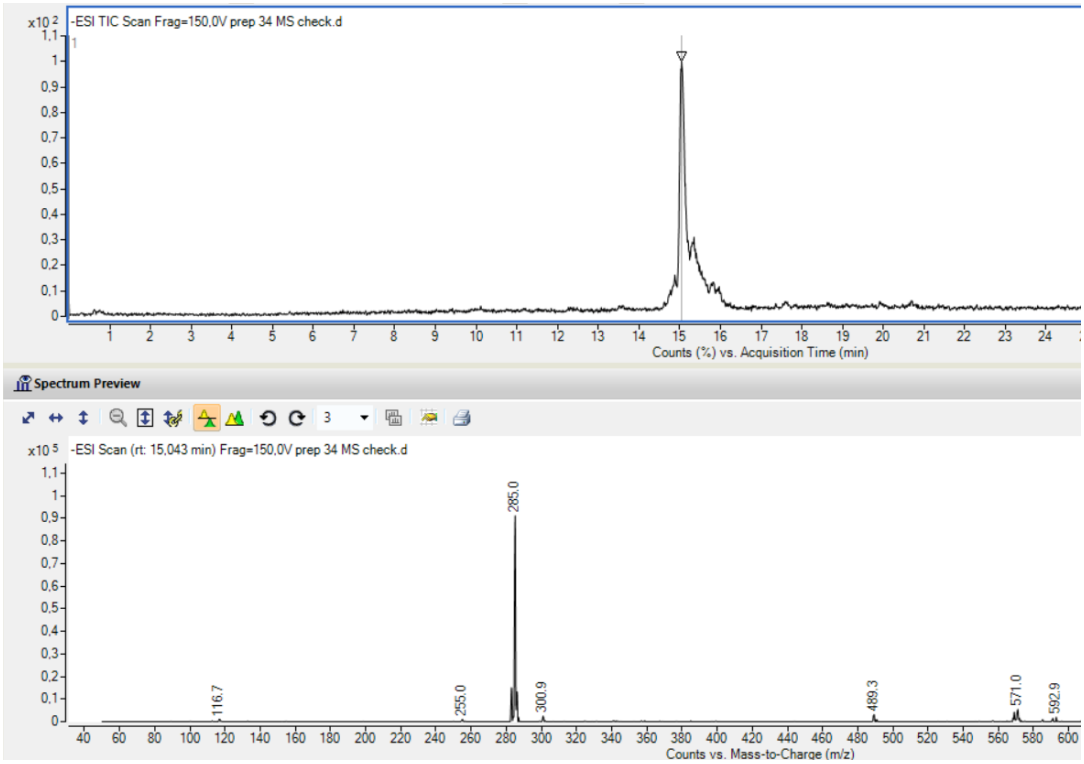

Figure A 3 MS prep 34 m/z$^-$ 285 assumed luteolin.

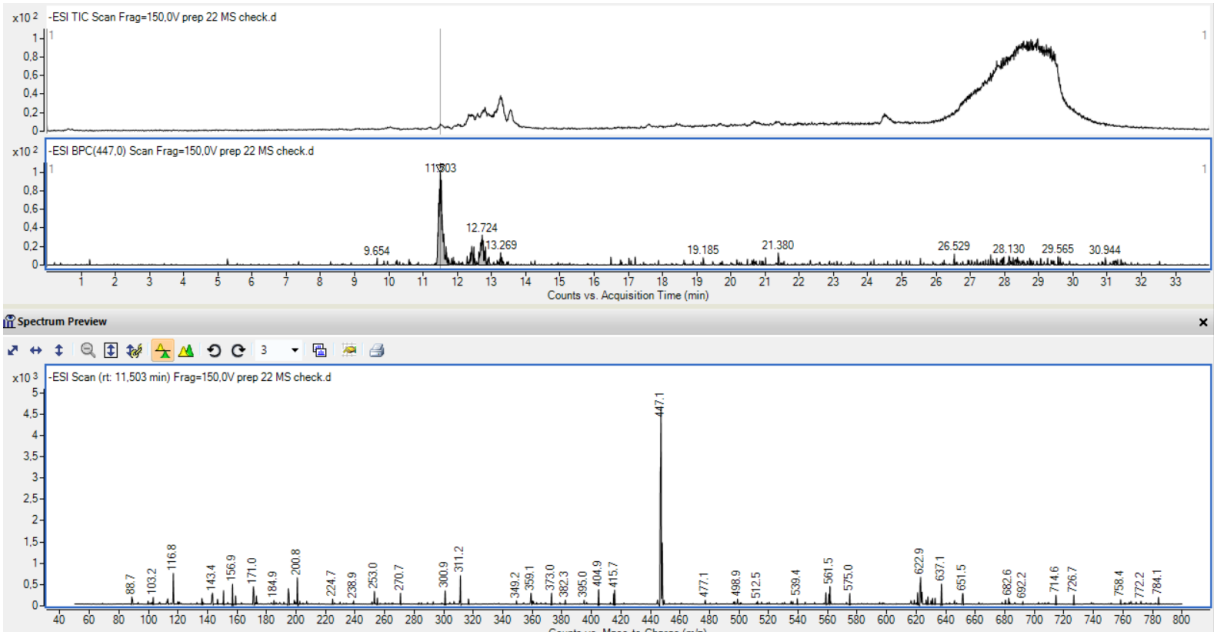

Figure A 4 MS prep 22 m/z$^-$ 447,1 assumed luteolin 7-O-glucoside.

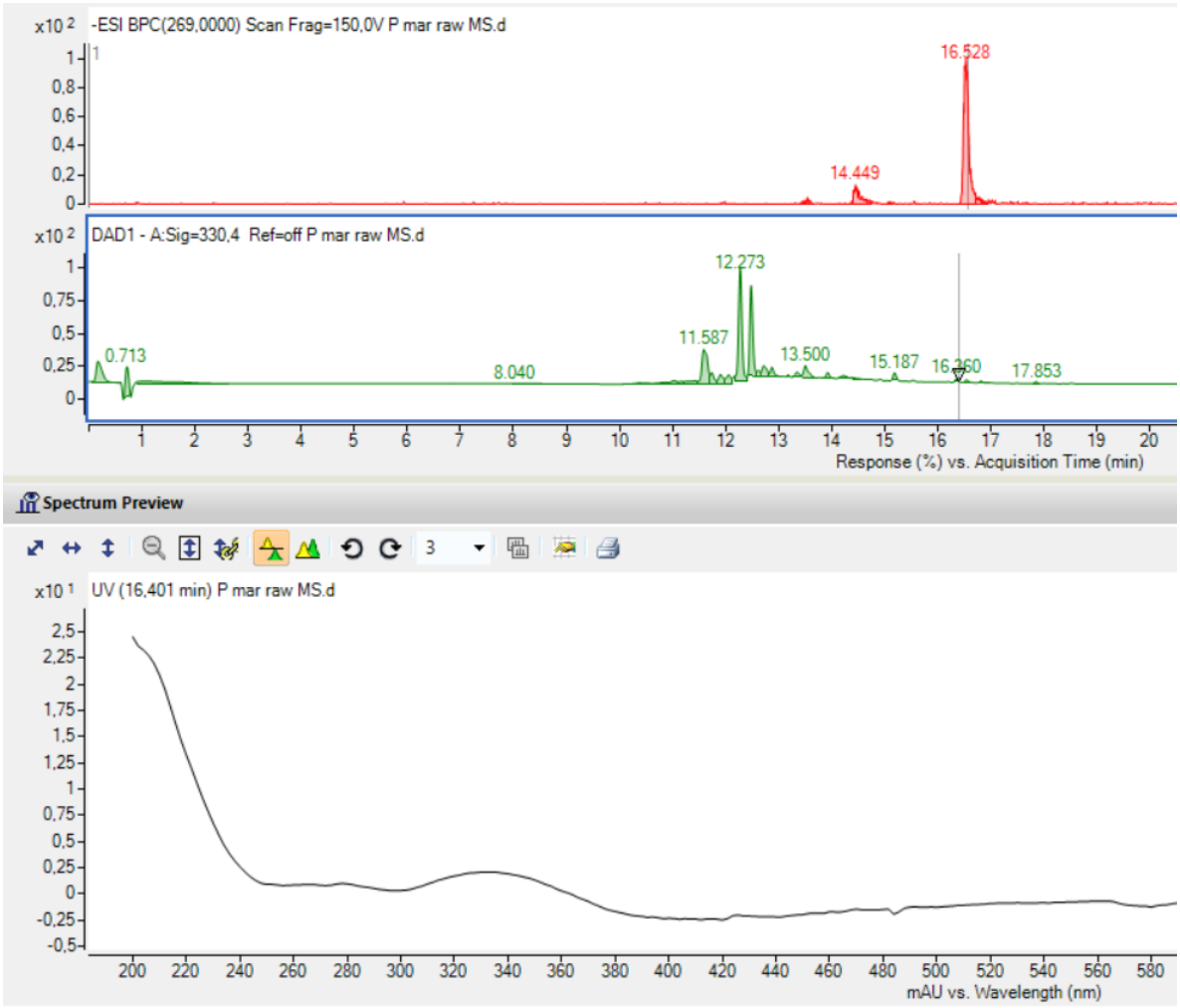

Figure A 5 LC-MS of m/z^{-} 269 assumed apigenin. UV peak at 335.

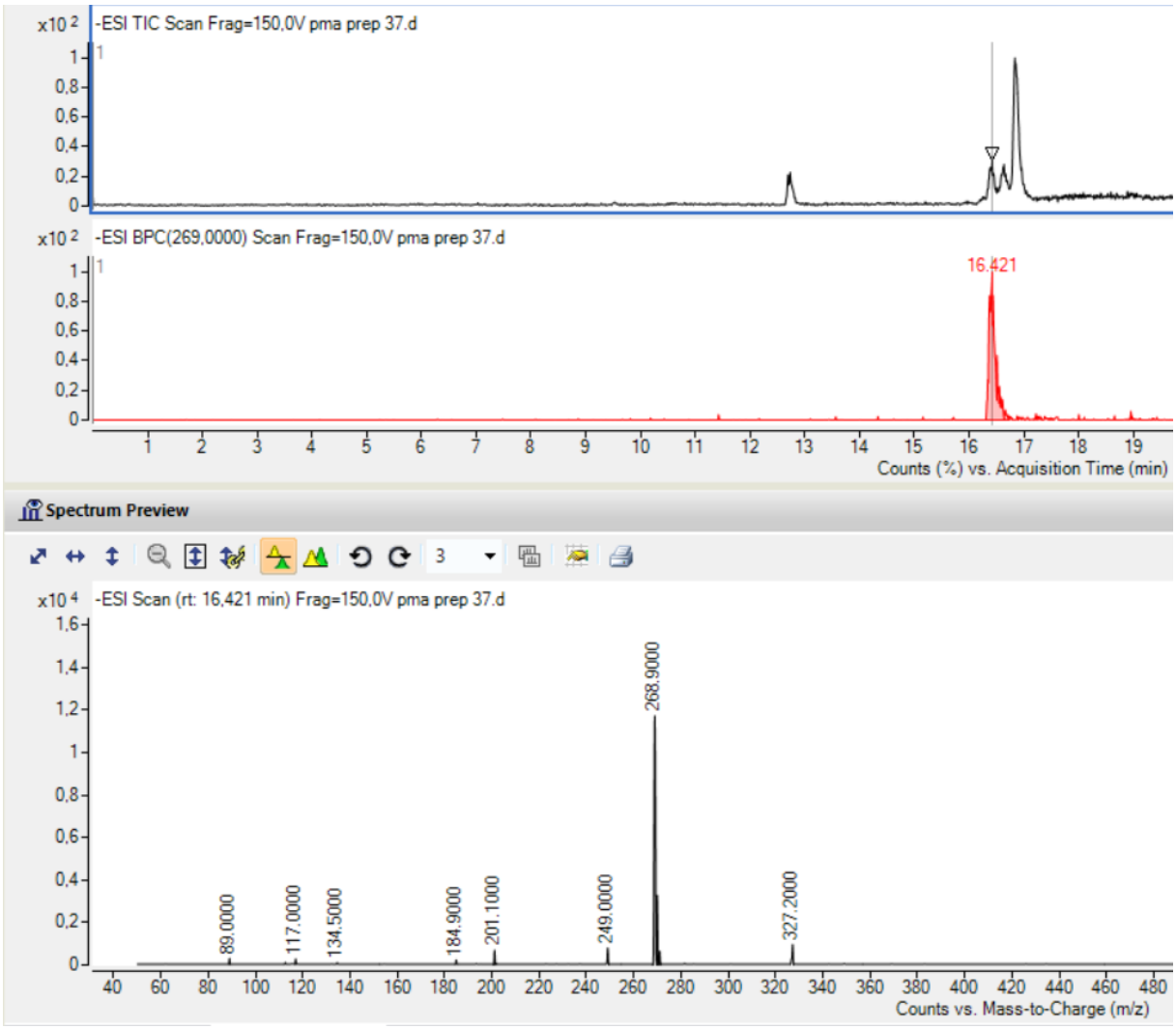

Figure A 6 LC-MS of prep 37, contains masses corresponding to apigenin (m/z^- 269) and tricin (m/z^- 329)

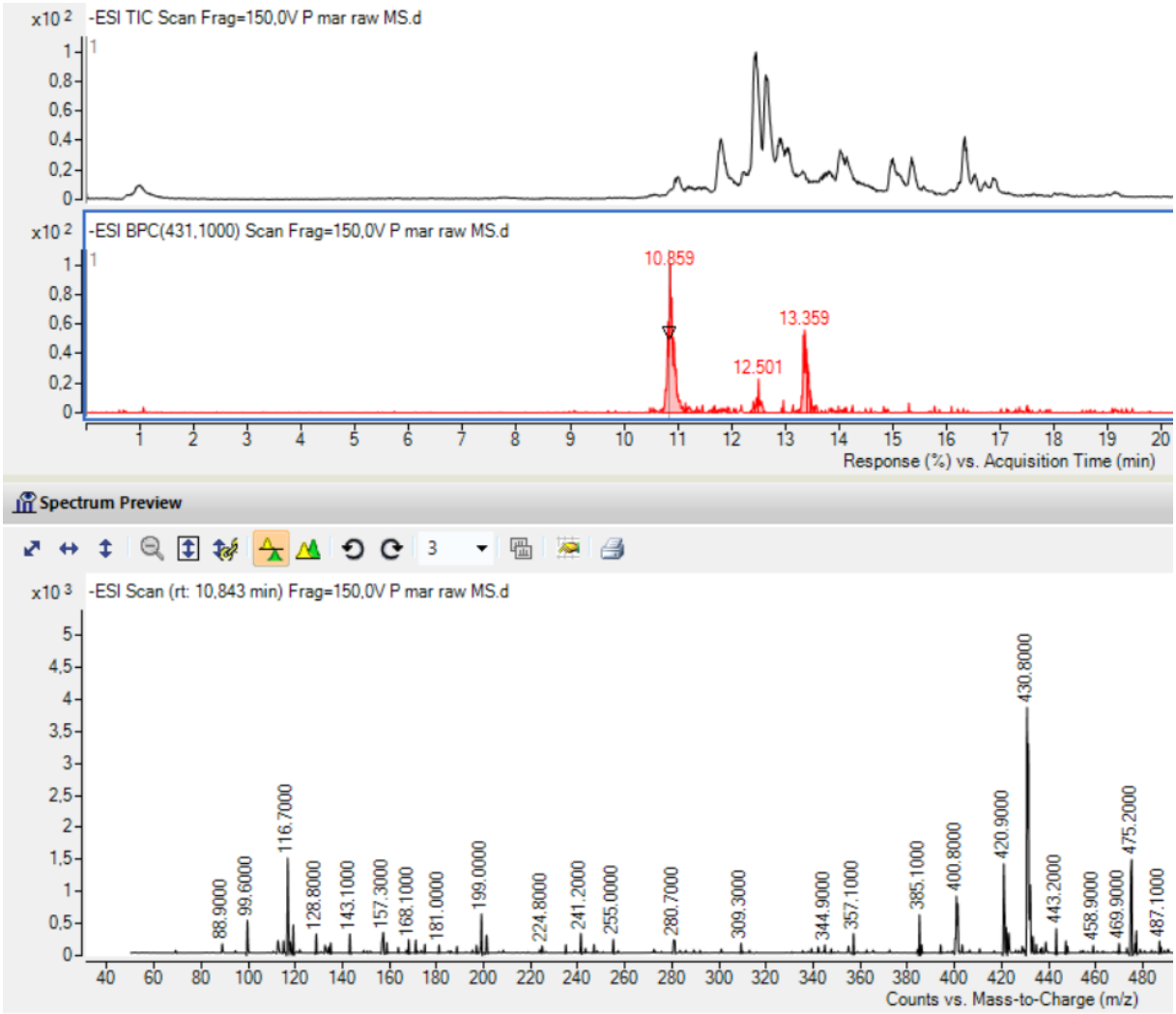

Figure A 7 LC-MS of crude XAD-7 purified *Plantago maritima* showing suspected apigenin glucoside (m/z^- 431) mass.

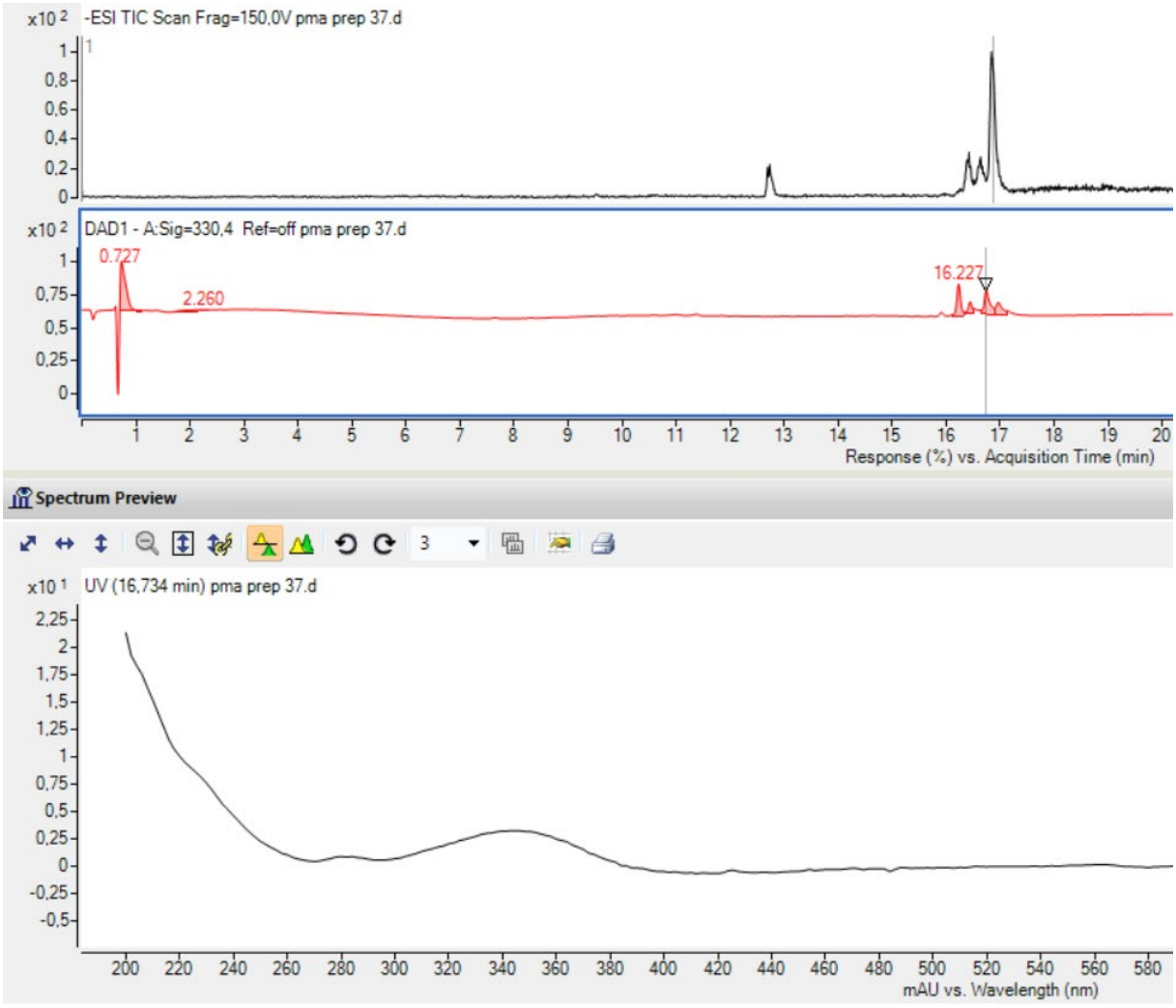

Figure A 8 LC-MS prep 37 with UV/vis spectrum of suspected tricin (m/z^- 329) peak.

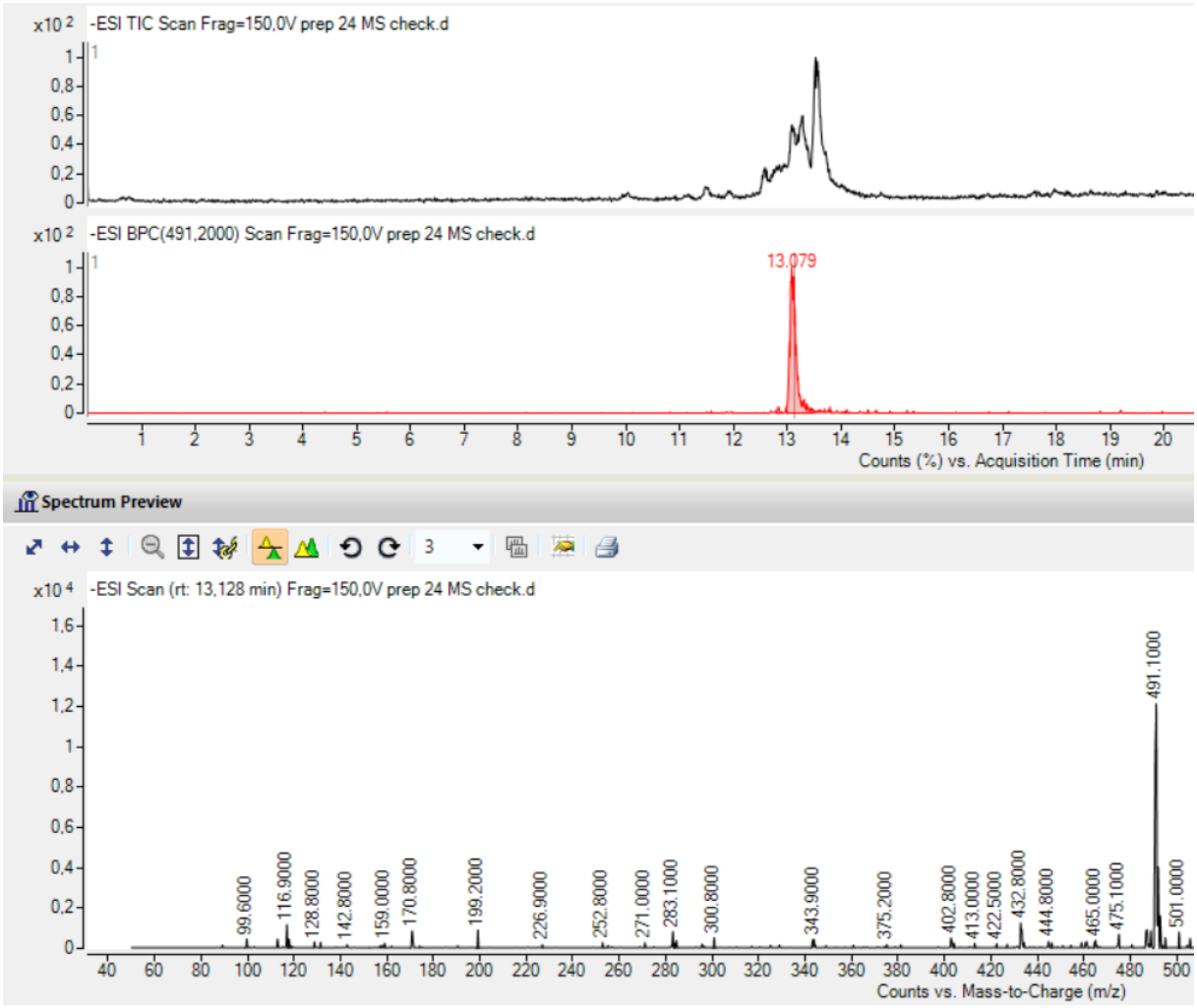

Figure A 9 LC-MS of m/z$^-$ 491.1 assumed tricin glucoside.

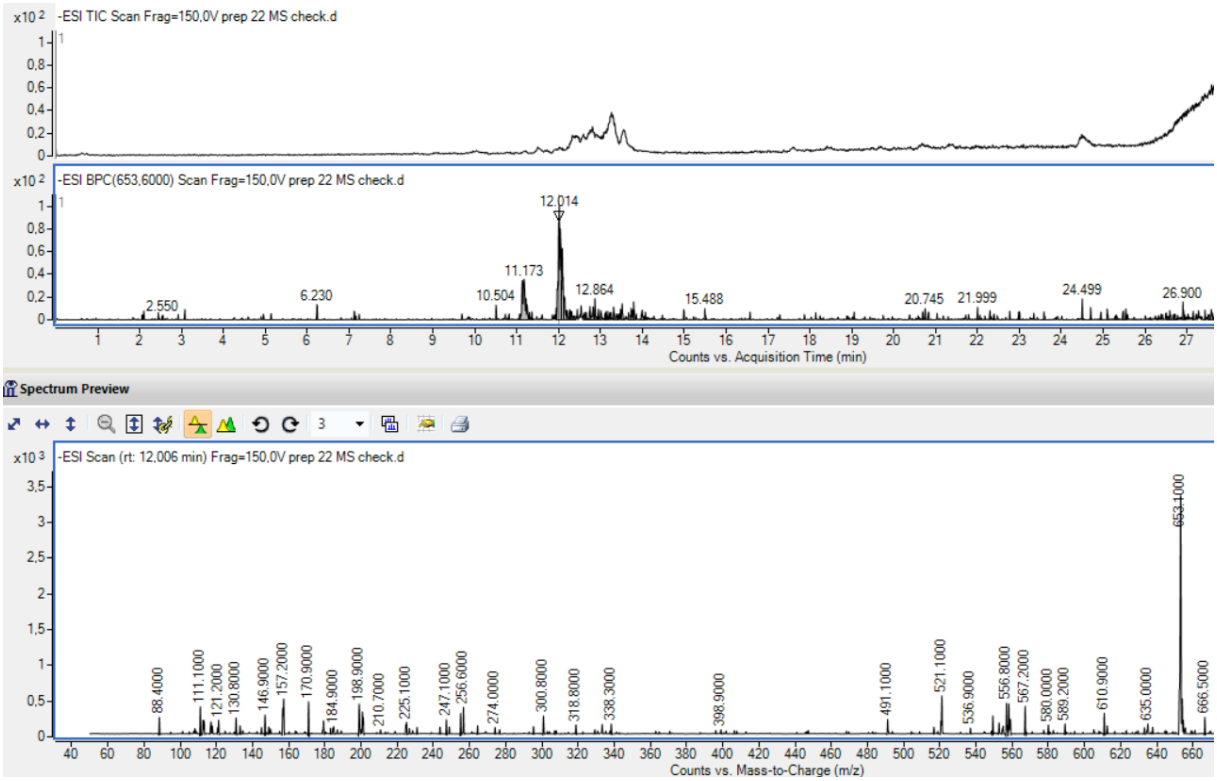

Figure A 10 LC-MS of prep 22 with m/z$^-$ 653.1 assumed tricin diglucoside.

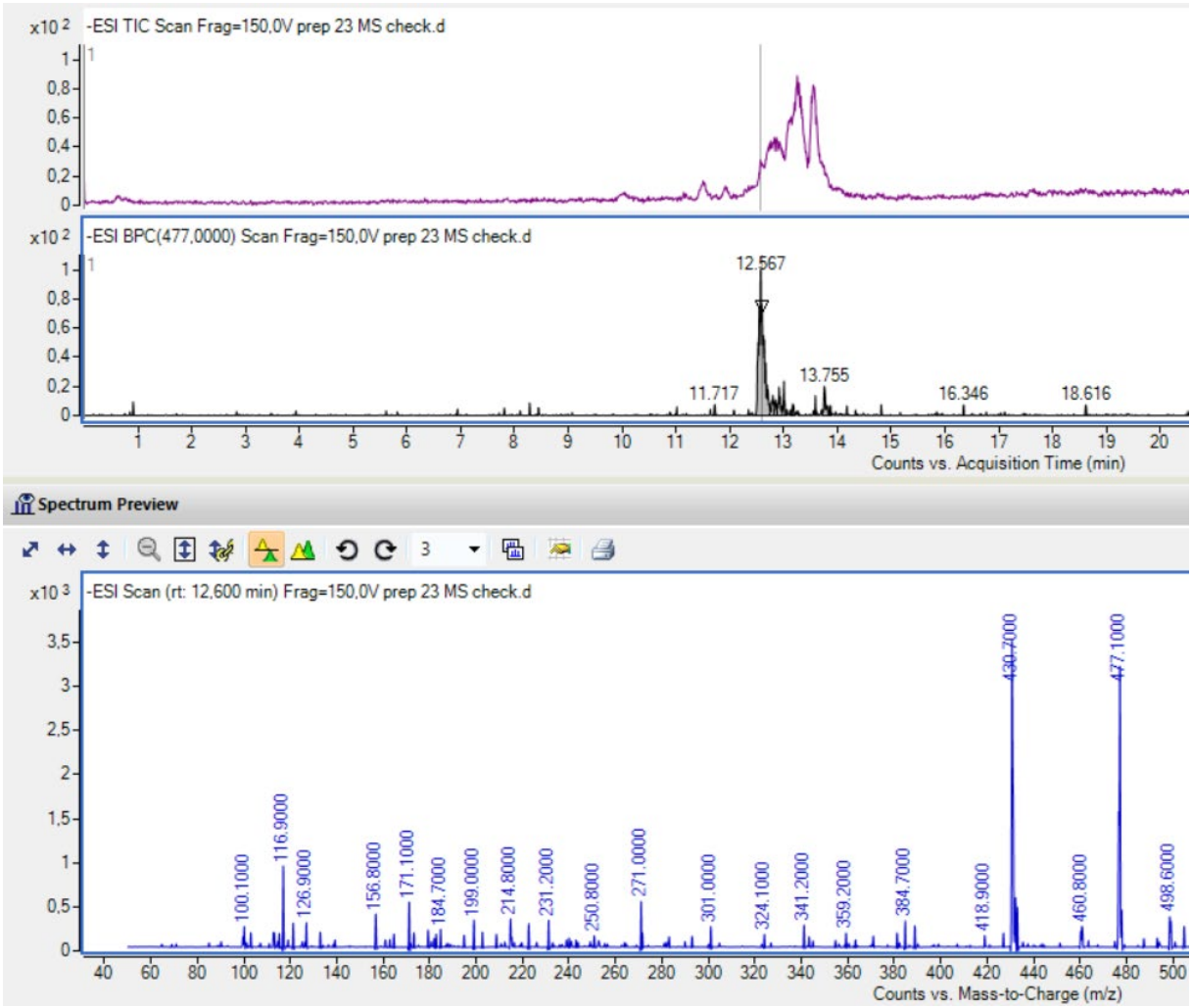

Figure A 11 LC-MS of prep 23, m/z$^-$ 477.1 assumed nepitrin.

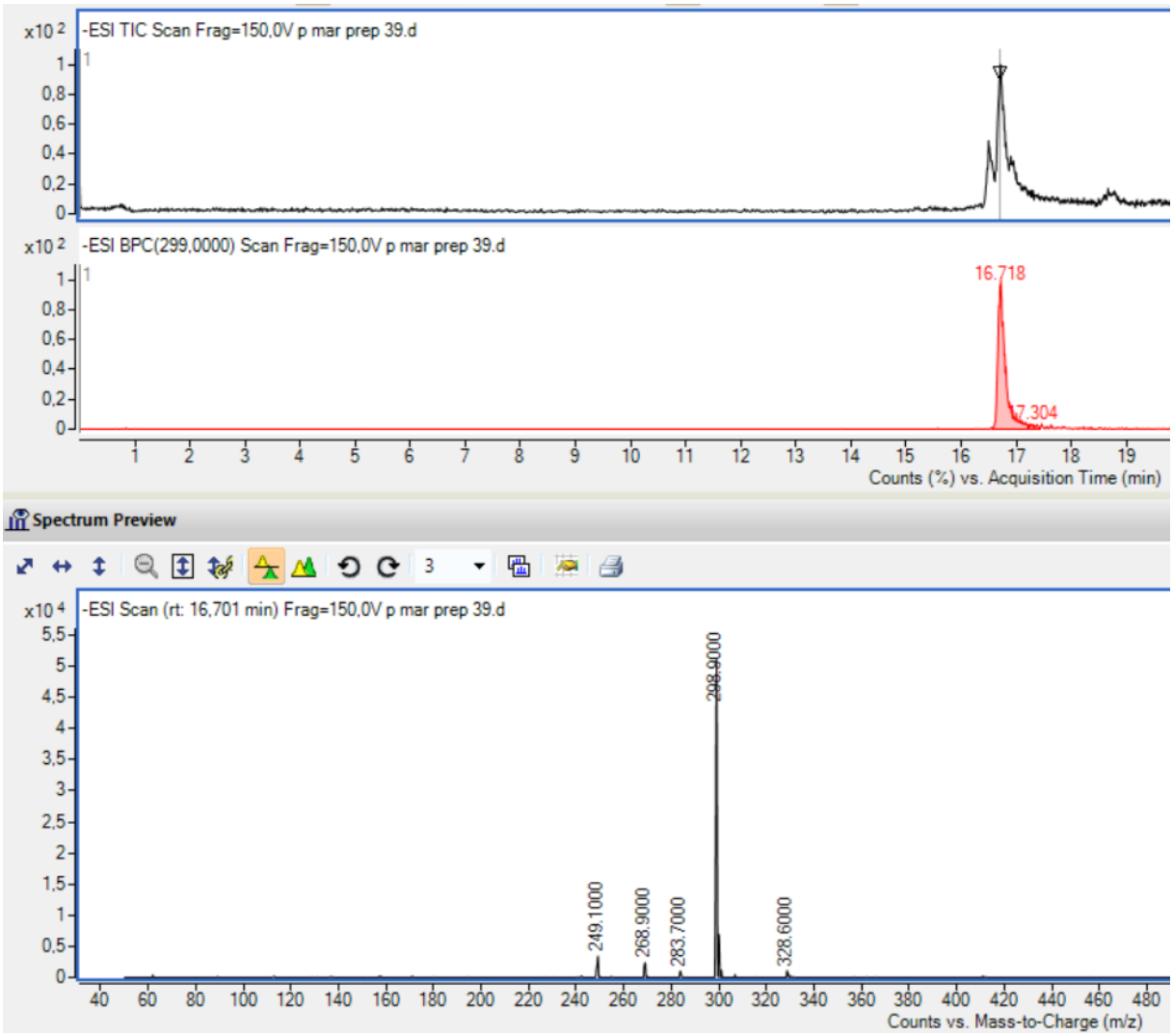

Figure A 12 LC-MS of prep 39, m/z$^-$ 298.9 assumed diosmetin/chrysoeriol.

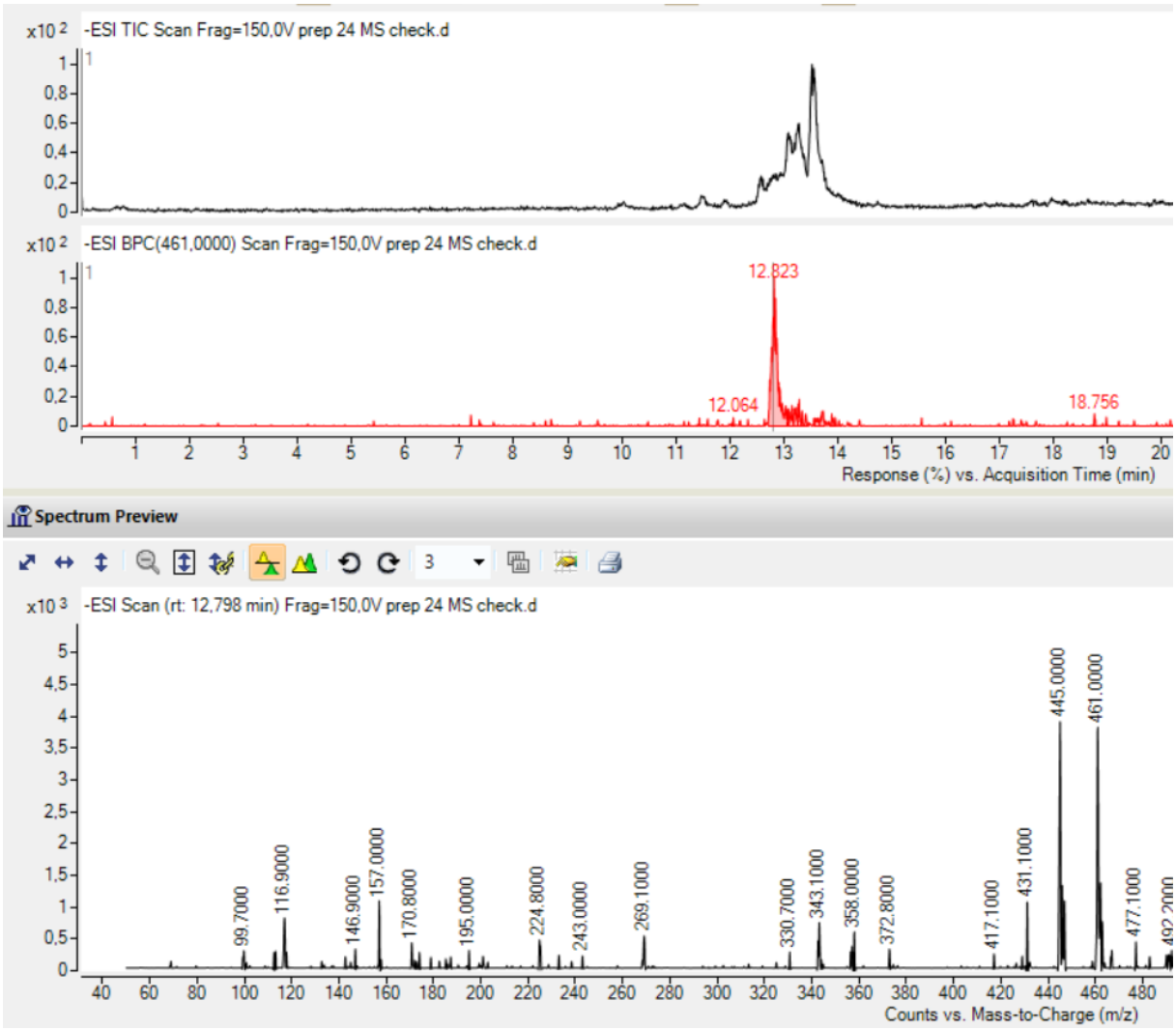

Figure A 13 LC-MS of prep 24 m/z$^-$ 461.0 assumed luteolin glucuronide.

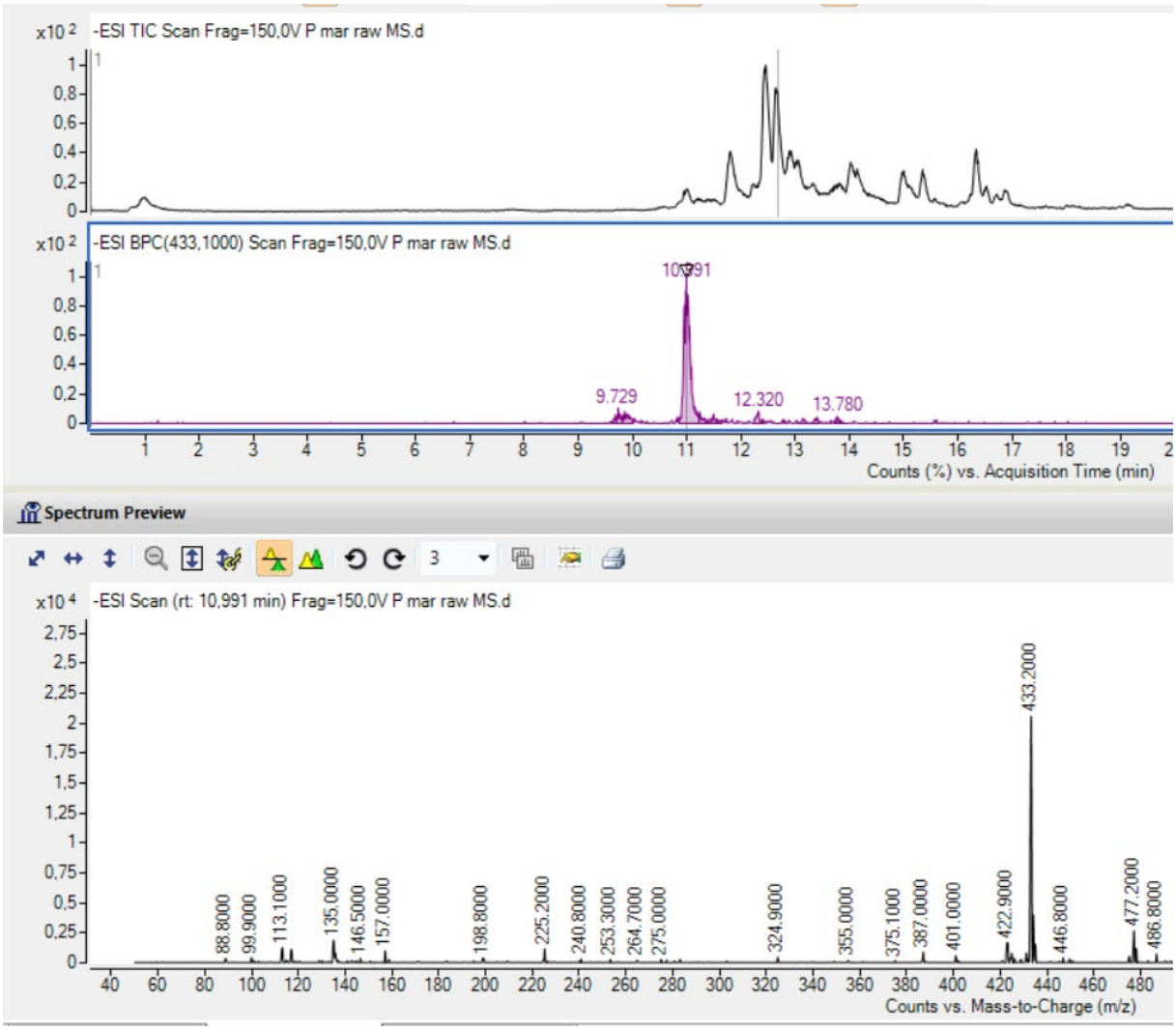

Figure A 14 LC-MS of crude, m/z^{-} 433,2 assumed quercetin arabinoside.

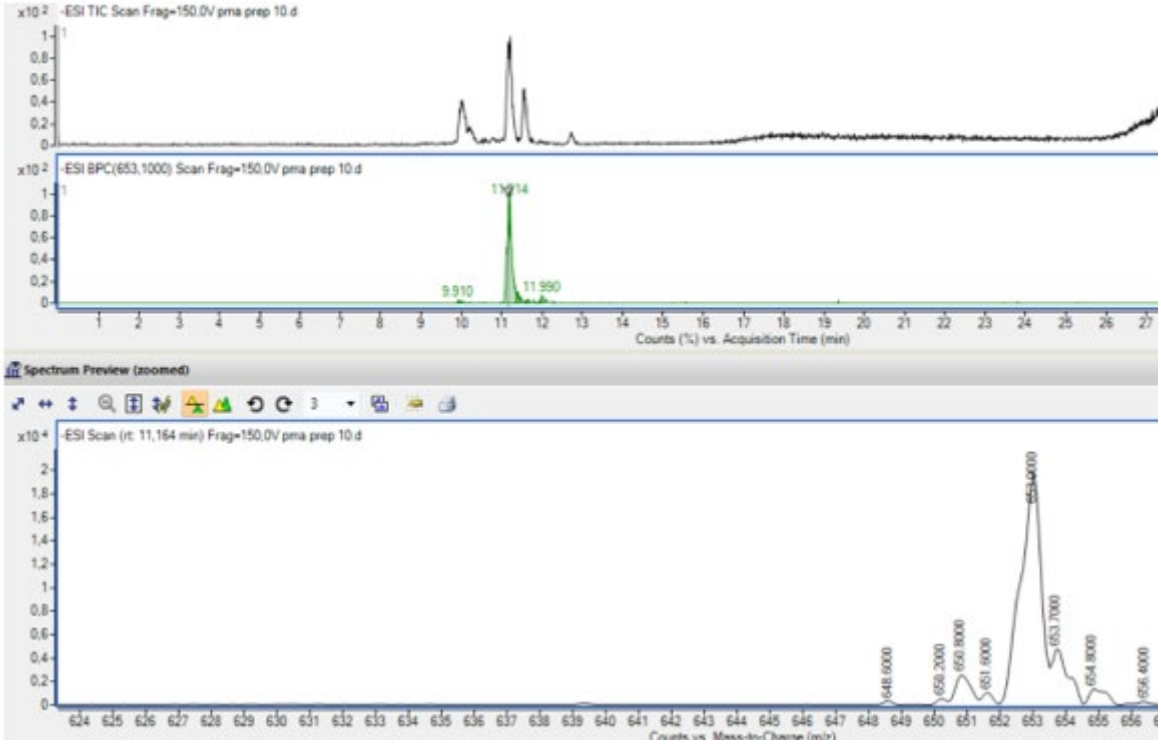

Figure A 15 LC-MS of main peak in prep 10 m/z^{-} of 653.1 suspected of being campneoside I.

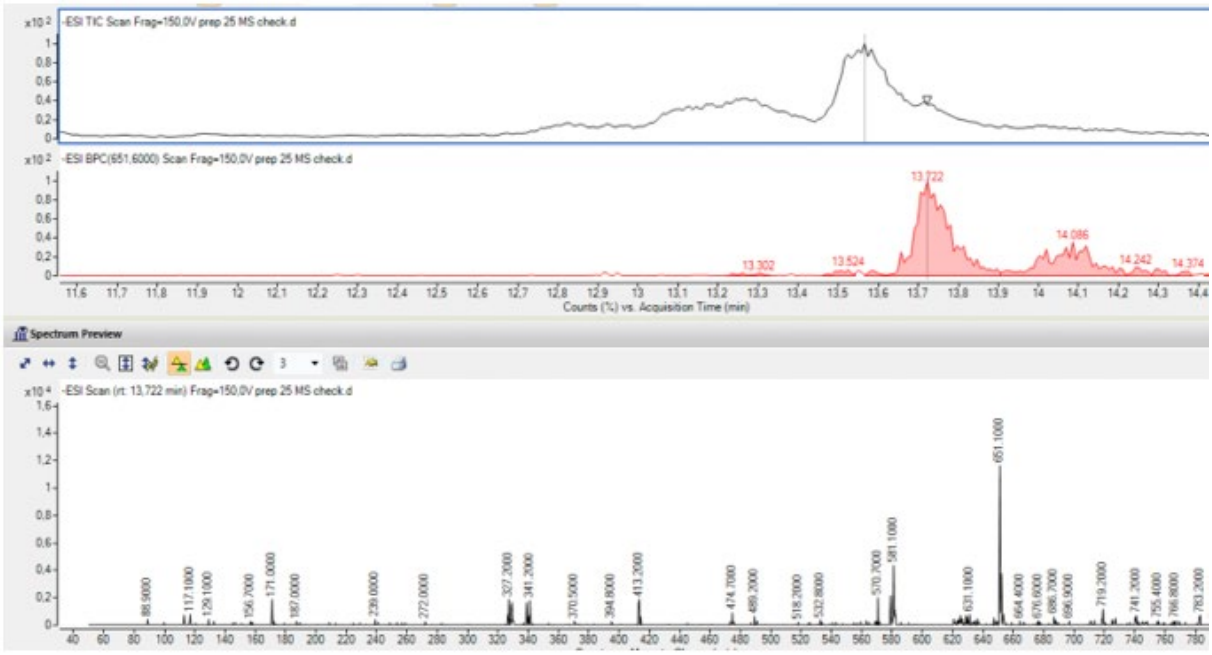

Figure A 16 LC-MS of main peak in prep 25 m/z- of 651 suspected of being martynoside.

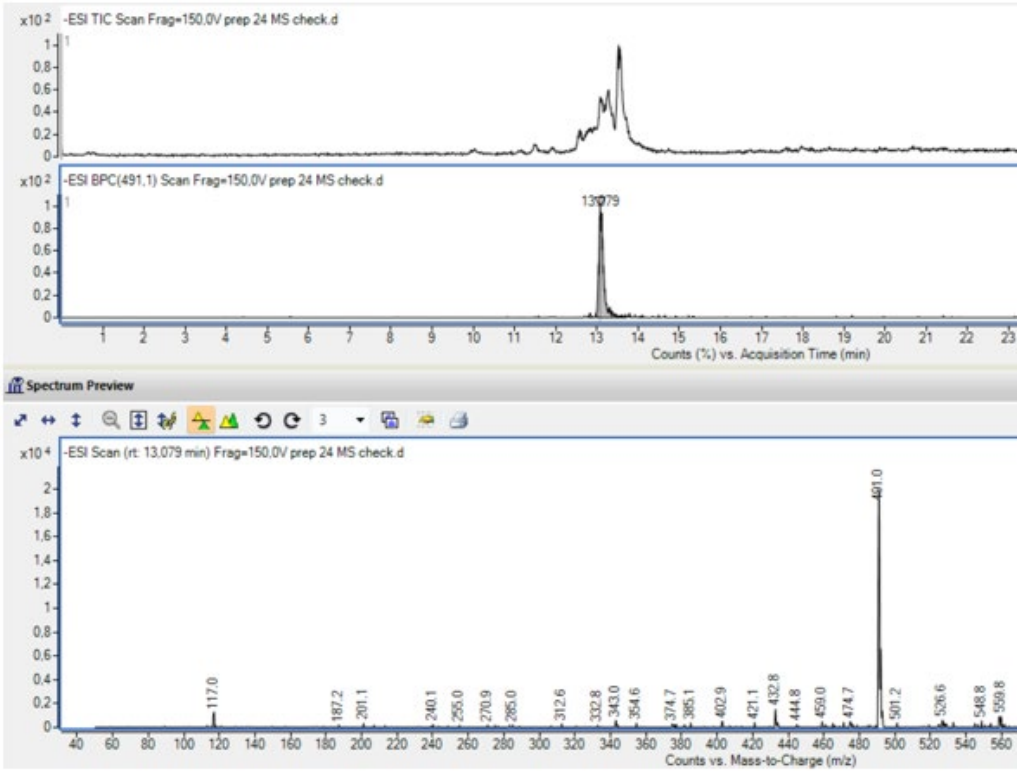

Figure A 17 LC-MS tricin glucoside (m/z$^-$ 491).

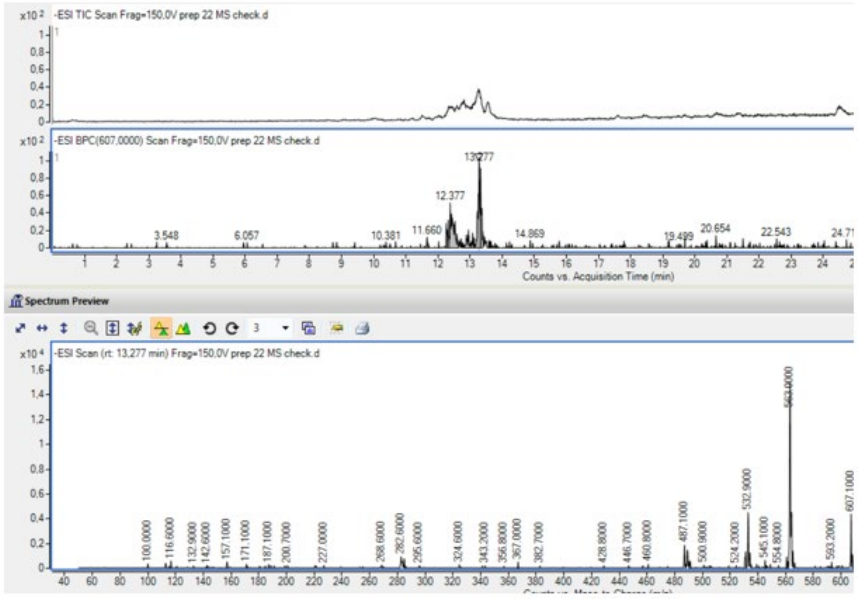

Figure A 18 LC-MS diosmetin rutinoside (m/z$^-$ 607).

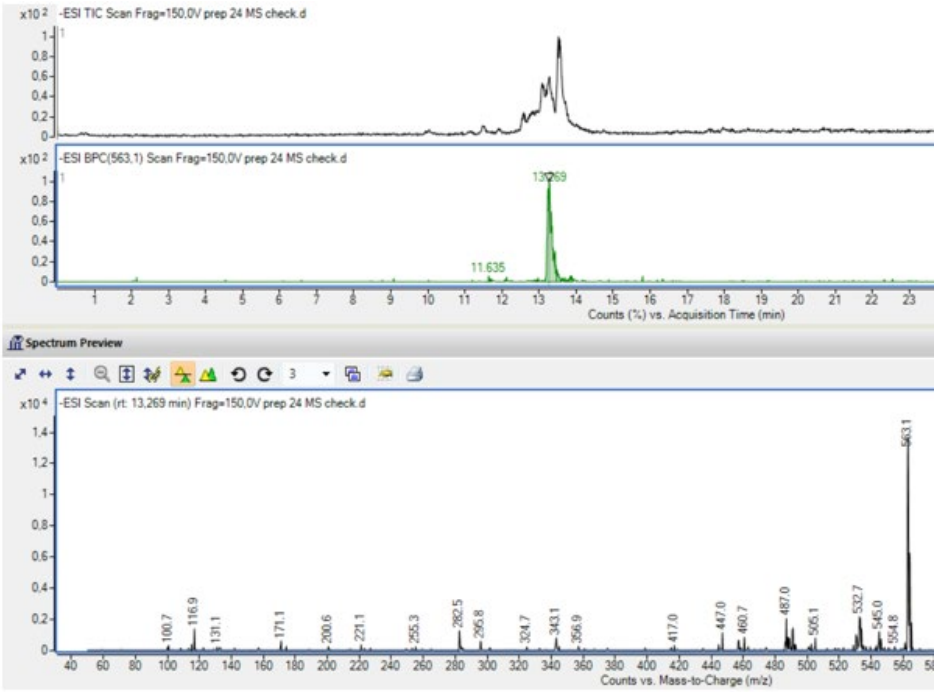

Figure A 19 LC-MS apiin (apigenin 7-apioglucoside) (m/z$^-$ 563.1).

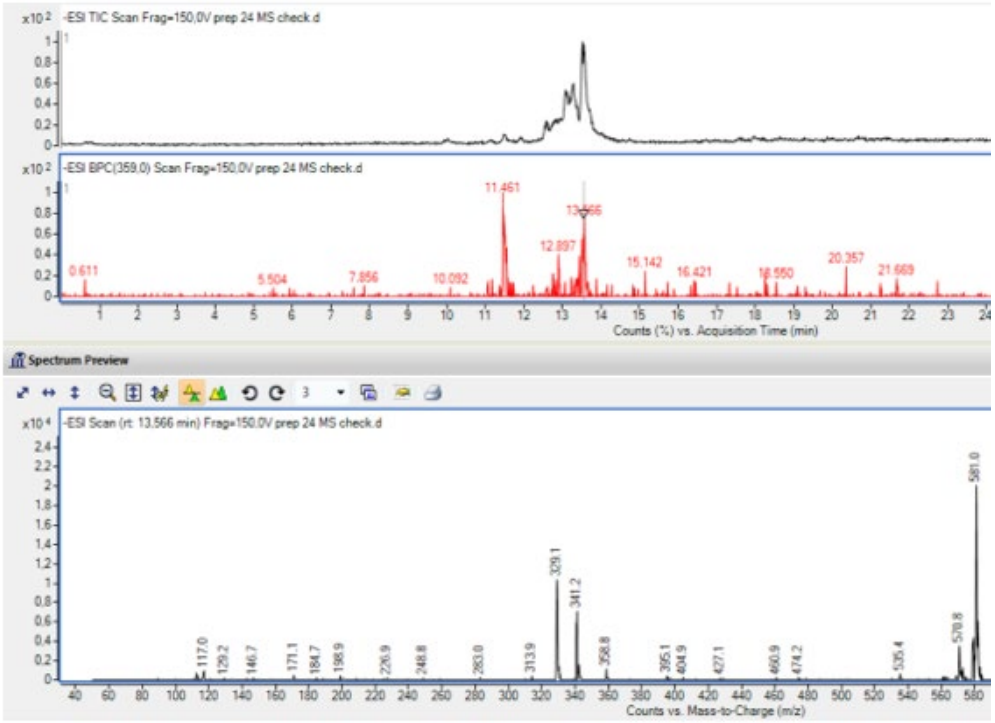

Figure A 20 LC-MS rosmarinic acid (m/z$^-$ 359).

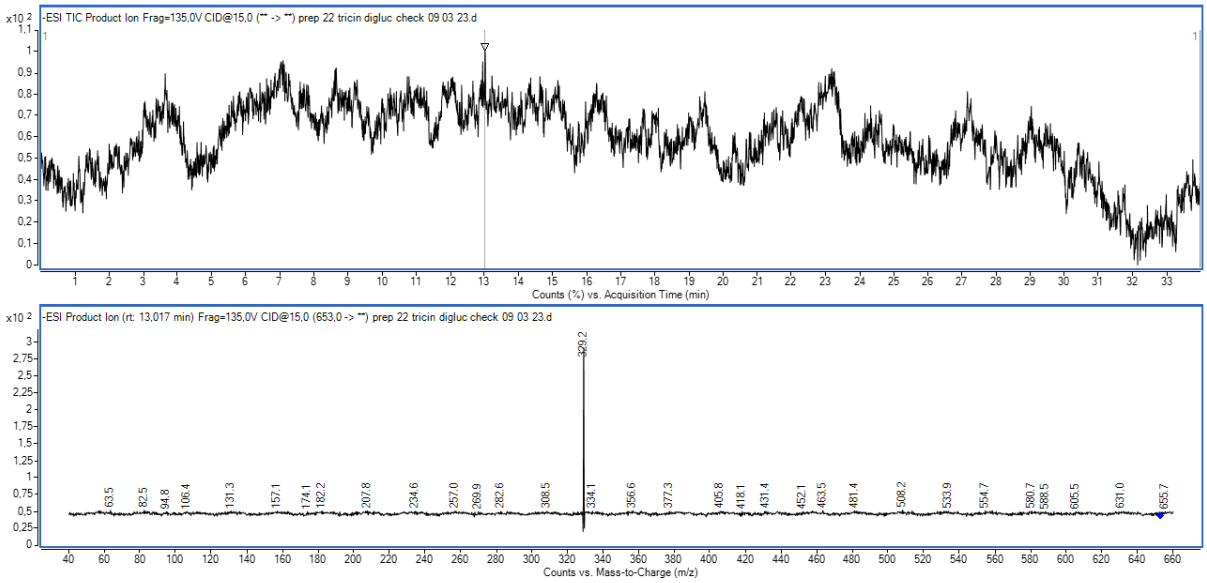

Figure A 21 LC-MS/MS of prep 22 checking for tricin diglucoside (m/z$^-$ 653.1).

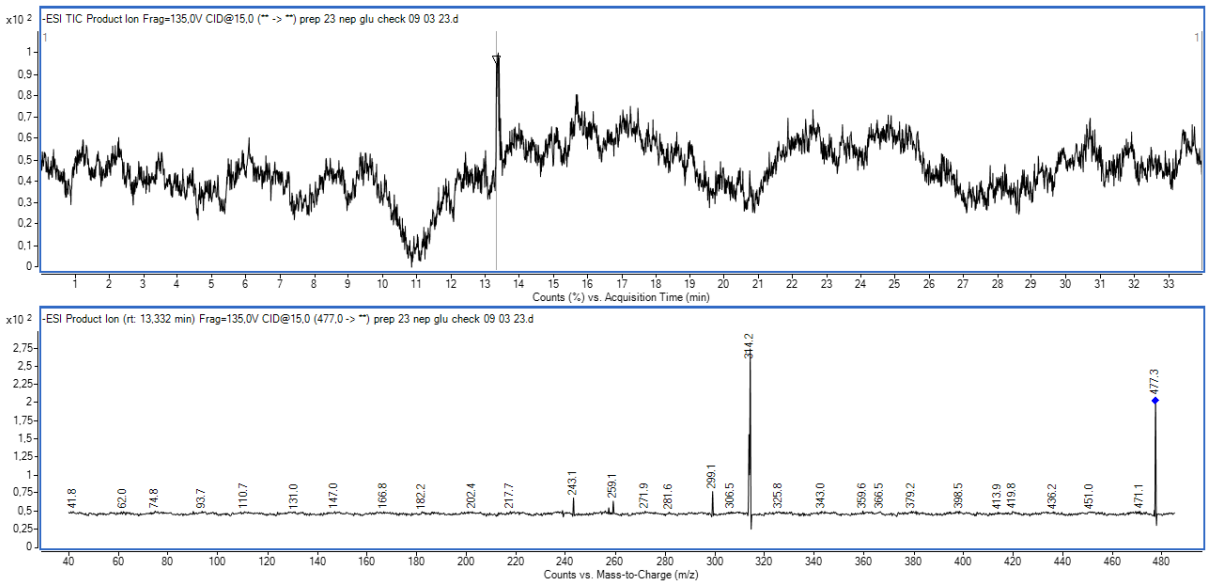

Figure A 22 LC-MS/MS of prep 22 checking for nepitrin (nepetin glucoside) (m/z$^-$ 447.1).

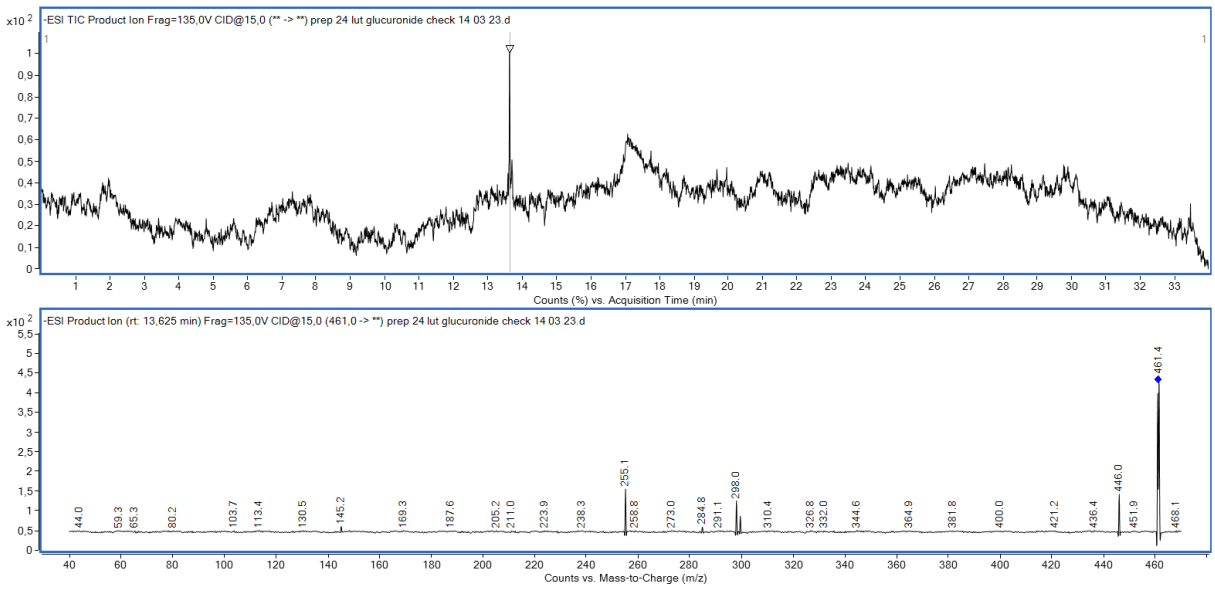

Figure A 23 LC-MS/MS of prep 24 checking for luteolin glucuronide (m/z^- 461).

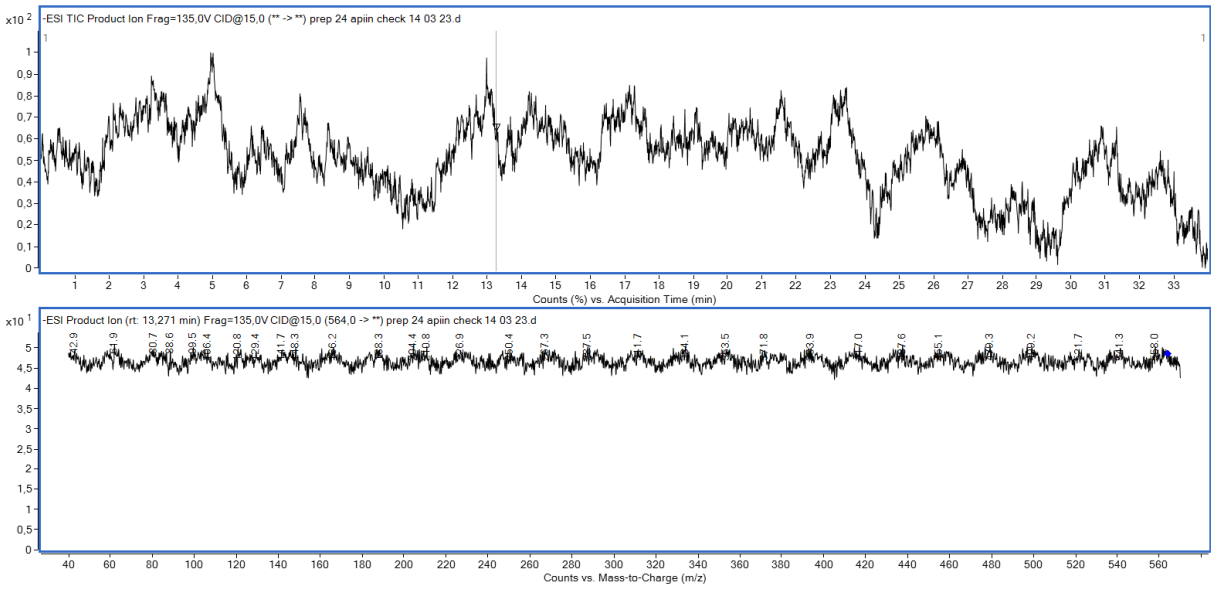

Figure A 24 LC-MS/MS of prep 24 checking for apiin (m/z^- 563.1).

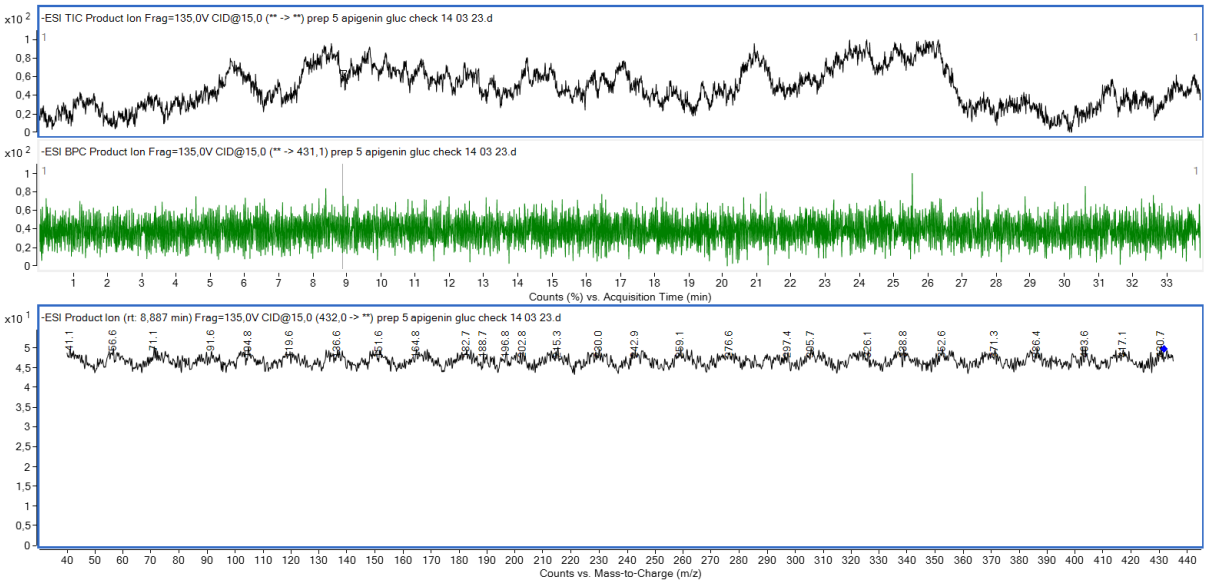

Figure A 25 LC-MS/MS of prep 5 checking for apigenin glucoside (m/z$^-$ 431.1).

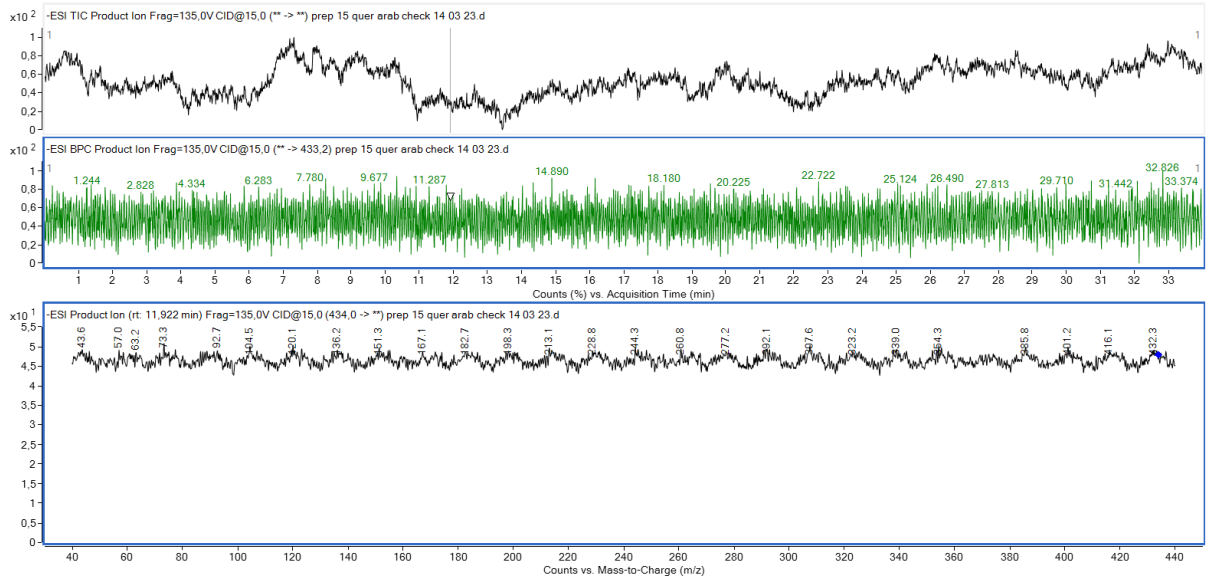

Figure A 26 LC-MS/MS of prep 15 checking for quercetin arabinoside (m/z$^-$ 433).

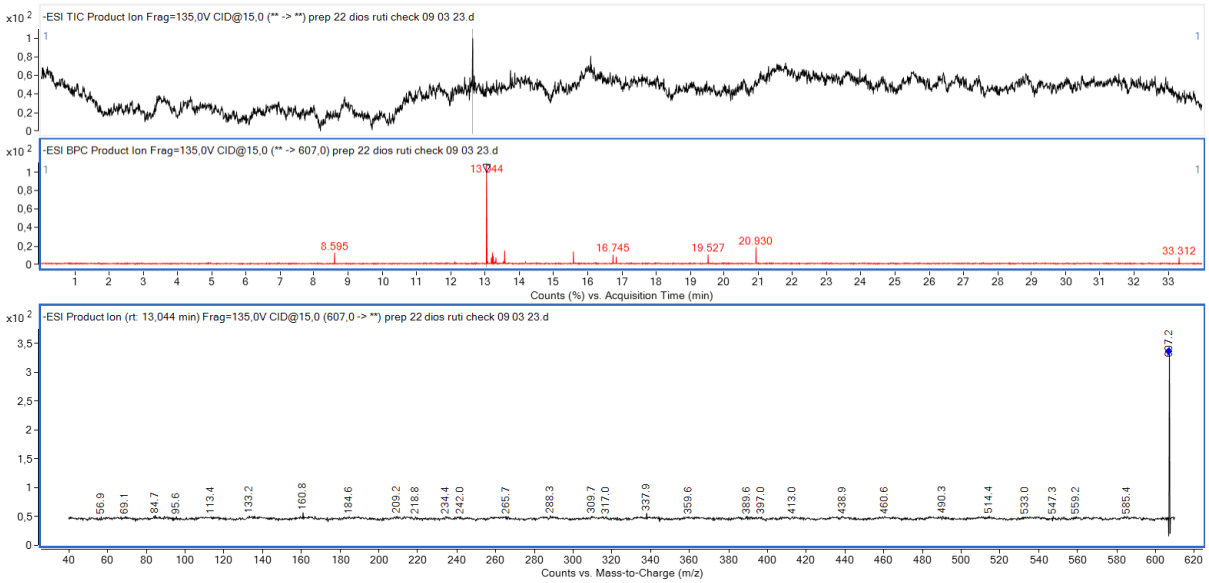

Figure A 27 LC-MS/MS of prep 22 checking for diosmetin rutinoside (m/z^- 607).

Appendix B. UV HPLC figures used for reference in results and discussion.

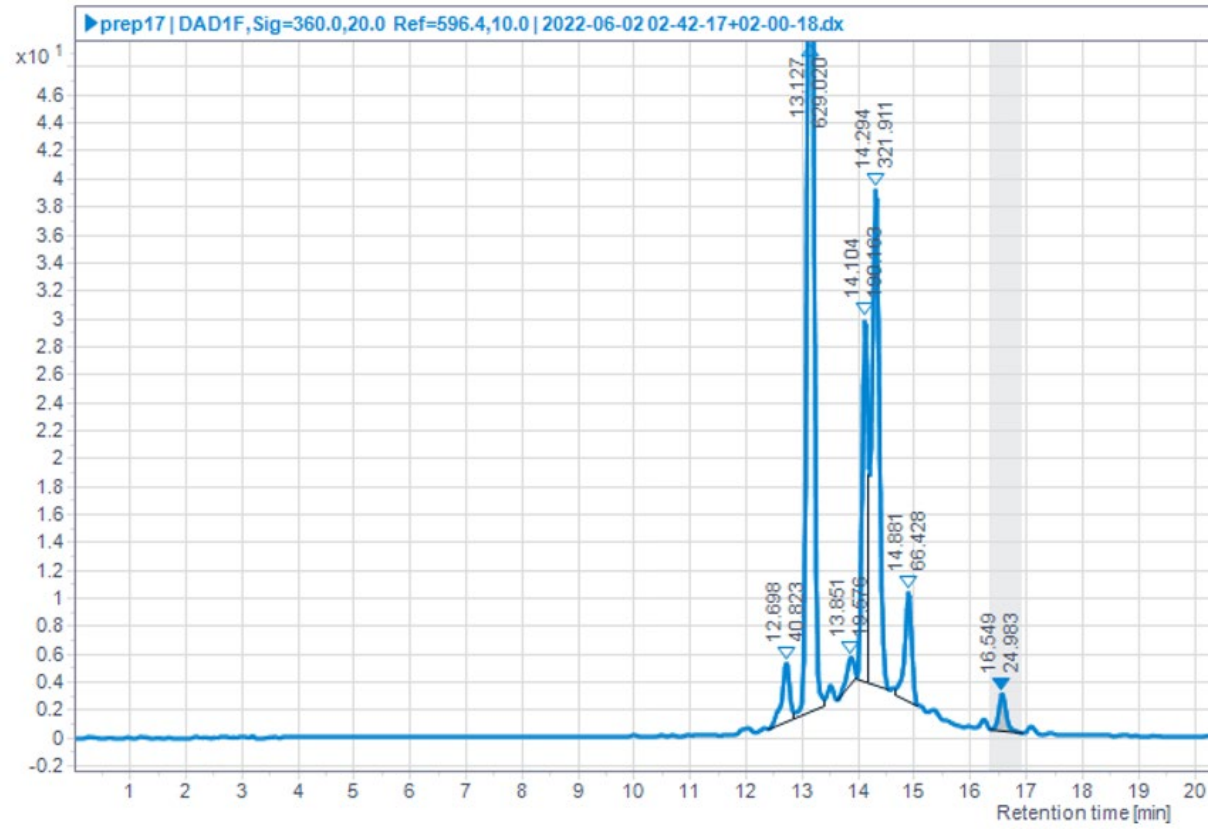

Figure B 1 HPLC of prep prep 17, major peak (Rt 13.127) tentatively containing plantamajoside.

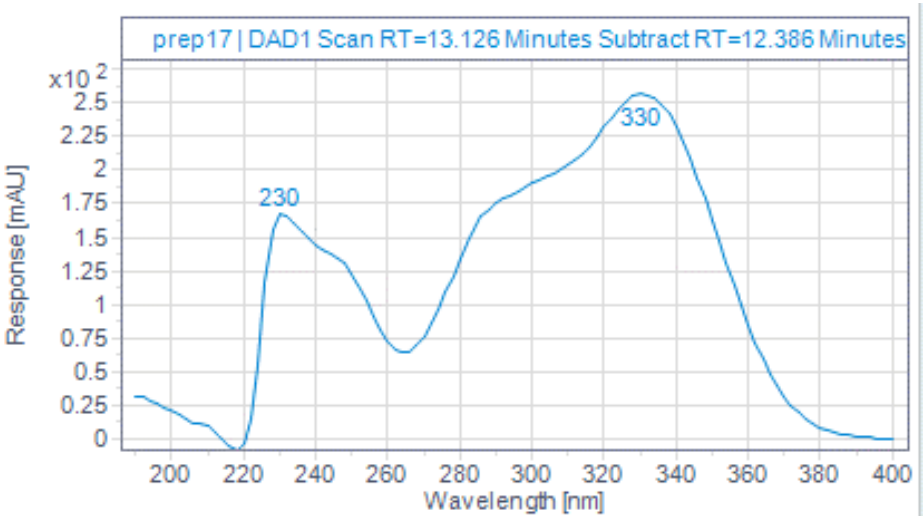

Figure B 2 UV profile of major peak in prep 17 at Rt=13.126 min.

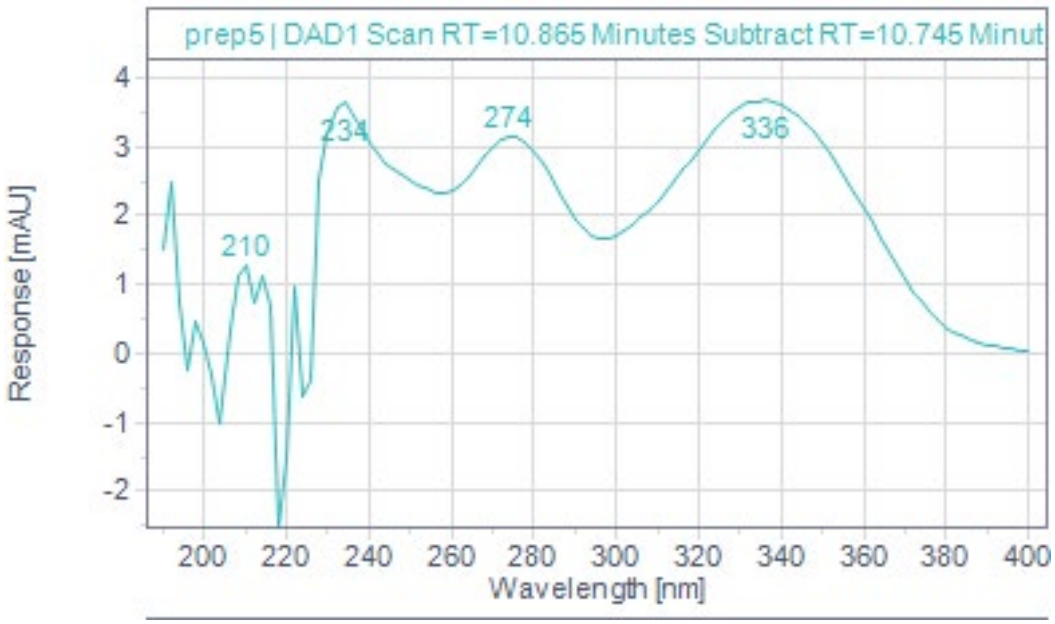

Figure B 3 UV spectrum of medium peak in prep 5 (336 and 274nm) tentatively containing apigenin glucoside.

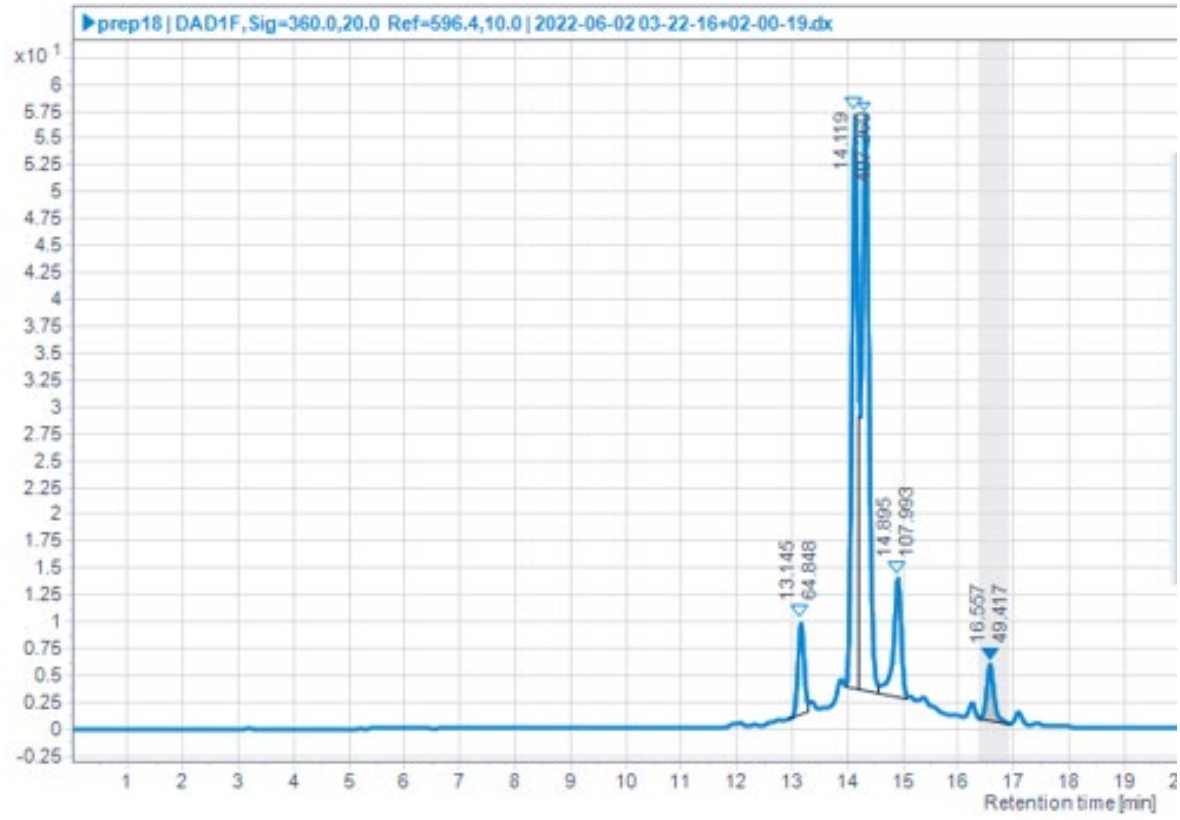

Figure B 4 Prep 18, minor peak (Rt 13.148 min) tentatively containing verbascoside.

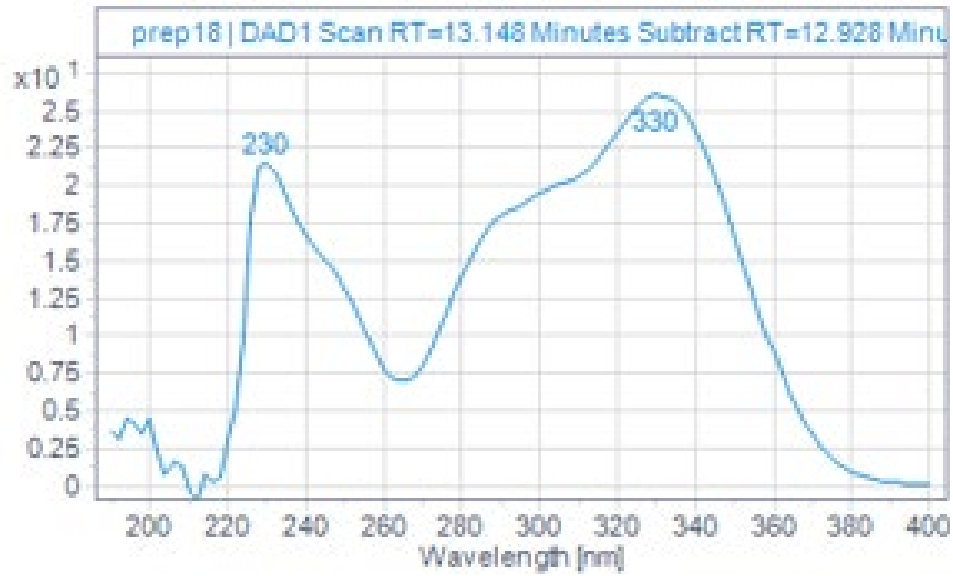

Figure B 5 UV of prep 18 tentatively containing verbascoside.

Prep sample 18 was also analyzed using LC-MS and no plantamajoside peak was found. A lack of plantamajoside suggests that it is instead verbascoside that is present, LC-MS also supports this.

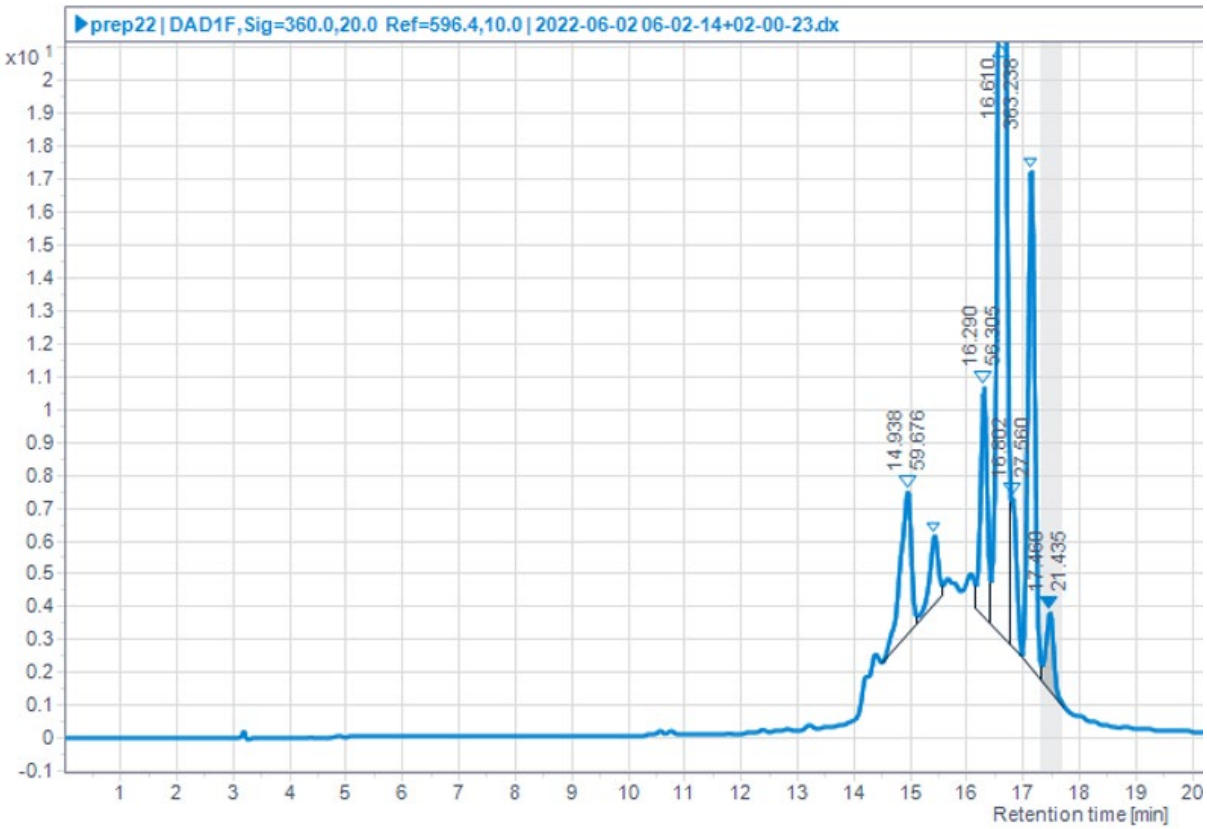

Figure B 6 HPLC of prep sample 22, major peak (Rt 16.610 min) tentatively containing luteolin 7 – O – glucoside.

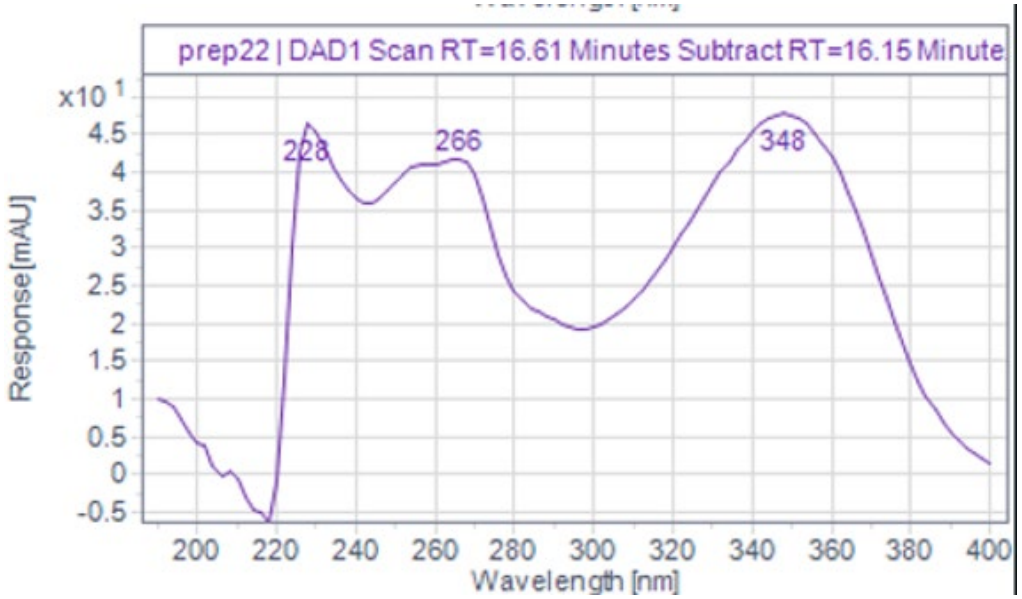

Figure B 7 UV chromatogram of dominant peak in prep 22.

The UV/vis spectra showing λmax = 348 with a local λmax = 266 suggests luteolin 7-O-glucoside (Lin, Lu, and Harnly 2007).

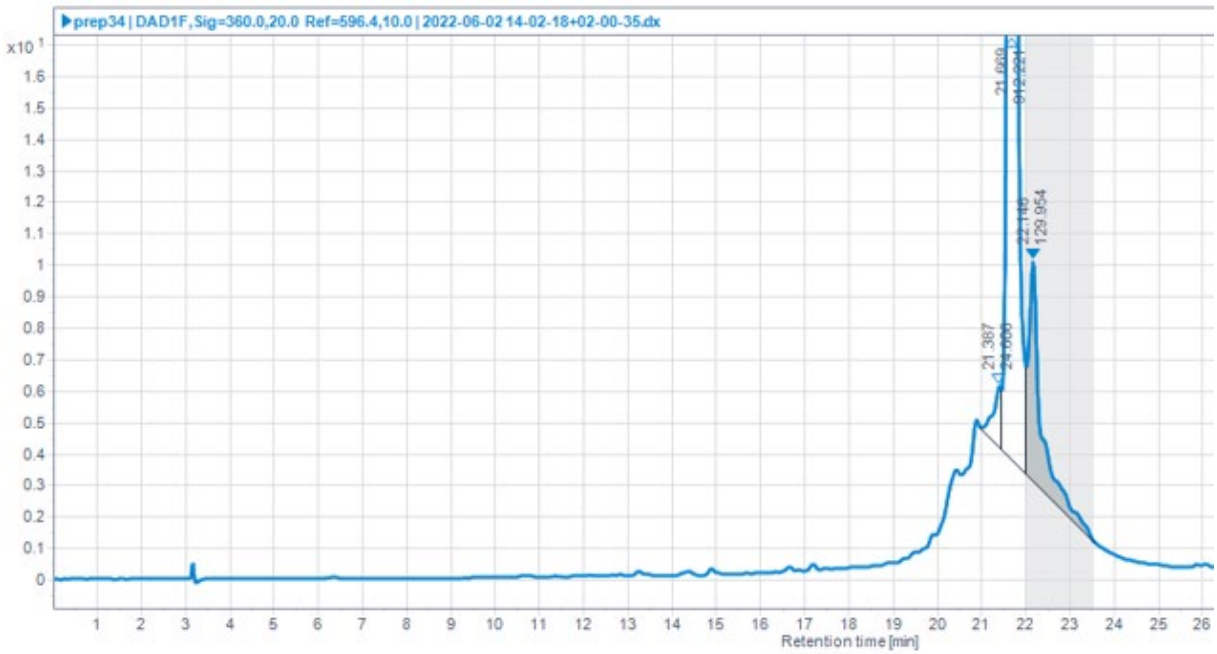

Figure B 8. chromatogram of HPLC prep 34, major peak (Rt 26.672 min) tentatively containing luteolin.

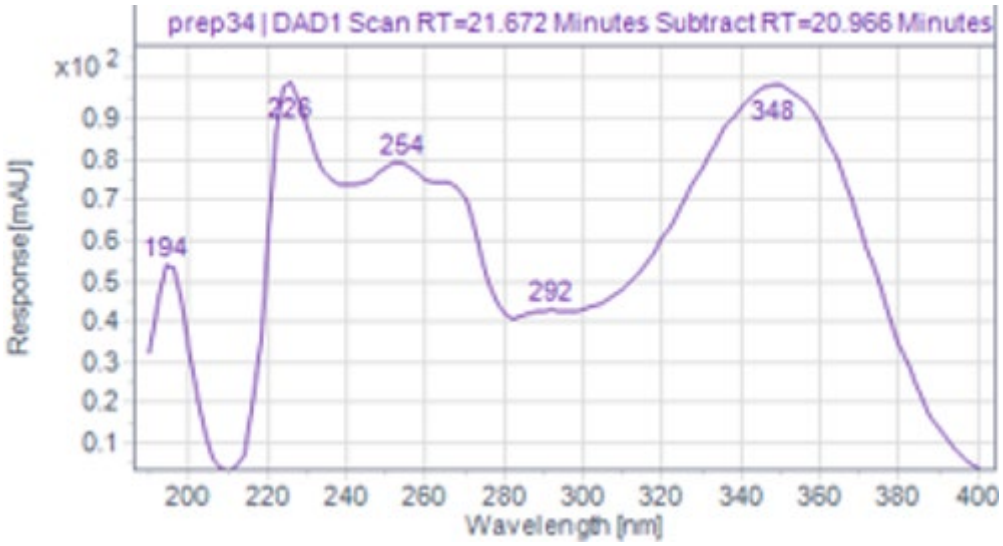

Figure B 9 UV chromatogram of dominant peak (Rt 21.672 min) in prep 34The UV/vis spectra showing λmax =348 with a local λmax = 254 and 226 suggests luteolin. LC-MS shows a major peak with m/z- 285 which corresponds with said peak containing luteolin.

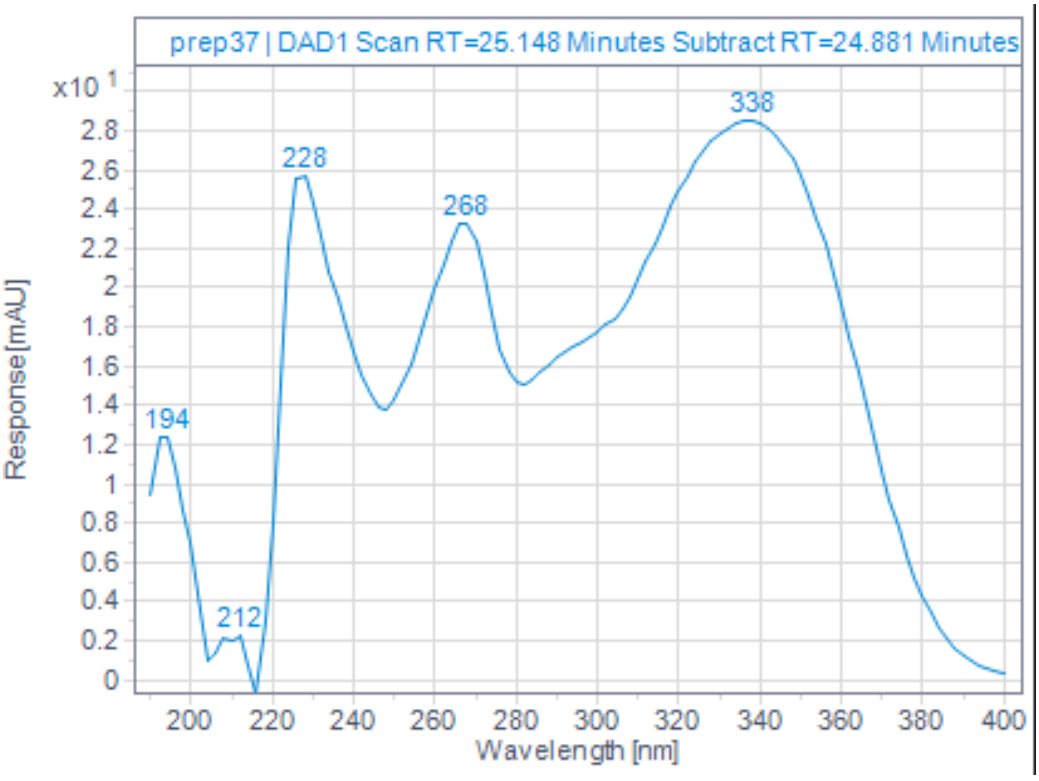

Figure B 10 UV chromatogram of dominant peak (Rt 25.148 min) in prep 37 tentatively containing apigenin.

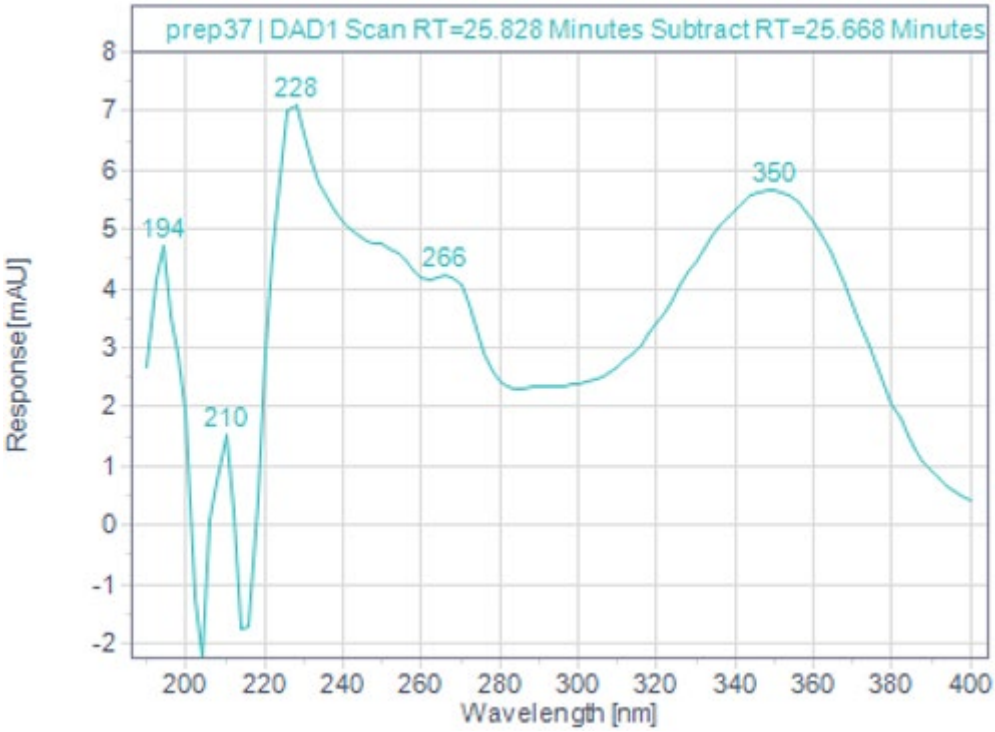

Figure B 12 UV spectra of tentatively tricin peak (Rt 25.828 min) in *Plantago maritima* prep 37.

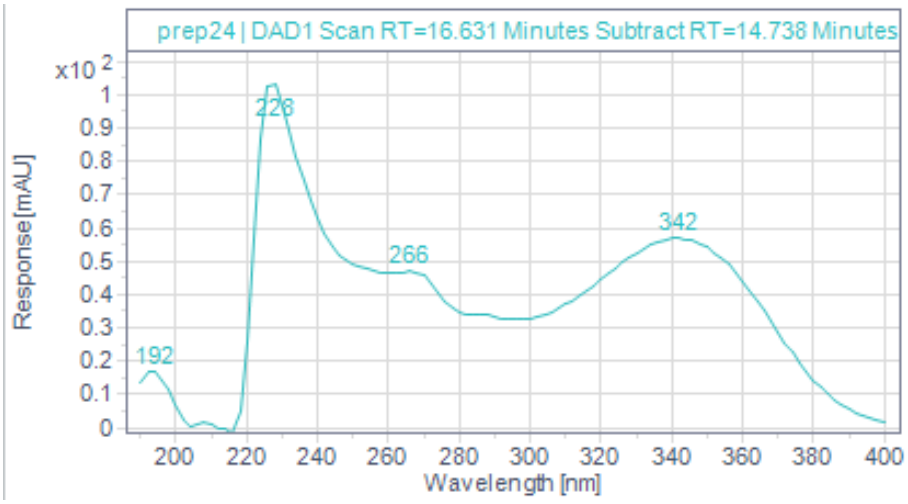

Figure B 13 UV spectra of prep 24 peak (Rt 16.631 min) tentatively tricin glucoside.

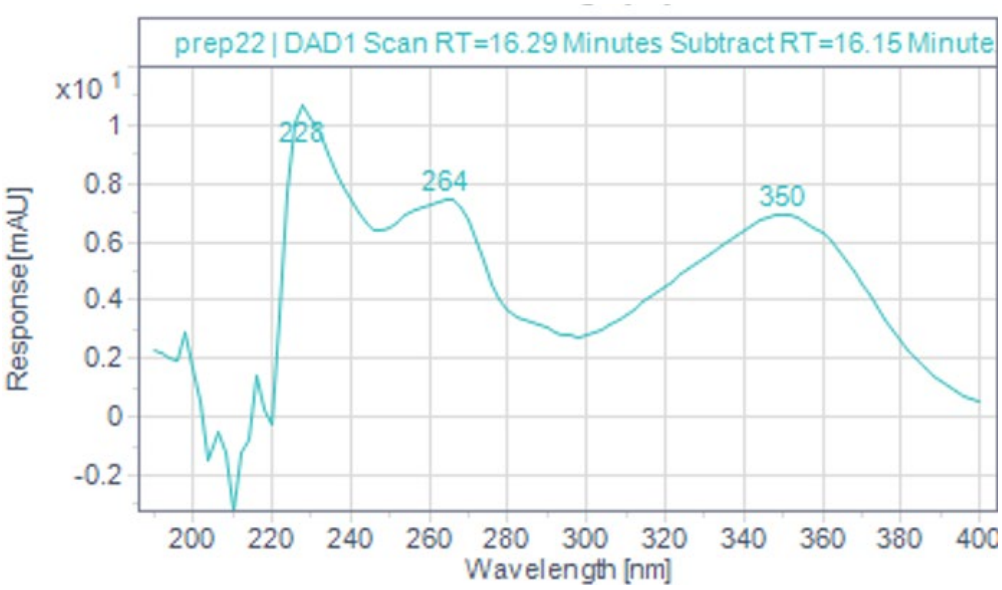

Figure B 14 UV spectra prep 22 (Rt 16.29 min) tentatively tricin diglucoside.

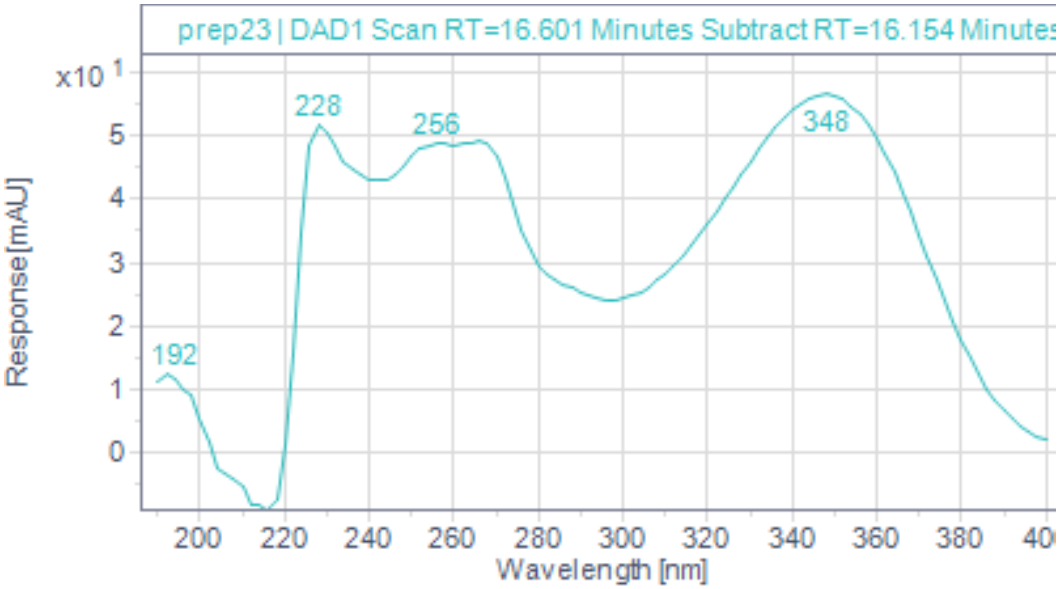

Figure B 15 UV spectra prep 23 (Rt 16.601 min) tentatively nepitrin (6-methoxy luteolin 7 glucoside).

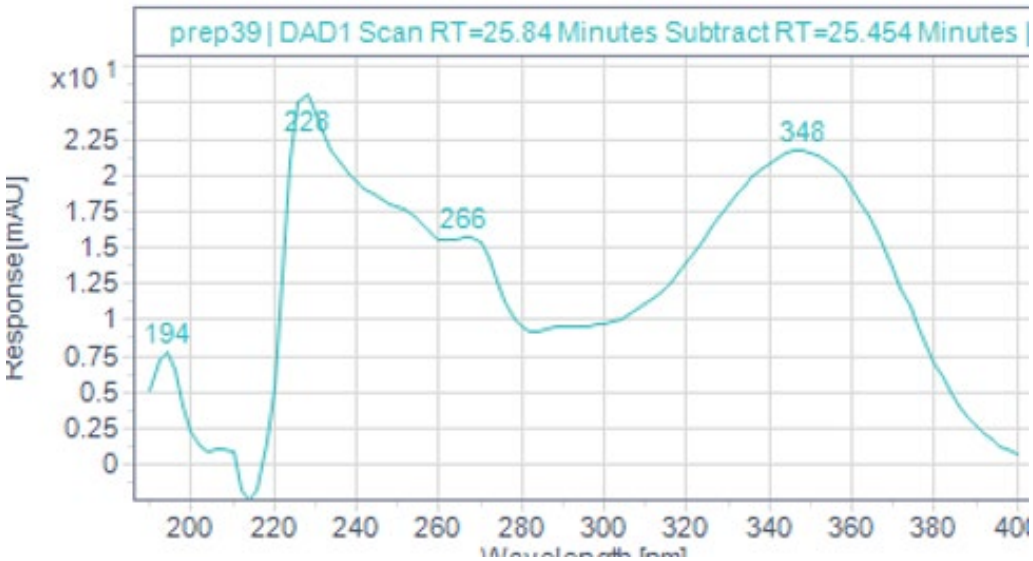

Figure B 16 UV spectra prep 39 (Rt 25.84 min) tentatively diosmetin/chrysoeriol.

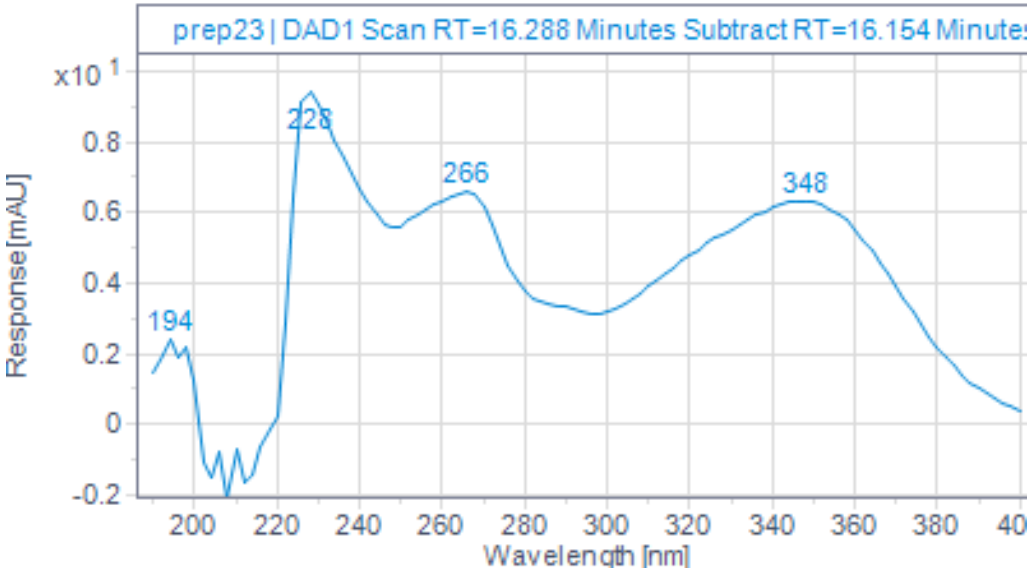

Figure B 17 UV spectra prep 23 (Rt 16.288 min) tentatively luteolin glucuronide.

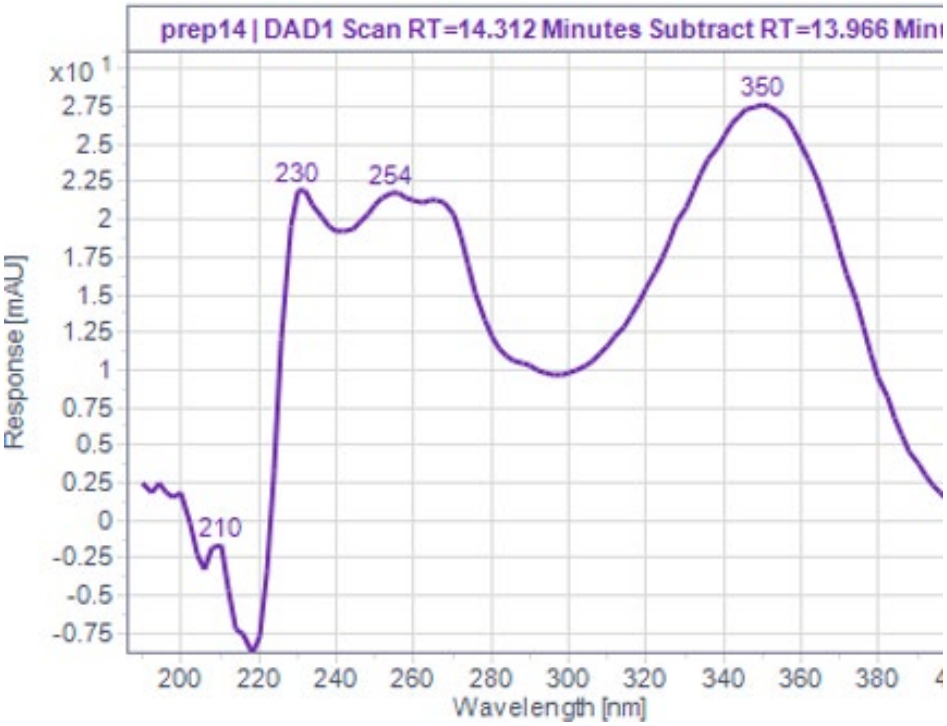

Figure B 18 UV spectra prep 14 (Rt 14.312 min) tentatively quercetin arabinoside.

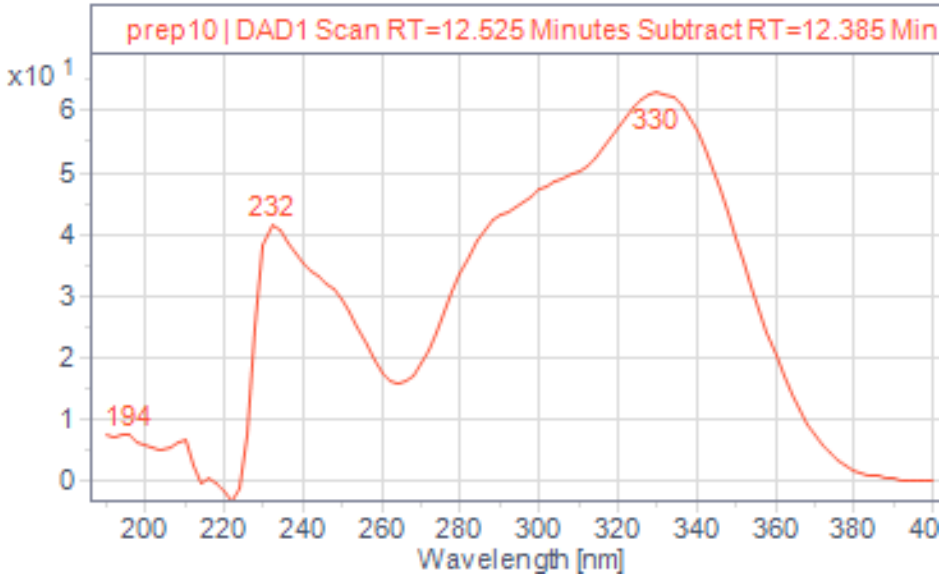

Figure B 19 UV/vis spectra of prep 10 main peak (Rt 12.525 min), tentatively containing campneoside I.

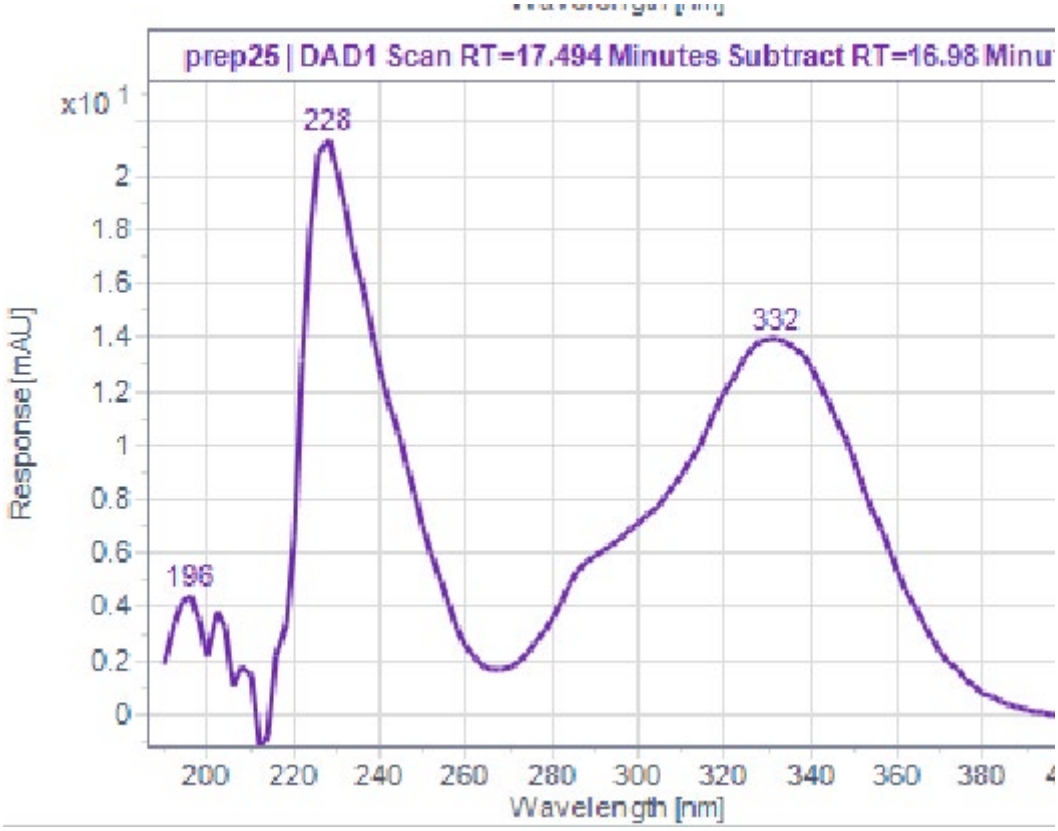

Figure B 20 UV/vis spectra of prep 25 main peak (Rt 17.494 min), tentatively containing martynoside.

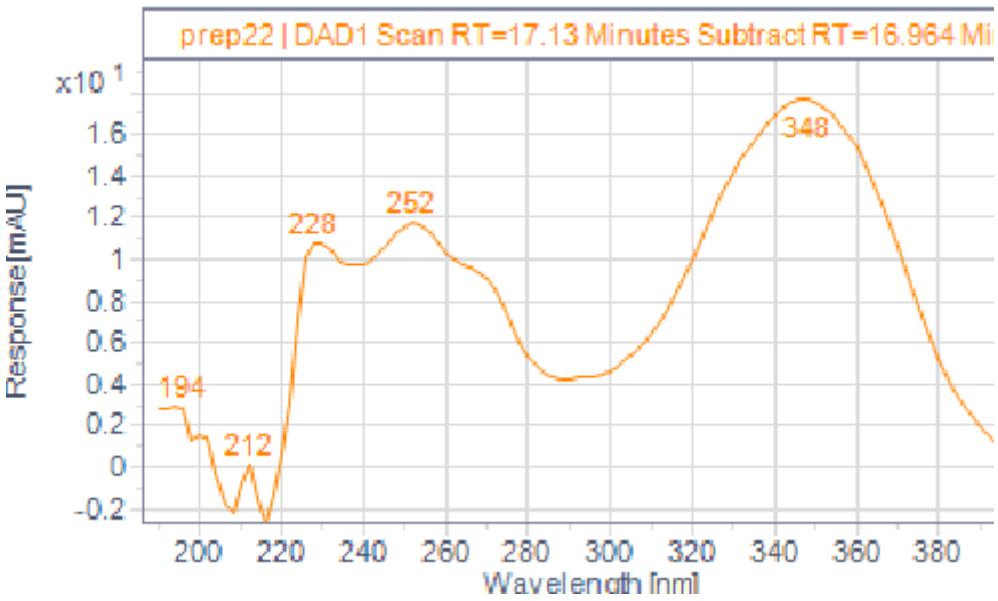

Figure B 22 UV/vis spectra of prep 22 (Rt 17.13 min) measured UV 348 252 tentatively containing diosmetin rutinoside.

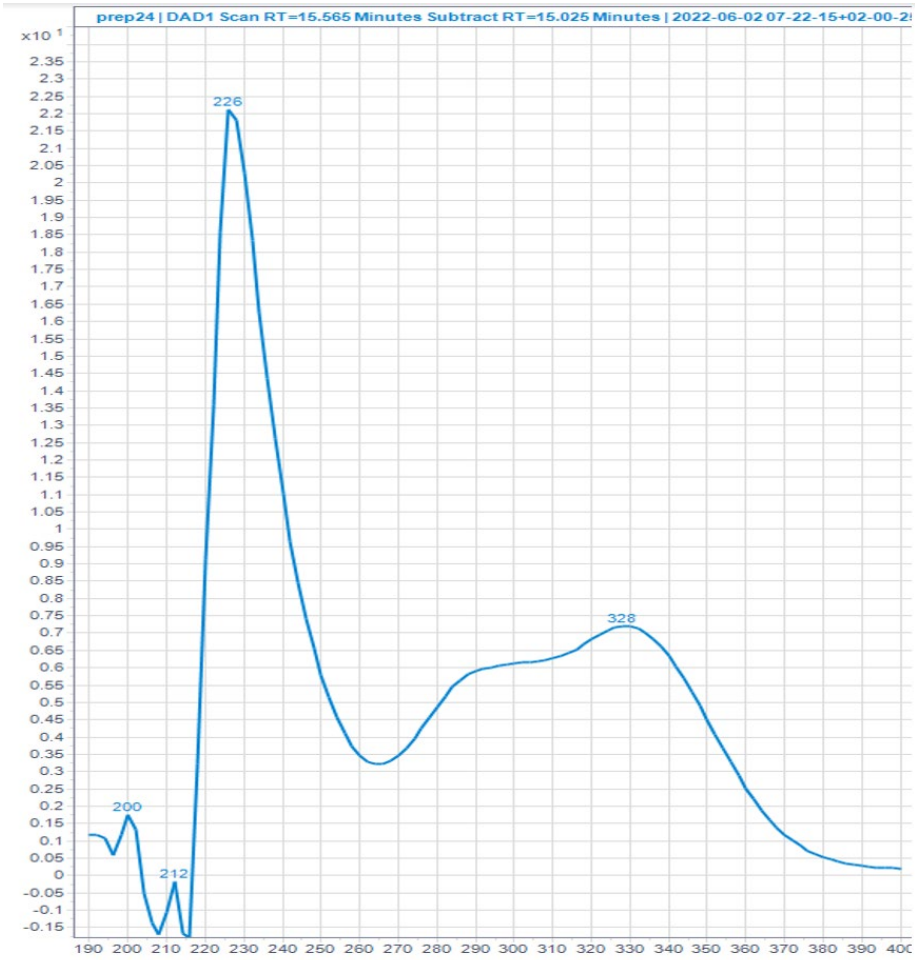

Figure B 23 UV/vis spectra of crude (Rt 15.565 min) tentatively rosmarinic acid.

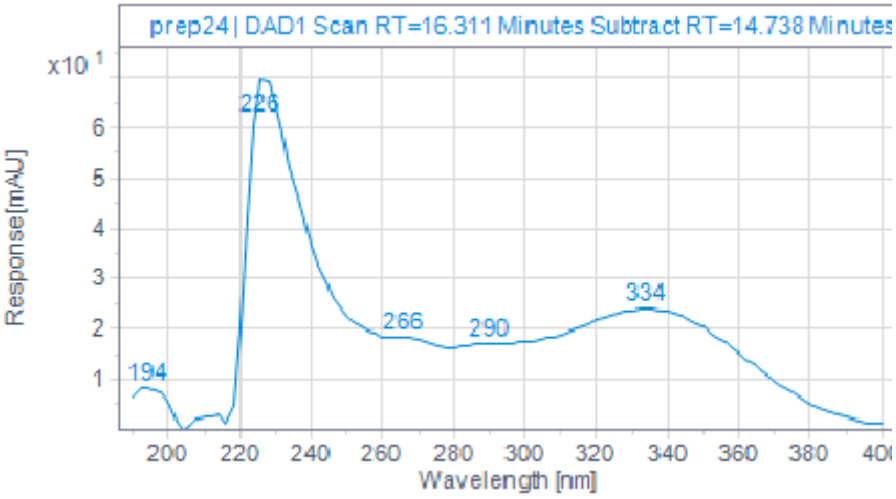

Figure B 24 UV/vis spectra of prep 24 (Rt 16.311 min) tentatively containing apiin.

4 References

Alipieva, Kalina, Liudmila Korkina, Ilkay Erdogan Orhan, and Milen I. Georgiev. 2014. "Verbascoside — A Review of Its Occurrence, (Bio)Synthesis and Pharmacological Significance." *Biotechnology Advances*, From Plants to Pharmacy Shelf: Recent Trends in Leads Finding and Bioproduction, 32 (6): 1065–76. https://doi.org/10.1016/j.biotechadv.2014.07.001.

"Alpha(α) and Beta(β) Glucose: Comparison, Structures, Explanation." 2022. *PSIBERG* (blog). January 1, 2022. https://psiberg.com/alpha-and-beta-glucose/.

"Angiosperms - NatureWorks." n.d. Accessed April 15, 2023. https://nhpbs.org/natureworks/nwep14f.htm.

Arnold, Ulrike W., Christian Zidorn, Ernst P. Ellmerer, and Hermann Stuppner. 2002. "Iridoid and Phenolic Glycosides from Wulfenia Carinthiaca." *Zeitschrift Für Naturforschung C* 57 (11–12): 969–75. https://doi.org/10.1515/znc-2002-11-1202.

Bakke, Nadia Maria. 2020. "Analysis of Flavonoids In," 36.

Beara, Ivana N., Marija M. Lesjak, Emilija Đ. Jovin, Kristina J. Balog, Goran T. Anačkov, Dejan Z. Orčić, and Neda M. Mimica-Dukić. 2009. "Plantain (Plantago L.) Species as Novel Sources of Flavonoid Antioxidants." *Journal of Agricultural and Food Chemistry* 57 (19): 9268–73. https://doi.org/10.1021/jf902205m.

Beara, Ivana N., Marija M. Lesjak, Dejan Z. Orčić, Nataša Đ. Simin, Dragana D. Četojević-Simin, Biljana N. Božin, and Neda M. Mimica-Dukić. 2012. "Comparative Analysis of Phenolic Profile, Antioxidant, Anti-Inflammatory and Cytotoxic Activity of Two Closely-Related Plantain Species: Plantago Altissima L. and Plantago Lanceolata L." *LWT - Food Science and Technology* 47 (1): 64–70. https://doi.org/10.1016/j.lwt.2012.01.001.

Bernatek, Erling Reinholdt, Einar Uggerud, and Bjørn Pedersen. 2019. "karbohydrater – kjemi." In *Store norske leksikon*. http://snl.no/karbohydrater_-_kjemi.

Bertin, Lorenzo, Francesco Ferri, Alberto Scoma, Leonardo Marchetti, and Fabio Fava. 2011. "Recovery of High Added Value Natural Polyphenols from Actual Olive Mill Wastewater through Solid Phase Extraction." *Chemical Engineering Journal*, Special Section: Symposium on Post-Combustion Carbon Dioxide Capture, 171 (3): 1287–93. https://doi.org/10.1016/j.cej.2011.05.056.

Budzianowska, Anna, and Jaromir Budzianowski. 2022. "A New Flavonoid, a New Phenylethanoid Glycoside and Related Compounds Isolated from the Inflorescences of Plantago Lanceolata L." *Natural Product Research* 36 (15): 3813–24. https://doi.org/10.1080/14786419.2021.1888289.

Budzianowska, Anna, Lutosława Skrzypczak, and Jaromir Budzianowski. 2004. "Phenylethanoid Glucosides from in Vitro Propagated Plants and Callus Cultures of Plantago Lanceolata." *Planta Medica* 70 (9): 834–40. https://doi.org/10.1055/s-2004-827232.

Cory, Hannah, Simone Passarelli, John Szeto, Martha Tamez, and Josiemer Mattei. 2018. "The Role of Polyphenols in Human Health and Food Systems: A Mini-Review." *Frontiers in Nutrition* 5 (September): 87. https://doi.org/10.3389/fnut.2018.00087.

Davey, Matthew P., David N. Bryant, Ian Cummins, Trevor W. Ashenden, Phillip Gates, Robert Baxter, and Robert Edwards. 2004. "Effects of Elevated CO2 on the Vasculature and Phenolic Secondary Metabolism of Plantago Maritima." *Phytochemistry* 65 (15): 2197–2204. https://doi.org/10.1016/j.phytochem.2004.06.016.

Duynstee, Howard I., Martijn C. de Koning, Huib Ovaa, Gijs A. van der Marel, and Jacques H. van Boom. 1999. "Synthesis of Verbascoside: A Dihydroxyphenylethyl Glycoside with Diverse Bioactivity." *European Journal of Organic Chemistry* 1999 (10): 2623–32. https://doi.org/10.1002/(SICI)1099-0690(199910)1999:10<2623::AID-EJOC2623>3.0.CO;2-K.

Enerstvedt, Kjersti Hasle. 2018. "ANALYSIS OF POLYPHENOLIC CONTENT IN MARINE AND AQUATIC ANGIOSPERMS FROM NORWEGIAN COASTAL WATERS," 170.

ERSÖZ, TAYFUN, DENİZ TAŞDEMİR, İHSAN ÇALIŞ, and CHRIS IRELAND. 2002. “Phenylethanoid Glycosides from Scutellaria Galericulata.” *Turkish Journal of Chemistry* 26 (4): 465–72. https://doi.org/-.

evan. 2014. “Benchtop Biochemistry: Looking at Glucose Anomers with Spinsolve.” *Magritek* (blog). December 23, 2014. https://magritek.com/2014/12/23/benchtop-biochemistry-looking-at-glucose-anomers-with-spinsolve/.

Falcone Ferreyra, Maria Lorena, Sebastián Rius, and Paula Casati. 2012. “Flavonoids: Biosynthesis, Biological Functions, and Biotechnological Applications.” *Frontiers in Plant Science* 3. https://www.frontiersin.org/articles/10.3389/fpls.2012.00222.

Feng, Wei-sheng, Hao Zhiyou, and Meng Li. 2017. “Isolation and Structure Identification of Flavonoids.” In . https://doi.org/10.5772/67810.

“Figure 6: Schematic Representation of the Electrospray Ionization Process.” 2022. ResearchGate. March 9, 2022. https://www.researchgate.net/figure/Schematic-representation-of-the-electrospray-ionization-process_fig31_225050758.

Fiz, M. Paz Velázquez, Ana M. Díaz Lanza, and Lidia Fernández Matellano. 2000. “Polyphenolic Compounds from Plantago Lagopus L.” *Zeitschrift Für Naturforschung C* 55 (11–12): 877–80. https://doi.org/10.1515/znc-2000-11-1205.

Fleming, Ian, and Dudley Williams. 2020. *Spectroscopic Methods in Organic Chemistry*. Springer Nature.

Fraser, Christopher M., and Clint Chapple. 2011. “The Phenylpropanoid Pathway in Arabidopsis.” *The Arabidopsis Book / American Society of Plant Biologists* 9 (December): e0152. https://doi.org/10.1199/tab.0152.

“Gamle Tegninger Av Strandkjempe.” 2022. 2022. https://www.rolv.no/bilder/galleri/tegninger/plantago_maritima.htm.

Goufo, Piebiep, Rupesh Kumar Singh, and Isabel Cortez. 2020. “A Reference List of Phenolic Compounds (Including Stilbenes) in Grapevine (Vitis Vinifera L.) Roots, Woods, Canes, Stems, and Leaves.” *Antioxidants (Basel, Switzerland)* 9 (5): E398. https://doi.org/10.3390/antiox9050398.

Harrata, Kamel. 1995. “Mass Spectrometry Tutorial (Dr. Kamel Harrata) | Chemical Instrumentation Facility | Iowa State University.” 1995. https://www.cif.iastate.edu/mass-spec/ms-tutorial.

Heldt, Hans-Walter, and Birgit Piechulla. 2021. *Plant Biochemistry*. Academic Press.

“HPLC Help Center.” 2021. 2021. https://www.idex-hs.com/literature-tools/educational-materials/hplc-center/.

Janković, Teodora, Gordana Zdunić, Ivana Beara, Kristina Bekvalac, Dejan Pljevljakusic, Danijela Stešević, and Katarina Šavikin. 2012. “Comparative Study of Some Polyphenols in Plantago Species.” *Biochemical Systematics and Ecology* 42 (June): 69–74. https://doi.org/10.1016/j.bse.2012.02.013.

“JEOL USA Blog | A Quick Introduction to Triple-Quadrupole Mass Spectrometry.” 2022. February 23, 2022. https://www.jeolusa.com/BLOG/triple-quad-mass-spectrometry.

Kahraman, Hüseyin. 2019. “The Importance of L-Rhamnose Sugar.” *Biomedical Journal of Scientific & Technical Research* 21 (3): 15906–8. https://doi.org/10.26717/BJSTR.2019.21.003606.

Kawada, Toshinari, Yuko Yoneda, Ryuji Asano, Ippei Kan-no, and Walther Schmid. 2006. “Synthesis of Plantamajoside, a Bioactive Dihydroxyphenylethyl Glycoside from Plantago Major L.” 60 (5): 492–97. https://doi.org/10.1515/HF.2006.081.

Kawashty, S. A., E. Gamal-el-din, M. F. Abdalla, and N. A. M. Saleh. 1994. “Flavonoids of Plantago Species in Egypt.” *Biochemical Systematics and Ecology* 22 (7): 729–33. https://doi.org/10.1016/0305-1978(94)90058-2.

Kotova, Elina, Semen Kotov, and A. Kotov. 2021. “STUDY OF CHROMATOGRAPHIC FINGERPRINT OF FLAVONOID COMPOUNDS OF THE BUR-MARIGOLD HERB.” *Scientific Study & Research: Chemistry & Chemical Engineering, Biotechnology, Food Industry* 22 (April).

Lech, Katarzyna, Katarzyna Witkoś, and Maciej Jarosz. 2014. “HPLC–UV–ESI MS/MS Identification of the Color Constituents of Sawwort (Serratula Tinctoria L.).” *Analytical and Bioanalytical Chemistry* 406 (15): 3703–8. https://doi.org/10.1007/s00216-013-7589-3.

Lee, Seon-Hye, Heon-Woong Kim, Min-Ki Lee, Young Jin Kim, Gelila Asamenew, Youn-Soo Cha, and Jung-Bong Kim. 2018. “Phenolic Profiling and Quantitative Determination of Common Sage (Salvia Plebeia R. Br.) by UPLC-DAD-QTOF/MS.” *European Food Research and Technology* 244 (9): 1637–46. https://doi.org/10.1007/s00217-018-3076-6.

Li, B., D. H. Robinson, and D. F. Birt. 1997. “Evaluation of Properties of Apigenin and [G-3H]Apigenin and Analytic Method Development.” *Journal of Pharmaceutical Sciences* 86 (6): 721–25. https://doi.org/10.1021/js960383s.

Li, Mi, Yunqiao Pu, Chang Geun Yoo, and Arthur J. Ragauskas. 2016. “The Occurrence of Tricin and Its Derivatives in Plants.” *Green Chemistry* 18 (6): 1439–54. https://doi.org/10.1039/C5GC03062E.

Lin, Long-Ze, and James M. Harnly. 2007. “A Screening Method for the Identification of Glycosylated Flavonoids and Other Phenolic Compounds Using a Standard Analytical Approach for All Plant Materials.” *Journal of Agricultural and Food Chemistry* 55 (4): 1084–96. https://doi.org/10.1021/jf062431s.

Lin, Long-Ze, Shengmin Lu, and James M. Harnly. 2007. “Detection and Quantification of Glycosylated Flavonoid Malonates in Celery, Chinese Celery, and Celery Seed by LC-DAD-ESI/MS.” *Journal of Agricultural and Food Chemistry* 55 (4): 1321–26. https://doi.org/10.1021/jf0624796.

Ludick, N.J.J. 2020. “Method Development for Extraction and HPLC Analysis of Kaempferol, Chrysin and Quercetin.” N.J.J. Ludick.

Maréchal, Eric. 2019. “Marine and Freshwater Plants: Challenges and Expectations.” *Frontiers in Plant Science* 10: 1545. https://doi.org/10.3389/fpls.2019.01545.

Mark, T. D. 1982. “Fundamental Aspects of Electron Impact Ionization.” *International Journal of Mass Spectrometry and Ion Physics*, Mass Spectrometry Advances 1982, 45 (December): 125–45. https://doi.org/10.1016/0020-7381(82)80103-4.

McDowall, R. D. 2012. “Getting It Write?,” November. accessed 22.02.2022 https://www.chromatographyonline.com/view/quadrupole-mass-analysers-introduction.

Mo, Zaharie, Radu N, Pirvu L, Bostan M, Voicescu M, Begea M, Constantin M, Voaides C, Babeanu N, and Roman V. 2022. “Studies Regarding the Pharmaceutical Potential of Derivative Products from Plantain.” *Plants (Basel, Switzerland)* 11 (14). https://doi.org/10.3390/plants11141827.

Moldoveanu, Serban, and Victor David. 2012. *Essentials in Modern HPLC Separations*. Newnes.

Morita, Hiroyuki, Ikuro Abe, and Hiroshi Noguchi. 2010. “1.06 - Plant Type III PKS.” In *Comprehensive Natural Products II*, edited by Hung-Wen (Ben) Liu and Lew Mander, 171–225. Oxford: Elsevier. https://doi.org/10.1016/B978-008045382-8.00022-8.

Murai, Yoshinori, Hiroaki Setoguchi, Junichi Kitajima, and Tsukasa Iwashina. 2015. “Altitudinal Variation of Flavonoid Content in the Leaves of Fallopia Japonica and the Needles of Larix Kaempferi on Mt. Fuji.” *Natural Product Communications* 10 (3): 1934578X1501000308. https://doi.org/10.1177/1934578X1501000308.

Packard, Hewlett. 1998. “Basics of LC/MS.” https://www.agilent.com › support › documents.

Panche, A. N., A. D. Diwan, and S. R. Chandra. 2016. “Flavonoids: An Overview.” *Journal of Nutritional Science* 5 (December): e47. https://doi.org/10.1017/jns.2016.41.

Patel, Manish Kumar, Avinash Mishra, Santlal Jaiswar, and Bhavanath Jha. 2020. “Metabolic Profiling and Scavenging Activities of Developing Circumscissile Fruit of Psyllium (Plantago Ovata Forssk.) Reveal Variation in Primary and Secondary Metabolites.” *BMC Plant Biology* 20 (1): 116. https://doi.org/10.1186/s12870-020-2318-5.

Pavia, Donald L., Gary M. Lampman, George S. Kriz, and James A. Vyvyan. 2014. *Introduction to Spectroscopy*. Cengage Learning.

PHONE, BESØKSADRESSE Kristine Bonnevies husBlindernvn 31 0371 OSLO POSTADRESSE Postboks 1066 Blindern 0316 OSLO and FAX. n.d. “Monosakkarid - Institutt for biovitenskap.” Accessed

January 21, 2022. https://www.mn.uio.no/ibv/tjenester/kunnskap/plantefys/leksikon/m/monosakkarid.html.
"Plant Kingdom Plantae." 2022. VEDANTU. 2022. https://www.vedantu.com/biology/plant-kingdom-plantae, https://www.vedantu.com/biology/plant-kingdom-plantae, https://www.vedantu.com/biology/plant-kingdom-plantae, https://www.vedantu.com/biology/plant-kingdom-plantae.
"Plantago Major - Common Plantain." n.d. Accessed November 24, 2022. https://eflora.neocities.org/Plantago%20major.html.
"*Plantago Maritima*." 2020. In *Wikipedia*. https://en.wikipedia.org/w/index.php?title=Plantago_maritima&oldid=993355635.
"Plantago Maritima - an Overview | ScienceDirect Topics." 2022. 2022. https://www.sciencedirect.com/topics/agricultural-and-biological-sciences/plantago-maritima.
"Plantago Maritima - Artsdatabanken." 2022. 2022. https://artsdatabanken.no/taxon/Plantago%20maritima/102536.
Pradas Del Real, Ana Elena, Jose Silvan, Sonia de Pascual-Teresa, Ana Guerrero, Pilar García, M.C. Lobo, and Araceli Pérez-Sanz. 2017. "Role of the Polycarboxylic Compounds in the Response of Silene Vulgaris to Chromium." *Environmental Science and Pollution Research* 24 (February). https://doi.org/10.1007/s11356-016-8218-4.
"Preparative Liquid Chromatography - an Overview | ScienceDirect Topics." 2022. 2022. https://www.sciencedirect.com/topics/chemistry/preparative-liquid-chromatography.
Ravn, Helle, and Leon Brimer. 1988. "Structure and Antibacterial Activity of Plantamajoside, a Caffeic Acid Sugar Ester from Plantago Major Subs Major." *Phytochemistry* 27 (11): 3433–37. https://doi.org/10.1016/0031-9422(88)80744-1.
Ravn, Helle Weber, Laurence Mondolot, Mary T. Kelly, and Anne Mette Lykke. 2015. "Plantamajoside — A Current Review." *Phytochemistry Letters* 12 (June): 42–53. https://doi.org/10.1016/j.phytol.2015.02.002.
Sævdal Dybsland, Cecilie, Trine Bekkby, Kjersti Hasle Enerstvedt, Olav M. Kvalheim, Eli Rinde, and Monica Jordheim. 2021. "Variation in Phenolic Chemistry in Zostera Marina Seagrass along Environmental Gradients." *Plants* 10 (2): 334. https://doi.org/10.3390/plants10020334.
Samuelsen, Anne Berit. 2000. "The Traditional Uses, Chemical Constituents and Biological Activities of Plantago Major L. A Review." *Journal of Ethnopharmacology* 71 (1): 1–21. https://doi.org/10.1016/S0378-8741(00)00212-9.
Sanna, Federico, Giovanna Piluzza, Giuseppe Campesi, Maria Giovanna Molinu, Giovanni Antonio Re, and Leonardo Sulas. 2022. "Antioxidant Contents in a Mediterranean Population of Plantago Lanceolata L. Exploited for Quarry Reclamation Interventions." *Plants* 11 (6): 791. https://doi.org/10.3390/plants11060791.
Santos, Alda E dos, Ricardo M Kuster, Kristie A Yamamoto, Tiago S Salles, Renata Campos, Marcelo DF de Meneses, Márcia R Soares, and Davis Ferreira. 2014. "Quercetin and Quercetin 3-O-Glycosides from Bauhinia Longifolia (Bong.) Steud. Show Anti-Mayaro Virus Activity." *Parasites & Vectors* 7 (March): 130. https://doi.org/10.1186/1756-3305-7-130.
Shekarchi, Maryam, Homa Hajimehdipoor, Soodabeh Saeidnia, Ahmad Gohari, and Morteza Hamedani. 2012. "Comparative Study of Rosmarinic Acid Content in Some Plants of Labiatae Family." *Pharmacognosy Magazine* 8 (March): 37–41. https://doi.org/10.4103/0973-1296.93316.
"Strandkjempe (Plantago Maritima)." 2022. 2022. https://www.rolv.no/bilder/galleri/medplant/plan_mar.htm.
Torres-Vega, Jeniffer, Sergio Gómez-Alonso, José Pérez-Navarro, Julio Alarcón-Enos, and Edgar Pastene-Navarrete. 2021. "Polyphenolic Compounds Extracted and Purified from Buddleja Globosa Hope (Buddlejaceae) Leaves Using Natural Deep Eutectic Solvents and Centrifugal Partition Chromatography." *Molecules* 26 (8): 2192. https://doi.org/10.3390/molecules26082192.

Wilson, Angela. 1985. “Flavonoid Pigments of Butterflies in the Genus Melanargia.” *Phytochemistry* 24 (8): 1685–91. https://doi.org/10.1016/S0031-9422(00)82535-2.

Wishart, D. S., C. Knox, A. C. Guo, R. Eisner, N. Young, B. Gautam, D. D. Hau, et al. 2009. “HMDB: A Knowledgebase for the Human Metabolome.” *Nucleic Acids Research* 37 (Database): D603–10. https://doi.org/10.1093/nar/gkn810.

Xu, Jinju, Chaoying Tong, Qiachi Fu, Keke Guo, Shuyun Shi, and Yecheng Xiao. 2020. “Comprehensive Polyphenolic Profile of Plantago Depressa Using High-Speed Countercurrent Chromatography Off-Line with High-Performance Liquid Chromatography–Diode Array Detector–Quadrupole Time-of-Flight Tandem Mass Spectrometry.” *EFood* 1 (1): 94–105. https://doi.org/10.2991/efood.k.191101.001.

YMDB, YMDB. 2022. “L-Arabinose (YMDB00893) - Yeast Metabolome Database.” 2022. http://www.ymdb.ca/compounds/YMDB00893.

Zaghloul, Mona, and Ahmed Zaghloul. 2000. “A New Phenylpropanoid from the Aerial Parts of Plantago Crassifolia Forsk.” *Mans J Pharm Sci* 16 (January): 56–68.

华玉强. 2006. Luteolin-7-O-bata-glucuronide and its extracting process and application thereof. China CN1793156A, filed July 11, 2005, and issued June 28, 2006. https://patents.google.com/patent/CN1793156A/en.